



Review

Advanced Polymer Electrolytes in Solid-State Batteries

Ningaraju Gejjiganahalli Ningappa, Anil Kumar Madikere Raghunatha Reddy and Karim Zaghib *

Department of Chemical and Materials Engineering, Concordia University, 1455 De Maisonneuve Blvd. West, Montreal, QC H3G 1M8, Canada; ningaraju.ningappa@mail.concordia.ca (N.G.N.); anil.mr@concordia.ca (A.K.M.R.R.)

* Correspondence: karim.zaghib@concordia.ca

Abstract: Solid-state batteries (SSBs) have been recognized as promising energy storage devices for the future due to their high energy densities and much-improved safety compared with conventional lithium-ion batteries (LIBs), whose shortcomings are widely troubled by serious safety concerns such as flammability, leakage, and chemical instability originating from liquid electrolytes (LEs). These challenges further deteriorate lithium metal batteries (LMBs) through dendrite growth and undesirable parasitic reactions. Polymer electrolytes (PEs) have been considered among the few viable options that have attracted great interest because of their inherent non-flammability, excellent flexibility, and wide electrochemical stability window. However, practical applications are seriously limited due to the relatively low ionic conductivity, mechanical instability, and short operational life cycle. This review covers the recent developments in the field and applications of polymer electrolytes in SSBs, including solid polymer electrolytes (SPEs), gel polymer electrolytes (GPEs), and composite polymer electrolytes (CPEs). The discussion comprises the key synthesis methodologies, electrochemical evaluation, and fabrication of PEs while examining lithium-ion's solvation and desolvation processes. Finally, this review highlights innovations in PEs for advanced technologies like lithium metal batteries and beyond, covering emerging trends in polymer materials and advancements in PE performance and stability to enhance commercial applications.



Citation: Ningappa, N.G.; Madikere Raghunatha Reddy, A.K.; Zaghib, K. Advanced Polymer Electrolytes in Solid-State Batteries. *Batteries* **2024**, *10*, 454. <https://doi.org/10.3390/batteries10120454>

Academic Editors: Hirotoshi Yamada and Diana Golodnitsky

Received: 12 November 2024

Revised: 16 December 2024

Accepted: 19 December 2024

Published: 23 December 2024



Copyright: © 2024 by the authors. Licensee MDPI, Basel, Switzerland. This article is an open access article distributed under the terms and conditions of the Creative Commons Attribution (CC BY) license (<https://creativecommons.org/licenses/by/4.0/>).

1. Introduction

High consumer demand for electronics and a greater need for energy storage have fueled intensive research on rechargeable battery system technologies. With the rapid growth of electric vehicles and energy storage systems, the need for more advanced battery technologies that can provide better energy density and more safety features becomes critical [1–5]. Safety is a critical issue primarily due to the flammability of organic liquid electrolytes [6,7]. In contrast, SSEs, which serve as electrolytes and separators, are anticipated to mitigate these safety risks [8,9]. SEs have excellent thermal stability and, accordingly, no risk regarding safety for temperatures as high as 200 °C. In contrast, liquid electrolytes pose a risk starting from as low a temperature as 70 °C. Furthermore, SEs offer significant advantages, such as leak-proof operation and a wider electrochemical stability range compared to liquid electrolytes, which are limited to a narrower window, typically under 4.2 [10–13]. SSEs are seen as the most promising solution for the next generation of SSBs, particularly when paired with high-energy metallic anodes and high-voltage cathode materials (nickel-rich layered oxides, lithium-rich layered oxides, high-voltage spinel oxides, high-voltage polyanionic compounds, etc.) that would lead to tremendous improvements in energy density of up to 20–50% [14–17]. In addition, the rigid structure of SEs could potentially reduce capacity losses and internal short circuits. These problems could also be overcome by further research. High ionic and low electronic conductivity can also

enable fast charging facilitated by SEs. These advantages of SEs create vast opportunities for developing innovative battery chemistries [18,19].

1.1. Overview and State of the Art

Faraday's Law, proposed in 1833, marked the first reported observation of ionic conduction in Ag_2S . There was a gap until the 1950s [20]. These cells are an early example of solid-state battery basic cells containing silver salts. Still, they perform poorly and work with voltages below 1 V without any reasonable discharge currents [21–23]. Rao [24] filed the first patent in 1969 for the Li/LiI/I_2 solid-state cell with a film LiI electrolyte prepared with about 3 V of open circuit voltage. In 1970, a report was published on the movement of lithium ions in lithium halides in LMBs. Afterward, Liang et al. [25] created solid-state cells (Li/LiI and heavy metal SS cells) to solve the problems of iodine vapor diffusion in I_2 -based cathodes [21,25,26]. These LiI batteries became polarized and, therefore, unmendable, even if the energy density reached 100–200 Wh/kg [27]. Even so, these LiI batteries became polarized and, therefore, unmendable, even if the energy density of the batteries reached 100–200 Wh/kg [28]. Rechargeable SSBs based on lithium were created at the end of the 1970s. Since 1973, poly(ethylene oxide) has been applied for the purpose of conducting the alkali ions in lithium batteries as SSEs [21,29].

Studies on new polymer SSEs with lithium salts were conducted in subsequent works. Lithium-ion conductors with high ionic conducting capacity, systems for storing and transforming energy, and solid ionic electrolytes were also developed by scientists in the 1980s–1990s. Goodenough and coworkers [28,30] constructed a superionic conductor of sodium comprising $\text{Li}_{1.3}\text{Al}_{0.3}\text{Ti}_{1.7}(\text{PO}_4)_3$ in 1976, and in 1989, a report of high ionic conductivity was recorded. In 1993, a bulk conductive high perovskite, $\text{Li}_{0.34}\text{La}_{0.51}\text{TiO}_{2.94}$ (10^{-3}S/cm), was reported, and in 2003, the garnet-type material $\text{Li}_7\text{La}_3\text{Zr}_5\text{O}_{12}$ was used as an ionic conductor due to fast ionic conduction reported in 2007 [31,32]. In 1999, Birke and colleagues [33] reported that oxide-based electrolytes exhibit high ionic conductivity and strong mechanical properties. These and materials with sulfide-type structures and weak lithium–sulfur bonds were able to conduct lithium ions with high ionic conductivity in the 1980s [34]. The successful demonstration of LIBs with carbonate electrolytes in the 1990s meant that the research around SSBs reached a standstill. Still, the demand for more energy-dense and safer ASSB technology sparked research on SSBs again. In 2011, the use of a sulfide-based electrolyte, $\text{Li}_{10}\text{GeP}_2\text{S}_{12}$, which has very high conductivity, was presented, which expanded the possibilities of SSB applications, and this research group exceeded their achievement in 2016 (Figure 1) [8,35]. The materials are prepared via solid-state reactions with sintering, such as $\text{LiY}_{0.15}\text{Zr}_{1.85}(\text{PO}_4)_3$ (LYZP) and $\text{Na}_3\text{Zr}_2(\text{PO}_4)(\text{SiO}_4)_2$ (NZPS), to improve ionic conductivity and chemical stability [36]. Florian Strauss et al. [37] recognized that SSBs in 2020 would use solid ceramic electrolytes instead of liquids. Material examples include $\text{Li}_6\text{PS}_5\text{Cl}$, while surface coatings such as Li_2ZrO_3 improve interface stability and reduce side reactions. In 2021, Jordi Sastre et al. [38] mentioned that $\text{Li}_7\text{La}_3\text{Zr}_2\text{O}_{12}$ has high ionic conductivity and stability against lithium metal, while the polycrystalline LLZO may cause the growth of lithium dendrite. In 2023, Faruk Okur and his team [39] pointed out that Li-garnet, especially LLZO, is suitable for lithium metal anodes because of its high ionic conductivity and stability. Ongoing research on improving ionic conductivity and mitigating lithium dendrite formation in SSBs is up and coming, considering its wide-scale application to electric vehicles and renewable energy systems.

SSBs have emerged as a leading energy storage technology driven by the limitations of state-of-the-art LIBs that use liquid electrolytes, which have reached their theoretical energy density limits ($250 \text{ Wh}\cdot\text{kg}^{-1}$ and $600 \text{ Wh}\cdot\text{L}^{-1}$) and face safety concerns due to toxic and flammable components [40–43]. Replacing these liquid electrolytes with SSEs enhances safety and improves energy density and stability. SSEs can be organic or inorganic, with inorganic options like ceramic oxides, sulfides, and salt-solidified polymers. At the same time, hybrid electrolytes that integrate both solid and liquid components further boost ionic conductivity, electrode contact, and mechanical strength. Studies show that

adding small amounts of liquid or polymer electrolytes at the interface between SSEs and electrodes effectively reduces self-discharge in full cells, increasing their capacity and cycle life. SSBs, particularly with lithium metal anodes, offer the potential for higher energy densities with minimal risk of thermal runaway, making them a safer alternative for high-demand applications [44,45]. Furthermore, by integrating high-capacity, high-voltage cathode materials, SSBs could achieve energy densities up to $400 \text{ Wh}\cdot\text{kg}^{-1}$ and $900 \text{ Wh}\cdot\text{L}^{-1}$, far surpassing conventional LIBs [46,47].

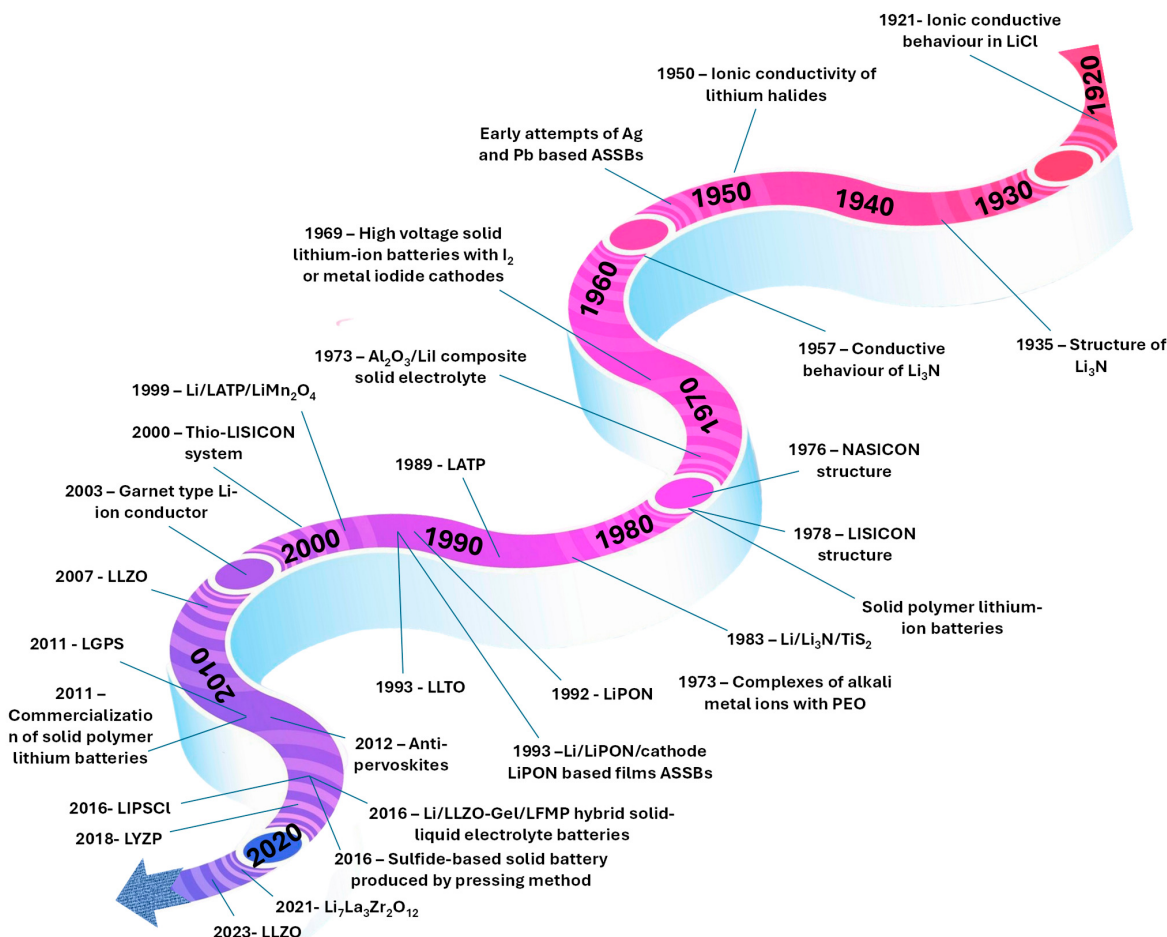


Figure 1. Timeline of key developments in SSBs.

1.2. Structural Design and Operating Mechanisms of SSBs

SSBs operate in the same fashion as conventional LIBs. An SSB cell consists of three main parts: the anode (negative electrode), from which electrons are released into the external circuit; the electrolyte, where ion transport between the anode and cathode takes place; and the cathode (positive electrode), onto which electrons are taken in from an external circuit. This leads to oxidation of the anode and reduction in the cathode throughout the discharging process, through which ions wander from the anode to the cathode through the SEs. Charging reverses this process [48].

SSBs can be categorized into three geometric types, each with a distinct design and material-specific mechanisms.

1. **Thin-Film SSBs:** Thin-film SSBs are ultra-thin, usually less than $15 \mu\text{m}$ in total thickness (Figure 2a). Such a design is highly advantageous for long-term stable cycling applications. In the thin architecture, the transport distance for Li^+ is minimized, which is important because thin-film SSBs normally use SEs with relatively low ionic conductivity, such as LPO. In this configuration, lithium metal usually serves as the anode, while LiCoO_2 is one of the typical cathode compositions. In the discharge

process, the lithium ions from the anode traverse the thin LiPON layer to the cathode while the electrons pass through the outer circuit. The structure minimizes ion transport resistance and leads to stable cycling, though the low areal capacity limits energy output for larger applications.

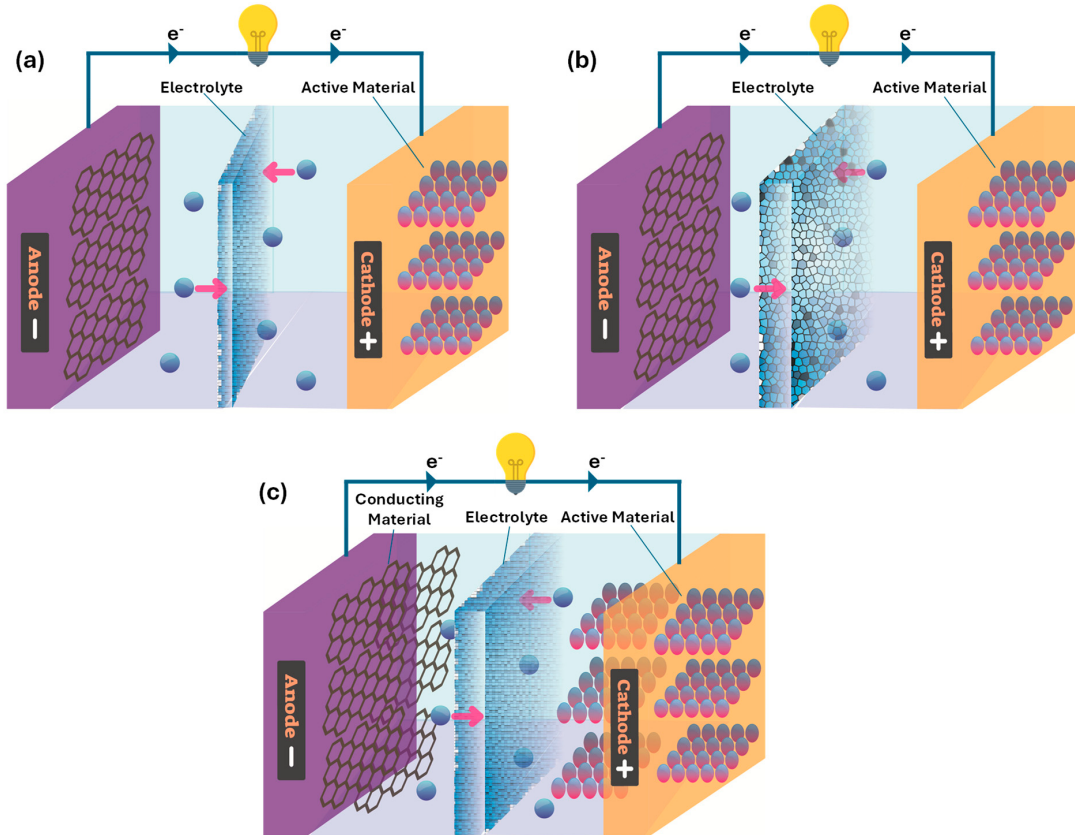


Figure 2. The layouts of (a) thin-film SSB, (b) three-dimensional SSB, and (c) bulk-type SSB.

2. 3D SSBs: The 3D SSBs use an interconnected electrode/electrolyte structure that maximizes the surface area of ion transport, thus offering superior energy density and power. Lithium metal or its alloys are normally used as the anode materials in such configurations, with SEs based on garnets being rather popular due to their stability and ionic conductivity. Due to this 3D structure, ions can flow through higher surface areas for high discharge rates and rapid charging. During the discharge process, lithium ions will migrate across the 3D network of the SE from the anode to the cathode, and electrons will move externally, thereby achieving efficient energy release. However, because of the greater interfacial contact area and complex geometries, uniform and stable interfaces in the 3D architecture might not be so easily achieved (Figure 2b).
3. Bulk-type SSBs: These involve thick electrodes, normally hundreds of microns, and these batteries are targeted for applications in which high energy density is required. Solid electrolytes with strong ionic conductivity are selected for this type of battery. Sulfide-based SEs such as lithium thiophosphate represent commonly used options due to their effectiveness in conducting lithium ions at ambient temperatures. The anode, in most cases, is lithium metal or lithium alloy. The cathode is manufactured from high-capacity materials such as NMC and LFP. The SE allows Li^+ ions to pass between the thick layers of the anode and cathode during the discharging process, whereas electrons move through the external circuit. Compared with these, bulk SSBs possess higher energy density and longer cycle life. Still, the thick structure would be

unfavorable for ionic transport efficiency, and thus, careful control of the interfacial contact and stability is required (Figure 2c) [49–51].

1.3. The Role of Electrolytes and the Importance of PEs

SSBs are gaining significant attention as next-generation energy storage technologies due to their potential for higher safety and energy density than conventional liquid electrolyte systems. While liquid electrolyte-based systems, such as rechargeable batteries and supercapacitors, are prone to leakage and volatility, SSBs use SEs that enhance thermal stability and provide wider electrochemical stability windows, critical for achieving high power densities and efficient battery performance [52,53]. Operating safely over a broad temperature range from -50 to 20 °C, SEs are suitable for extreme conditions where liquid electrolytes may decompose, freeze, or evaporate [14,16]. SEs generally fall into three categories: inorganic, organic, and composite (Figure 3). Inorganic SEs, such as ceramics, offer high ionic conductivities (over 10^{-4} S/cm) and excellent thermal stability due to their rigid structures. Still, they may suffer from interfacial contact issues with electrodes, impacting their performance [54,55]. Organic SEs provide flexibility suitable for flexible battery designs, although they generally have lower lithium-ion conductivities ($<10^{-5}$ S/cm at room temperature) and may be prone to oxidation at high voltages [56,57]. Composite SEs combine ceramic and polymeric components to enhance ionic conductivity and interfacial compatibility, thus advancing the potential for efficient, safe, high-performance SSBs [14].

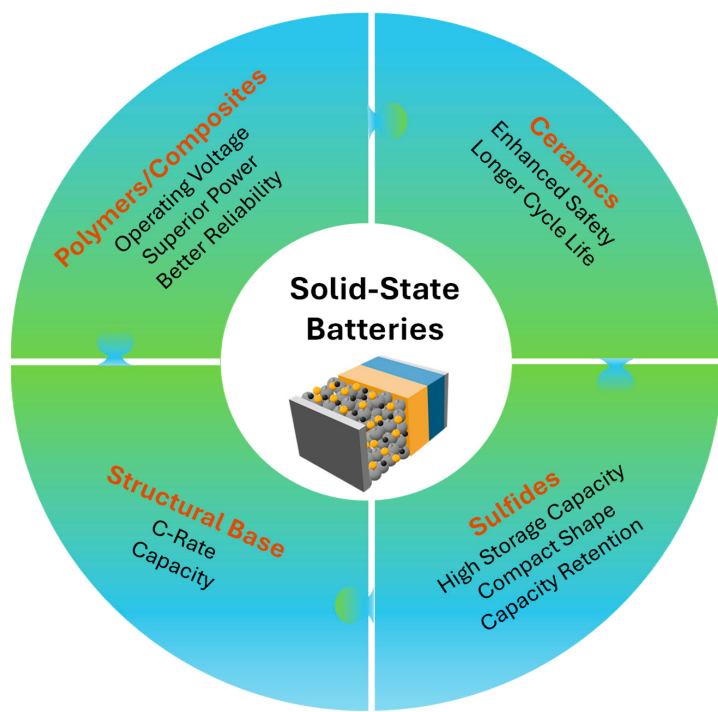


Figure 3. Advantages of SSEs.

PBSEs are particularly promising due to their favorable chemical, mechanical, and electrochemical properties, with SPEs allowing lithium-ion conduction through a polymer chain matrix. SPEs address leakage and flammability issues associated with liquid electrolytes while offering robust interface contact, processability, and cost-effectiveness [58]. Generally composed of a polymer matrix, lithium salt, and additives, SPEs face some challenges with ionic conductivity at room temperature due to segmental motion constraints [59–61]. Since the discovery of ion conductivity in PEO in 1973 and its proposed use in solid-state lithium batteries, polymer electrolytes have expanded to include matrices such as PVDF, PAN, PVA, PVP, PEG, and PMMA for diverse applications [62–67]. Further classified as SPEs, GPEs, and CPEs, advancements in polymer matrices, blending, and

adding inorganic fillers are helping to improve room-temperature ionic conductivity [68,69]. These developments in polymer electrolytes and interface engineering are pivotal for the future of high-performance, safe energy storage technologies.

1.4. Challenges and Limitations

SSEBs encounter various challenges that impede their broad adoption. These comprise low ionic conductivity, narrow electrochemical stability windows, poor mechanical properties, dendrite formation, interfacial impedance, and electrode compatibility [70–74]. SEs have benefits, improved safety, and higher energy density than LEs. They offer good thermal management effects on the cell, and their mechanical stability can be much better than that of a porous polymer, etc. However, there are some limitations to the following solid electrolyte solutions, e.g., brittleness for ceramic electrolytes or porosity and grain-boundary resistance. Also, scenarios related to dendrite formation occur under cyclic loads in the case of SPEs among electrochemical instabilities. These challenges require the improvement of interfacial stability, ionic conductivity, the electrochemical stability window, and compatibility with both anodes and cathodes in a smart electrolyte design. Key challenges in SSEs are as follows:

Lower Ionic Conductivity: One of the most critical challenges regarding PEs in SSBs is that they present low ionic conductivity in principle, especially at room temperature. SPEs have the advantage of flexibility and processability, but their ionic conductivity, in the range between 10^{-5} and 10^{-6} S/cm, is much lower than that of liquid or ceramic electrolytes. This is a consequence of the slow ion transport in the polymer matrix, which is somewhat controlled by the segmental motion of the polymer chains. Enhancement of the ionic conductivity without lowering the mechanical or thermal properties of the electrolyte remains a challenge [17,75]. Emily S. Doyle et al. [76] reported that the ionic conductivity of the polymer electrolyte was significantly low at 1.55×10^{-11} S/cm before being enhanced to 2.26×10^{-5} S/cm at 60 °C by incorporating crosslinked poly(ethylene glycol) units within a perfluoropolyether matrix (Figure 4a).

Poor Electrochemical Stability: The narrow electrochemical stability window of PEs also restricts their use in high-energy-density batteries. Since most PEs degrade at voltage levels higher than 4V, this results in parasitic reactions and leads to a high interfacial impedance between the electrolyte and electrodes. Such cathodes require improvement of the electrochemical stability window with current-limiting factors due to high working voltages, as used with nickel-rich layered oxides [77,78]. Xiaofei Yang et al. [79] herein report that PEO, the most commonly used SPE, suffers from limited ESW and cannot support voltages over 4 V. This has, in essence, been a significant barrier to its application in high-voltage SSLBs (Figure 4b).

Dendrite Formation: Dendrite growth is a fatal risk point for LMBs. Over time, dendrite lithium deposits that form needle-like structures can breach the PE and create internal short circuits, which cause battery failure. However, the limited mechanical strength of PEs makes it challenging to inhibit the growth of dendrites during extended cycling. Technical aspects like these pose a strong impediment to polymer-based SSBs on a commercial scale [77]. Moreover, the mechanical properties of the materials influence the dendrite growth; for example, a material with a higher modulus of elasticity, such as LLZO or glass Li₃PS₄, reduces the formation, whereas that from lower-modulus polymers, such as PVDF-HFP, promotes the growth of dendrites [80]. Furthermore, the distribution of lithium dendrites inside the PEs is heterogeneous, with growth from both the plating and the stripping electrodes, which is paramount in devising effective mitigation strategies (Figure 4c) [81].

Interfacial Stability: The formation of stable and low-resistance interfaces between PE and electrodes is required for high ion transport efficiency. Nevertheless, low interfacial adhesion or chemical incompatibility results in poor rate capability and cycling stability limited by higher interfacial resistance. In PEs, it is difficult to build stable SEIs at the lithium–metal interface, which inevitably leads to deteriorated long-term performance [82,83].

Temperature Sensitivity: The performance of PEs is very dependent on temperature. However, they have poor ionic conductivities at lower temperatures, making them unsuitable for colder regions. By contrast, very high temperatures can enhance ionic conductivity, but at the expense of mechanical stability, because PEs can become soft or decompose. This poses a challenge in terms of maintaining good performance over a broad temperature range [84]. However, one of the PEs prepared by the method of in situ polymerization shows an ionic conductivity of $2.2 \times 10^{-4} \text{ Scm}^{-1}$ at -20°C , which could work stably at such an ultralow temperature. Conversely, PEs are also subjected to shrinkage and deformation under high temperatures, probably due to the catastrophic failure of batteries. For example, adding ionic liquids and zeolites has improved room temperature ionic conductivity and thermal stability up to 300°C [85].

Strength and Durability: This can be an improvement, but, while PEs are already more flexible than ceramic electrolytes, many lack the mechanical strength necessary for robust use in a vehicle. Over time, this repeated cycling and mechanical stress causes the cells to crack or split, eventually leading to structure failure for the battery itself. To this end, efforts are ongoing to boost the mechanical properties of PEs further by constituting composites and incorporating them with inorganic fillers [86,87].

Scalability and Manufacturing: PEs are easier to process than ceramics or sulfides overall, but there are numerous challenges in scaling their production while retaining quality and performance properties. PEs need to be synthesized to have good ionic conductivity and mechanical strength, which fundamentally depend on nano-structural control. The ability to produce defect-free PEs at scale via cost-effective manufacturing processes is required for the scalable commercialization of their use [88,89].

The development of SSBs enables a crucial step in energy storage technology that will fix key safety and performance problems with conventional lithium-ion batteries. Using SSEs opens perspectives for innovative, high-energy-density batteries with superior thermal stability, enabling a variety of new battery chemistries that might play a key role in electric vehicles and renewable energy systems. Continuous study and development in this area promise great expectations for a safe, efficient, and high-capacity energy storage solution.

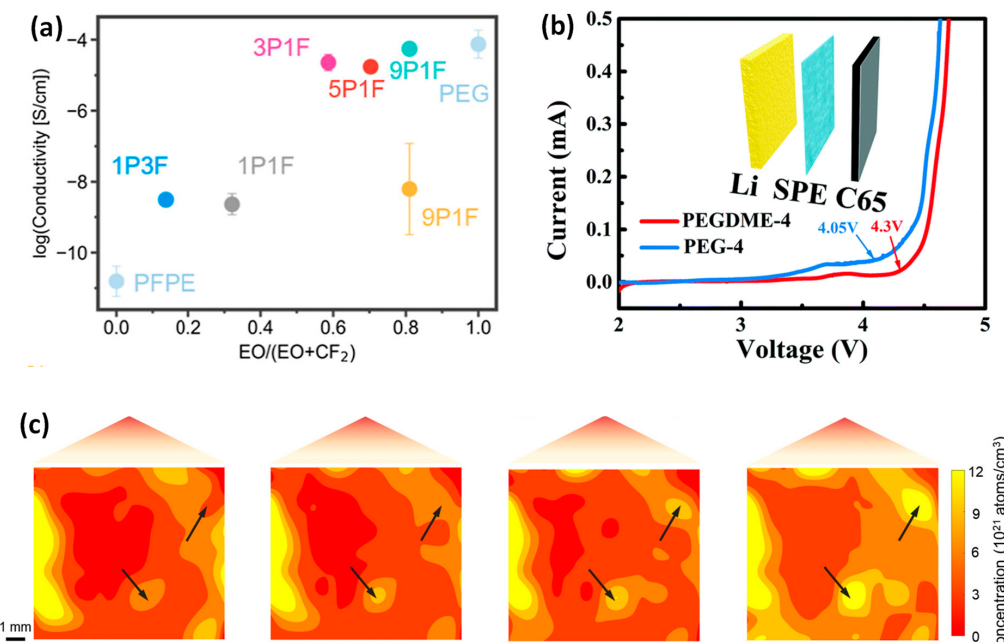


Figure 4. (a) Ionic conductivity at 60°C versus the Li^+ /EO ratio of 0.05 with different PEG/PFPE ratios [76]. (b) Electrochemical stability window of PEGDME-4 and PEG-4 SPEs. Adapted with permission from [79]. Copyright 2020, Royal Society of Chemistry. (c) Schematic structure formed in the PE upon Li stripping [81].

2. Characteristics of PEs

2.1. Performance Requirements

The PEs used in SSLPBs play the key roles of charge conduction and separation between the anode and cathode, which makes them extremely important for battery performance. PEs must have several key attributes to find practical applications. In practice, they would be expected to show ionic conductivities above 10^{-4} Scm⁻¹ (preferably even higher), ensuring fast ion passage with low system resistance and maintaining electronic insulating character to limit self-discharge [90–93]. Especially for Li⁺, the cation transference number (0.9–1) should be as high as possible to avoid concentration polarization, decrease overpotential, and enhance energy density. These approaches can be realized by grafting anions onto the polymer backbone or introducing accessory anion acceptors to confine anion movement in favor of Li⁺ transport [94,95]. Moreover, PEs should have superior chemical stability in terms of the chemical reaction with battery components and electrochemical and thermal stability with thermal degradation typically occurring at temperatures above 250 °C and a decomposition temperature (T_d) exceeding 200 °C to ensure safety across various conditions, including high-temperature environments or even short-circuiting/overcharging [96]. In addition, strong mechanical properties are needed to prevent dendrite growth and oxidation of the electrodes, which are required to achieve ideal metallically forced intimate contact during charging/discharging cycling. Moreover, a high electrochemical stability window (usually 4 to 5V vs Li/Li⁺) is also required for application in high-voltage cathode materials [97], and would significantly improve energy density over current state-of-the-art designs. Figure 5a below illustrates these key characteristics.

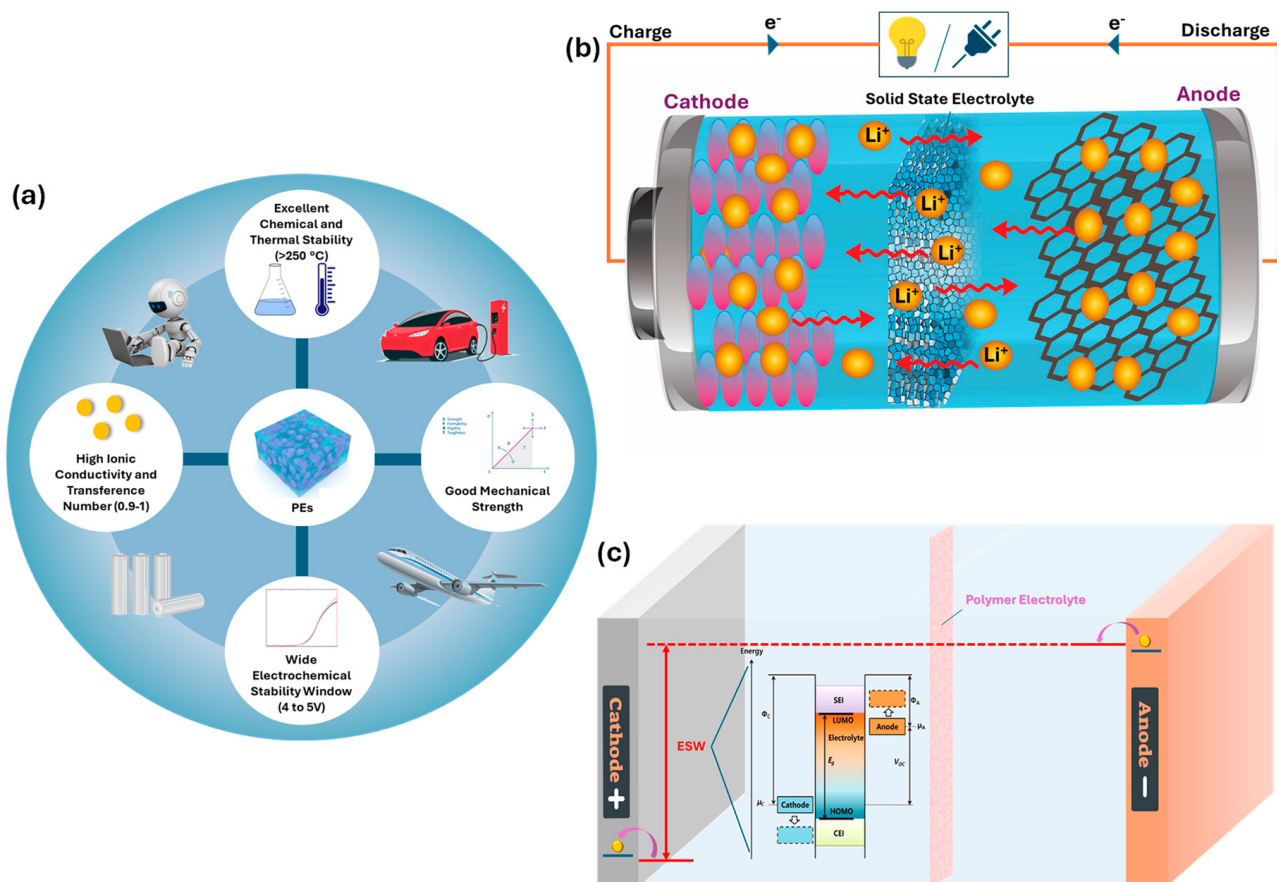


Figure 5. (a) Essential requirements for an ideal SSPE. (b) Ion-transfer mechanism in SPEs. (c) Schematic representation of the ESW and energy diagram of PEs.

2.1.1. Ion Transfer Mechanism

Researchers have been trying to explore the ion transport mechanism of SPEs from time to time since SPs became known [63,98–100]. Like conventional SPEs, high ion conductivity in PEs results from Li-salt dissociation. The polymer matrix must also effectively dissolve these lithium salts to enable the formation of complexes with lithium ions, which is essential for facilitating efficient ion transport. Ideally, the system would comprise a lithium salt with low lattice energy mixed with a polymer with a high dielectric constant, which would allow for both dissociation of the Li salts and ion mobility. Some polymers that contain polar functionalities, such as -O-, -C=O, -S-, -CN, and -P-, have been reported to dissolve Li⁺ salts and, thus, form polymer-Li salt complexes [40]. When the salt is chosen, it is essential to use a low-lattice-energy salt together with a polymer that has a desired dielectric constant; this can potentially produce an enhanced dissociation of lithium salts as well [101].

For SPEs, ionic conductivity is primarily influenced by free ions' mobility and availability. The segmental motion of the amorphous regions is the dominant cause of Li⁺ mobility. At lower temperatures, polymers with lower glass transition temperatures will have more chain flexibility and, as a result, more effortless segmental movements. Complexation and dissociation of Li⁺ ions occur between coordination sites in the polymer matrix while migrating under an electric field (Figure 5b). Upon heating, Li⁺ can hop between polymer chains through the free volume induced by the segmental motion in the polymer [102]. Moreover, ionic conduction may also propagate through certain crystalline forms in the PE. Unusually, lithium salts have cylindrical tunnels surrounded by pairs of polymer chains in their crystal lattices. In this framework, Li⁺ ions can coordinate with ether oxide bonds and transfer along these channels without any segmental movement of the polymer chains [75,103–106].

In the case of conductivities in PEs, the well-known relationships describing the temperature dependence of ion conductivity are (i) the Vogel–Tamman–Fulcher (VTF) and (ii) Arrhenius, between which there are two other forms.

Basic VTF equation formula:

$$\sigma = \sigma_0 T^{-1/2} \exp \left[\frac{-B}{T - T_0} \right] \quad (1)$$

where σ_0 represents the frequency factor for the number of charge carriers, B denotes the activation energy for ion conduction, T is the operating temperature, and T_0 is ($T_0 = T_g - 50$ K) the equilibrium glass transition temperature (T_g). The VTF model was first proposed for glassy and disordered materials to explain diffusion processes, and it shows that ionic conductivity is associated with the volume of the polymer, which participates in the ion hopping as well as the relaxation process.

This is the more familiar form of the Arrhenius equation.

$$\sigma = \sigma_0 \exp \left[\frac{-Ea}{kT} \right] \quad (2)$$

Ea —energy of activation, k —Boltzmann's constant, and σ and σ_0 —ion conductivities. Thus, the most prevalent model is the Arrhenius model, which also characterizes ion-hopping motion as being influenced by the long-range movement of the polymer matrix.

To evaluate ionic conduction properties, impedance spectroscopy was used, with the calculation of ionic conductivity expressed as:

$$\sigma = L / RA$$

In the above equation, L represents the thickness of the PE membrane (cm). The parameter R stands for the resistance of the electrolyte (ohm), and A refers to the area of the electrode (cm²) [107].

2.1.2. Electrochemical Stability Window

The ESW of PEs is essential when considering their application in high-energy-density SSBs. The ESW is the region of voltages where the electrolyte is stable, ideally 4–5 V, because it is compatible with high-voltage cathodes such as LiCoO_2 and $\text{LiNi}_{1x-y}\text{Co}_x\text{Mn}_y\text{O}_2$ [108–110]. This stability correlates strongly with the oxidation and reduction potentials of the electrolyte, which are commensurate with its HOMO and lowest unoccupied molecular orbital LUMO, respectively (Figure 5c) [111,112]. The broad ESW increases the electrolyte resistivity against failures, helping in efficient ion transport and inhibiting undesired side reactions at the anode and cathode interfaces. Cyclic voltammetry and linear sweep voltammetry are frequently used as measures for the ESW, whereby a sharp increase in current indicates oxidation, while no significant anodic current points to stability over high voltages [113]. Nevertheless, the classical techniques can overestimate the ESW for a small cover depth of geosynthetic reinforcement, so they have been extended to more accurate ones such as quasi-static LSV, which fits a precise measure due to applying an extension at voltage application time [114]. The same can be said about the polymer matrix interactions with lithium salts like LiTFSI, where structural reorganization and side reactions might reduce ESW [115]. As such, the optimization of the ESW by both improved testing methods and material design is critical for further improving PE performance in advanced LBs.

2.1.3. Mechanical and Thermal Stability

For SSBs, the potential of PEs is mostly determined by their mechanical stability. The challenge facing polymer designers is that the material needs to be strong and stiff enough to prevent mechanical deformation during these charge–discharge cycles. The properties of PEs are often polymers, and Young's modulus is the key determining factor in preventing battery problems like dendrite formation and electrolyte cracking that ultimately led to battery failure. The polymer matrix, being flexible and tough, is, therefore, key in maintaining the mechanical integrity of the electrolyte under extreme conditions. Results suggest that the combined approach (PEs supported by ceramic or inorganic fillers) is promising for improved mechanical properties and demonstrates a trade-off between flexibility and toughness. These modifications enhance the life cycle and electrochemical performance by reducing the interfacial degradation between PE and electrodes. Nonetheless, mechanical strength and good ionic conductivity still exist at different temperatures, and further optimization of polymer composition is needed for SSB applications [116–118].

The thermal stability of PEs used in SSBs constitutes an equally important factor in terms of safety and high-performance measures. Thermally stable polymer electrolytes, especially as compared to liquid electrolytes, lessen the risk of the system entering thermal runaway, a primary safety concern. The decomposition temperature of polymers bearing lithium salts, as these kinds of PEs, is influenced by the presence of salts in the polymer matrix. The thermal stability is enhanced upon an appropriate decision regarding the selection of lithium salts and polymer compositions, as every salt has one or two distinct polymers that enhance its stability or otherwise go down. To improve thermal performance and achieve safe and reliable SSBs, further development of new combinations of polymers and salts is required [119–121].

3. Types of Polymers Used as Electrolytes

3.1. Solid Polymer Electrolytes

SPEs are one class of material that provides a medium for ion transport in SSBs. They offer many advantages compared to their liquid counterparts, including much safer and more stable performances. They are especially critical in developing high-energy-density and safe lithium batteries that will be important for application in electric vehicles and portable electronics.

3.1.1. Dry Solid Polymer Electrolytes

DSPEs are one category of SPEs and are fully solid, i.e., there is no organic liquid solvent in a DSPE. PEO and its various derivatives have been extensively studied because of their attractive viscoelastic properties, high ion dissociation capability, and good mechanical and electrochemical stability [122,123]. PEO-based DSPEs show poor ionic conductivity, usually falling in the order of 10^{-8} to 10^{-7} Scm^{-1} because of their crystalline structure at room temperature and low ESW [124]. DSPEs typically operate as ion-coupled materials (the ions are still confined to the amorphous regions above T_g), requiring relatively high operating temperatures, like more than or equal to 60°C , for any reasonably high ionic conductivity [125]. Decreasing T_g to improve ion transport is a widely used method because it increases the segmental mobility of polymer chains due to its low interaction with Li ions and acts as a barrier to crystallinity. Polysiloxane, meanwhile, maintains an entirely amorphous state at room temperature among various polymer matrices with T_g lower than 0°C , such as PEO [126–128] and other candidate materials ranging from highly conductive polymers like polyphosphazene to elastic and mechanically robust ones like polypropylene oxide. The flexible Si-O-Si backbone of polysiloxanes with potential crosslinking sites makes polysiloxanes excellent backbones for an SPE because they exhibit ultralow T_g and chemical stability. The ionic conductivity of polysiloxane copolymers can reach a value of approximately 10^{-3} Scm^{-1} , and their ESWs are as wide as up to 5 V [129]. However, polysiloxanes (such as all low- T_g materials) can have a disadvantage: their low mechanical strength. Polyphosphazene and polypropylene oxide-based electrolytes show low T_g , facilitating the backbone chain movement in polymers; however, their mechanical properties need further improvement [130]. Crosslinking between polymers is a common way to give them some form of mechanical stability. Polycarbonate-based electrolytes have shown great potential to possess good ionic conductivity and wide ESWs, yet they still suffer from Li–metal anode incompatibility [131]. While many DSPEs utilizing single-polymer matrices reveal low room-temperature ionic conductivity (typically around 10^{-5} to 10^{-7} Scm^{-1}), which limits their practical use, various modification techniques like blending, copolymerization, and crosslinking modification for polymer bases, as well as the selection of innovative salt types and the integration of inorganic fillers, are employed to improve their ionic conductivity [132]. Therefore, future research will concentrate on enhancing the performance of DSPEs for advanced energy storage applications.

3.1.2. Polymer-In-Salt Electrolytes

PISEs show advanced energy storage systems for Li-ion and Na-ion batteries. These electrolytes are characterized by an extremely high lithium salt content, usually more than 50 wt%, due to the enhancement of ionic conduction and electrochemical stability (Figure 6(a1,a2)) [133–136,136–146]. Various studies have reported that the inclusion of different types of polymer matrices, such as PAN, PVDF-HFP, and polymeric ionic liquids, could greatly promote the transport of Li^+ -ions (Figure 6(b1–b5,c)) [134,137,139,143]. The structural features of these electrolytes facilitate more excellent ion transport and reduce other problems like dendrite growth, which is the major challenge in the advancement of LMBs [78,138,143].

Further, some specific fillers, for example, LLZTO and inorganic nanoparticles, have been incorporated into PISEs to enhance both electrochemical stability and mechanical properties and further increase the performance of batteries (Figure 6d) [135,136,141,142]. Some studies utilize in situ synthesis methods that provide a more efficient production process and better electrode interaction, hence minimizing complications with the solvent that remains after use. The progress of research technology highlights their flexibility and promise as key elements in future SSBs with the potential for enhanced energy storage capacity and better durability [146]. As research progresses, PISEs are expected to impact the movement toward more effective energy storage options. Findings related to PISEs are summarized in Table 1.

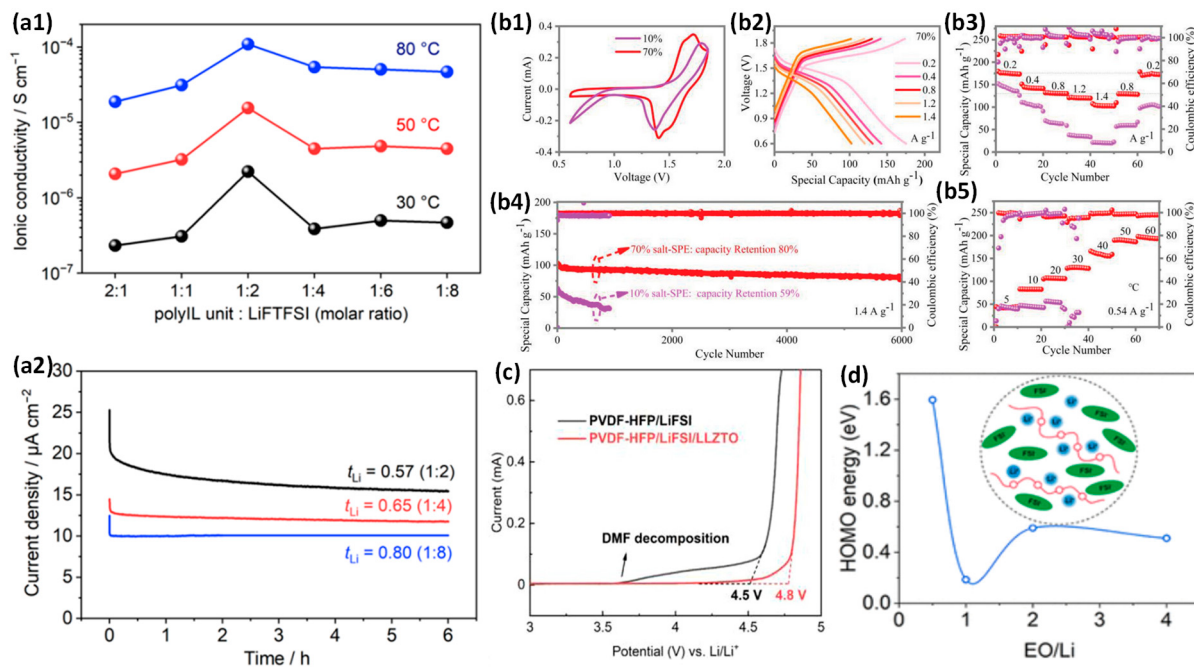


Figure 6. (a1) Ionic conductivity measurements as a function of different PISE units and LiTFSI ratios. (a2) The current time profile during 10 mV polarization and the Li-ion transference numbers for PISEs unit/LiTFSI. Adapted with permission from [133]. Copyright 2024, American Chemical Society. (b1–b5) LSV curves of PVDF-HFP/LiFSI and PVDF-HFP/LiFSI/LLZTO electrolytes. Adapted with permission from [137]. Copyright 2023, Wiley-VCH GmbH. (c) Electrochemical performance of Li||LFP full cells using the PVDFHFP/LiFSI electrolyte at room temperature, rate performances from 0.1 C to 5 C. Adapted with permission from [134]. Copyright 2022, Elsevier. (d) Schematic diagram of PISE structure. Adapted with permission from [135]. Copyright 2021, American Chemical Society.

Table 1. Key findings of PISEs.

Monomer	Solvent	Salt	Ionic Conductivities (Scm⁻¹) at Temperature (°C)	Lithium-Ion Transference Number (t_{Li^+})	ESW (V vs. Li/Li ⁺)	Discharge Specific Capacity (mAh g⁻¹)	Capacity Retention (%/Cycle)	Reference
PolyILs	ACN	LiTFSI and LiFSI	9×10^{-5} at 80	0.81	-	-	-	[133]
PVDF-HFP	DMF	LiFSI	1.67×10^{-3} at RT	0.27	4.5–4.8	142.2	97.2/300	[134]
PEO	-	LiFSI	2.7×10^{-4} at RT	-	4.5	-	74.4/186	[135]
DL-lactide, and 3-caprolactone	-	LiTFSI	8.9×10^{-5} at 30	0.6	5	180/0.1 C, 171/0.2 C, 164/0.3 C, 150/0.5 C, and 121/1 C	92.5/160	[136]
PAN	-	Zn(OTf ₂)	1.75×10^{-3} at RT	0.78 (Zn ²⁺)	9	190	80/6000	[137]
PCL	-	LiFSI	3.9×10^{-4} at 30	0.61	4.8	147/0.1 C, and 135/0.5 C	92/300	[138]
PEO or PAN	-	LiTFSI	8.5×10^{-5} at 30, and 1.8×10^{-4} at 60	0.62	5	92/1 C	98.8/100	[139]
SAPE (Solid state aqueous PE)	-	LiTFSI	3×10^{-3} , and 1.7×10^{-3} at 25	-	3.86	158	99.97/600	[140]

Table 1. Cont.

Monomer	Solvent	Salt	Ionic Conductivities (Scm^{-1}) at Temperature ($^{\circ}\text{C}$)	Lithium-Ion Transference Number (t_{Li^+})	ESW (V vs. Li/Li $^+$)	Discharge Specific Capacity (mAh g^{-1})	Capacity Retention (%/Cycle)	Reference
PVDF	NMP	LiTFSI	3.03×10^{-4} at 25	0.546	4.3	111.8	71/800	[141]
PAN	-	LiTFSI	4.44×10^{-4} at 25	0.61	-	643/0.05 C	54.7/120	[142]
PVDF-HFP	DMF	LiTFSI	1.24×10^{-4} at RT	0.53	4.7	146.6	86.8/800	[143]
PME-LiPVFM	-	LiTFSI	3.57×10^{-4} at RT	0.62	5	196.3/0.1 C, and 180.4/0.5 C	89.2/225	[144]
3-caprolactone (CL) and DL-lactide (LA)	-	LiTFSI	34×10^{-3} at 30	0.6	5	180/0.1 C, 171/0.2 C, 164/0.3 C, 150/0.5 C, and 121/1 C	92.5/160	[136]
P(EO-co-PO)-TMPTGE	-	LiFSI	2.30×10^{-3} at 30	0.69	4.6	141	95/200 and 96/50	[145]
PE/AO@PIS)	DMF	LiTFSI	0.12×10^{-3} at 25	0.43	4.7	131/10 C	93.6/400	[146]

3.1.3. Single-Ion-Conducting Polymer Electrolytes

Particularly, SICPEs have gained much attention in SSLMBs due to their selective promotion of the mobilization of Li-ions and because they can alleviate problems related to ion polarization and lithium dendrite formation. The basic structure of SICPEs is a polymer with covalently tethered anions, which assist in ionic conductivity and facilitate Li $^{+}$ -ion transport. Recent investigations support various mixes that enhance performance [147]. For example, Yang et al. [148] prepared PLIMTFSI/POEM composite material, which showed remarkable ionic conductivity and mechanical strength. David Fraile-Insagurbe et al. [149] similarly developed new SICPEs based on a LiPhTFSI-functionalized poly(ethylene-alt-maleimide) backbone with PEO and PEGDME, respectively, demonstrated by two types of symmetric lithium cells and complete cell configurations (Figure 7(a1–a4)). In addition, a study by the Zhang group [150] reported a semi-solid polymer electrolyte (PBSIL) containing vital ingredients, including solvate ionic liquid, which exhibited encouraging performance for commercial application. Other especially remarkable advances are the implementation of LiPCSI, which preserves electrochemical stability, by Hongyan Yuan and co-workers [151], as well as the design of a novel LiCTFPB structure (Figure 7b), which is the world's first SICPE developed by Hao Li et al. [152].

Efforts have also been directed towards applications of modern synthetic methodologies for preparing SICPEs with improved properties. These include, for example, designed and synthesized high-ionic conductive block copolymers using ring-opening polymerization and reversible addition–fragmentation chain-transfer (RAFT) polymerization [154]. Li et al. [153], bearing excellent safety and enhancing efficiency for lithium–metal batteries, explored carbon quantum dot (CQD)-derived single-ion conducting solid-state polymer electrolytes (SIC-SPEs) from PEO (Figure 7c). Conversely, Hai-Peng Liang et al. [155], developed a polysiloxane-based single-ion conductor with excellent mechanical and electrochemical properties. Second, another group showed the usage of a high-pore 3D semi-IPN polymer network to enhance the transference of lithium ions [156]. Also, a new structure of a quasi-solid-state polymer-brush electrolyte (SLIC-QSPBE) using bacterial cellulose and functional polymer tethers suggested novel directions in energy storage [153,157]. These developments represent a collaborative effort throughout the research community to refine SICPEs, thus driving high-scale innovation and applications for solid-state battery technology. Table 2 summarizes the recent findings of SICPEs.

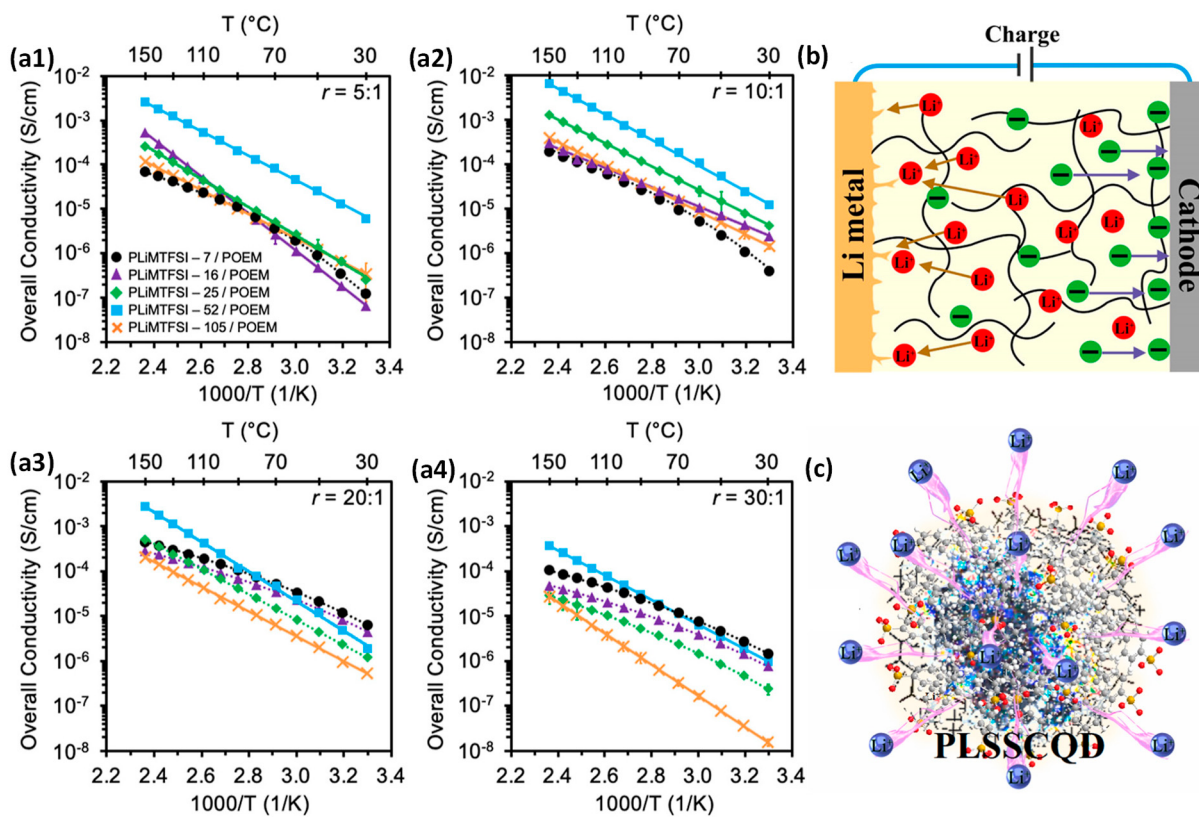


Figure 7. (a1–a4) Ionic conductivity trends with temperature for blend electrolytes at different ratios, showing data points and fitted lines. Adapted with permission from [148]. Copyright 2024, American Chemical Society. (b) Increasing concentration polarization leads to uneven lithium deposition, potentially causing dendrite formation. Adapted with permission from [151]. Copyright 2020, American Chemical Society. (c) Structure of PLSSCQD. Adapted with permission from [153]. Copyright 2020, Elsevier.

Table 2. Key properties and performances of SICPEs from recent studies.

Monomer	Solvent	Salt	Ionic Conductivities (Scm^{-1}) at Temperature ($^\circ\text{C}$)	Lithium-Ion Transference Number (t_{Li^+})	ESW (V vs. Li/Li^+)	Discharge Specific Capacity (mAh g^{-1})	Capacity Retention (%/Cycle)	Reference
PEGMEA	-	LiTFSI	$7.6 \times 10^{-6}/10^{-4}$ at 25/60	0.9	-	-	-	[147]
PLIMTFSI	-	TFSI	7×10^{-3} at 150	0.9	4.7	-	-	[148]
PEaMI	-	LiPhTFSI	7×10^{-6} at 70 7×10^{-7} at 25	Close to 1	25 70	160	45/100	[149]
PVDF-HFP	$[\text{Li}(\text{G4})][\text{TFSI}]$	LiTFSI	8×10^{-4}	0.75	-	183	75/1300	[150]
PEO	-	LiPCSI	7.33×10^{-5} at 60	0.84	5.53	141	85/80	[151]
TEG	-	LiCTFPB	3.53×10^{-6} at 25	0.92	4.8	162/0.1 C 155/0.2 C 145/0.5 C 131/1 C 91/2 C	89.8/200	[152]
PEO	-	Poly(lithium 4-styrene sulfonate)	2.02×10^{-4} at RT	0.94	4.4	155.9/0.2 C	94.3/100 96.3/50 91.2/300 83.4/1000	[153]

Table 2. Cont.

Monomer	Solvent	Salt	Ionic Conductivities (Scm^{-1}) at Temperature ($^{\circ}\text{C}$)	Lithium-Ion Transference Number ($t_{\text{Li}+}$)	ESW (V vs. Li/Li ⁺)	Discharge Specific Capacity (mAh g^{-1})	Capacity Retention (%/Cycle)	Reference
PSiO-PVDF-HFP	DMSO	LiPF ₆	0.4 mS cm ⁻¹ at 20, and 0.8 mS cm ⁻¹ at 40		4.8	170 to 125	80/150	[155]
PETEA	EC, and DMC	LiPF ₆	3.56×10^{-3} at RT	0.74	4.2	136.7/1 C 159.6/0.1 C	82.5/1000	[156]
TMC	-	LiM	3.7×10^{-6} at 70	0.91	4.8	145, and 118/20 C	2/10	[154]
PLiSTFSI	-	-	3.1×10^{-4} at RT		-	149, 134, 116, 99, and 83/0.1–0.5 C	111 m Ah g ⁻¹ /300	[157]

3.2. Gel Polymer Electrolytes

The development of GPEs has enabled the evolution of safe, high-energy-density SSBs. In this case, the liquid electrolytes are accommodated within the solid polymer structure, reaping the benefits associated with both liquid and solid electrolytes. PEO, PVDF, PMMA, and PAN are common polymer matrices that have encountered these unfavorable limitations when applied at room temperature. Recent studies, however, have revealed the potential of copolymer-based GPEs containing functional pendant groups that enhance Li-ion diffusion, redox safety, and fire-proof capacity (Figure 8a) [158–166]. Using ionic liquids and efficient salts containing lithium also contributed to reaching or surpassing the ionic conductivity of conventional liquid electrolytes. Plasticizer-assisted flame retardants have also bolstered the thermal stability and safety of GPE so that a high-energy-demanding application could be achieved [159,161].

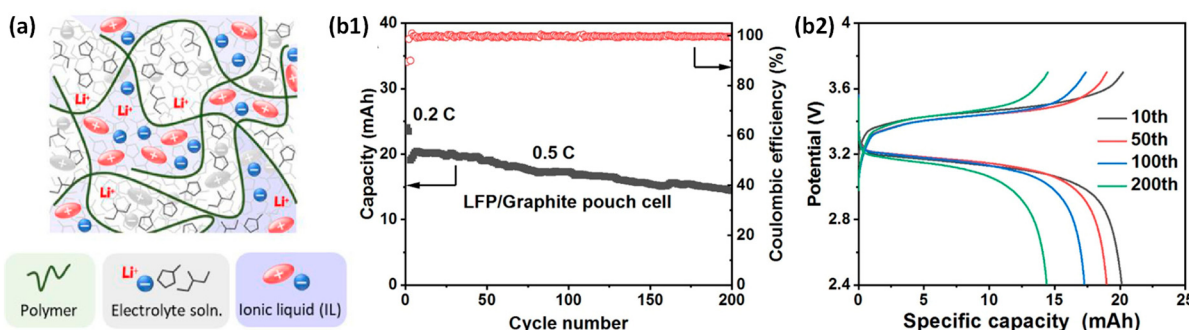


Figure 8. (a) Diagram showing micro-segregation in the gel structure. Adapted with permission from [166]. Copyright 2021, Elsevier. (b1,b2) Application of a LiFePO₄/graphite pouch battery with PA1D1-based GPE, highlighting cycling performance and charge/discharge curves. Adapted with permission from [167]. Copyright 2022, Elsevier B.V.

The performance of GPEs has been very receptive, with the ionic conductivity having values as high as 1.4×10^{-3} S/cm at room temperature [166]. They have excellent cycling stability, with some of their formulations retaining more than 90% capacity after 1000 cycles, and thus are suitable for use in Li-ion battery packs [159]. Moreover, heat generation has been minimized compared to traditional LEs, enhancing operational safety [166]. The design of the GPEs implies accelerating the movement of lithium ions, boosting the energy density, and extending the battery's cycle life. Nevertheless, more efforts must be conducted, especially on the formulation and polymerization technique, towards producing GPEs that are amenable for practical use in future energy storage technologies (Figure 8(b1,b2)) [165–167]. In addition, recent studies have highlighted the key properties and performance of GPEs, as summarized in Table 3.

Table 3. Key characteristics of GPEs studied in recent research.

Monomer	Solvent	Salt	Ionic Conductivities (Scm^{-1}) at Temperature ($^{\circ}\text{C}$)	Lithium-Ion Transference Number ($t_{\text{Li}^{+}}$)	ESW (V vs. Li/Li $^{+}$)	Discharge Specific Capacity (mAh g^{-1})	Capacity Retention (%/Cycle)	Reference
PEO	LEs	LiPF ₆ , and LiFSI	$7\text{--}9 \times 10^{-3}$ at RT	-	-	142.3	-	[165]
PEGDA and 2-hydroxyethyl methacrylate	DMF	LiTFSI	2.9×10^{-3} at 25		5.6	170/0.1 C	96/100	[159]
PVDF-HEP	PEGDME	LiTFSI	3.4×10^{-4} at RT	0.48	-	$1 \text{ mAh cm}^{-2}/10 \text{ C}$	98/60	[160]
PEO and PVDF	LEs	LiFSI, LiTFSI, and LiClO ₄	$>10^{-3}$ at RT	0.57	5.6	146	90/100	[161]
PMMA-SiO ₂ composite	-	-	0.41×10^{-3}	0.54	4.9	6.8 mAh cm^{-2}	$0.5 \text{ mAh cm}^{-2}/116$	[162]
PVDF-HEP	TEGDME	LiClO ₄ , LiPF ₆ , and LiTFSI	10^{-7} to 10^{-4}	0.3–0.9	4.9 (LiTFSI) 3.7 (LiPF ₆)	-	-	[163]
PEGM-Block Copolymer	EC, and DEC	LiPF ₆ , and LiNO ₃	2.7×10^{-4} at 25	0.68	4.2	168//0.1 C 151//0.2 C 136//0.5 C 118//1 C 99//2 C 89//3 C	$0.5 \text{ mAh cm}^{-2}/1200$	[164]
PAN, PEO, and PVDF	EC, and EMC	LiPF ₆ , and LiTFSI	$>10^{-3}$	0.77	-	159.7	84/200	[168]
PVDF-HEP	EC, and DMC	LiPF ₆	-	0.44	5	110.4	-	[166]
[P(AN-DEVP)]	-	LiPF ₆	1.4×10^{-3}	-	-	24.06	75.9/200	[167]
Polymer matrix	ILs	LiDFOB and LiFSI	1.0×10^{-3}	0.89	-	-	-	[158]

3.3. Composite Polymer Electrolytes

CPEs are a new generation of materials intended to improve the performance of SSBs, as they consist of polymers, lithium salts, and inorganic fillers aimed at increasing ionic conductivity, strength, and electrochemical stability. Such electrolytes generally involve using flexible polymer matrices, such as PEO, PAN, and PVDF, with Li-salts, e.g., LiTFSI. The interactions between components like PVA, PAN, LiTFSI, LATP, and SN are shown in Figure 9a. The addition of inorganic fillers—Li_{1.4}Al_{0.4}Ti_{1.6}(PO₄)₃-principal crystal structure material, garnet solid electrolyte (LLZO, LLTO), and the NASICON type of ceramics—is also essentially focused on the electrochemical properties of CPEs, which are enhanced through the elevation of Li-salt dissolution and the reduction in crystallinity. The lithium-ion transport pathways in CPEs, along with NMR results showing varying LLZO content, are depicted in (Figure 9(c1–c3)) [169–174]. However, while using active fillers improves ionic conductivity, using passive fillers increases the mechanical strength and thermal stability and, thus, the safety and stability of SSLBs [175–177].

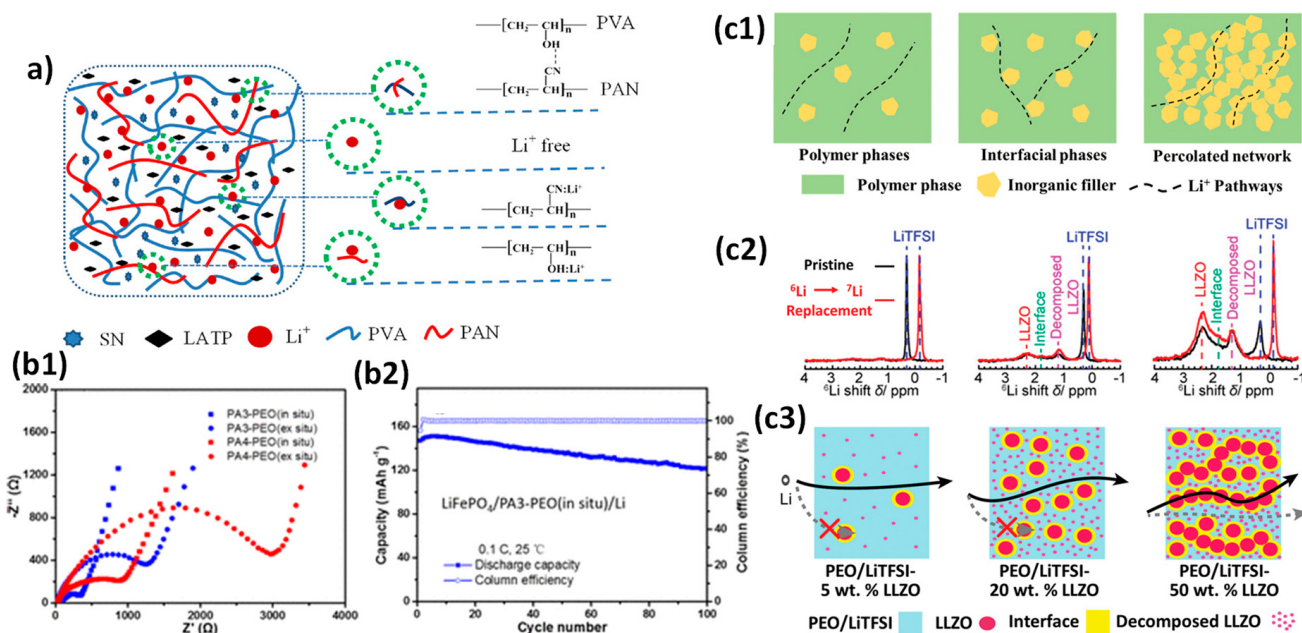


Figure 9. (a) Interactions between PVA, PAN, LiTFSI, LATP, and SN. Adapted with permission from [178]. Copyright 2020, American Chemical Society. (c1) Lithium-ion transport pathways in CPEs. (c2) ⁶Li NMR spectra for pristine and cycled PEO/LiTFSI-based CPEs with varying LLZO contents. (c3) Lithium-ion pathways in PEO/LiTFSI with different LLZO concentrations. Adopted with permission from [174]. Copyright 2018, American Chemical Society. (b1) ESI results. (b2) Cycling performance of LiFePO₄/PA₃-PEO (in situ)/Li cells at 25 °C. Adapted with permission from [179]. Copyright 2019, American Chemical Society.

The performance metrics of CPEs indicate their potential as promising candidates for ASSLBs. CPEs have been shown in many studies to develop high ionic conductivity; some results are as high as 2.21×10^{-5} Scm⁻¹ at room temperature in specific CPE designs (Figure 9(b1,b2)) [179,180]. In addition, the mechanical properties of CPEs have also been enhanced concerning tensile strength, reaching values over 9.5 MPa and improving reliability during the battery's charge and discharge [78,178]. So many optimal parameters regarding the electrical performance of CPEs have been attained with adequate cycling stability and capacity retention; some CPE samples have been shown to retain 98% or more capacity after 30 cycles. On the whole, understanding the issues related to the use of dendrite metal in secondary batteries, as well as interfacial stability and other issues, leads to the resolution of newer problems connected with energy storage devices with higher safety and improved overall performance. Latest developments in CPEs is summarized in Table 4.

Table 4. Overview of recent developments in CPEs.

Monomer	Activator	Lithium Salt	Ionic Conductivities (Scm ⁻¹) at Temperature (°C)	Lithium-Ion Transference Number (t_{Li^+})	ESW (V vs. Li/Li ⁺)	Discharge Specific Capacity (mAh g ⁻¹)	Capacity Retention (%/Cycle)	Reference
PEO	SiO ₂ , Al ₂ O ₃ , and LLZTO	LiTFSI LiClO ₄	4.42×10^{-4} at 55	0.72	5	118.6/0.1 C	99/750	[169]
PEO-SiO ₂	SiO ₂ , NASICON	LiCl ₄ LiTFSI	4.4×10^{-5} at 30 1.2×10^{-5} at 60	-	5.5	-	-	[170]
PEO-LLZTO	LATP, LLTO, and LLZO	LiTFSI	2.1×10^{-4} at 30	0.75	5.3	130/4 C	98/120	[171]

Table 4. Cont.

Monomer	Activator	Lithium Salt	Ionic Conductivities (Scm ⁻¹) at Temperature (°C)	Lithium-Ion Transference Number (t _{Li+})	ESW (V vs. Li/Li ⁺)	Discharge Specific Capacity (mAh g ⁻¹)	Capacity Retention (%/Cycle)	Reference
PEGDA	LATP, LLTO, and LLZO	LiTFSI	0.52 × 10 ⁻⁴ at RT	0.58	5	155/0.1 C	87/100	[172]
PVDF-CPE	LLTO	-	5.3 × 10 ⁻⁴ at 25 and increases to 1.42 × 10 ⁻³ at 80	-	5.1	121/1 C	99/100	[173]
PEO/LiTFSI-5 wt% PEO/LiTFSI-25 wt% LSGM CPE with LATP Nanoparticles Aligned Nanowires CPE PEO/LiTFSI-AAO CPE (ACPE)	-	LiTFSI	1 × 10 ⁻⁴ at 30 1 × 10 ⁻⁴ at 30 2 × 10 ⁻⁴ at RT 1.26 × 10 ⁻⁴ at 30 1.79 × 10 ⁻⁴ at 30	0.21 to 0.54	4.5	-	-	[175]
PEO-LiClO ₄ -Al ₂ O ₃ PEO-LiClO ₄ -TiO ₂	Al ₂ O ₃ , and TiO ₂	LiClO ₄	10 ⁻⁴ at 50 and 10 ⁻⁵ at 30 1.40 × 10 ⁻⁴ at 30	-	-	-	-	[176]
PEO-EC PMMA-based matrices	PF55, and AlCl33	-	10 ⁻³ 6.2 × 10 ⁻³	0.76 0.77	4.8	300	-	[177]
PEO-LAGP PEO-TiO ₂	TiO ₂ , LATP, or LAGP	LiTFSILiClO ₄	6.76 × 10 ⁻⁴ at 60 1.40 × 10 ⁻⁴ at 30	0.61	5	130	90/50	[180]
Poly(ethoxylated trimethylolpropane triacrylate) (PA3)	2-hydroxy-2-methyl-1-phenyl-1-propanone (HMPP)	-	2.21 × 10 ⁻⁵ at 25	-	4.7	147	82/100	[179]
PVA and PAN	Succinonitrile (SN)	LiPFSI	1.13 × 10 ⁻⁴ at 25	0.507	5.1	159.6/0.1	90.5/100	[178]
Polyimide	-	LiPFSI	2.3 × 10 ⁻⁴ at 30	-	-	176/10 C 156/5 C 138/2 C, and 125/1 C	-	[78]

3.4. Sustainable and Environmentally Friendly Polymers

Biopolymer electrolytes are considered an attractive, eco-friendly alternative to SSBs because they are derived from natural sources to enhance material costs and mitigate safety concerns. Blending biopolymers such as chitosan, pectin, and cassava starch with different lithium salts led to the advancement of ionic conductivity, thermal stability, and mechanical properties of SPEs. While different chitosan-lignocellulose composites have been investigated, ionic conductivities of up to 2.89 mS cm⁻¹ have been shown to point out the role of bio-based materials for scalable solutions for the purpose of meeting increased energy storage demands [181–185]. In this regard, cassava starch in its biodegradable form is used in an environmentally friendly way to enhance the physicochemical properties of the electrolytes themselves within Li⁺-ion battery systems. In the case of cassava starch electrolytes, they have been further improved by adding lithium salts like LiCl and Li₂SO₄, attaining values as high as 9.54 × 10⁻³ Scm⁻¹. The structure of the lignocellulosic matrix of chitosan is illustrated in Figure 10a. The P(HB-HV)-based gel electrolyte shows significant improvements in ionic conductivity and thermal stability, with conductivity increasing as temperature rises, outperforming typical liquid electrolytes. It maintains stable conductivity over time, with enhanced crystallization and melting temperatures due to crosslinking (Figure 10(b1,b2,c)) [186].

The performance parameters of the bio-polymer electrolyte unveil its potential and survivability in severe battery conditions. For example, a gel polymer electrolyte prepared from P3HB-3HV has exhibited ionic conductivity of over 8 × 10⁻⁴ Scm⁻¹ with thermal stability at high temperatures. Cycling stability and capacity retention are critical factors

for practical applications of SPEs. It is to be noted that the lignin-derived graft polymers not only improve the cycling performance, but also reduce the overall resistance in lithium metal batteries, displaying more than 99% capacity retention in 100 cycles. The type of lithium salt influences the electrochemical kinetics and molecular structure in the biopolymer matrix. LMBs using LPGP10 as the solid polymer electrolyte and LPG as the binder have demonstrated excellent long-term cycling performance, retaining 98% of their discharge capacity after 50 cycles, with reduced interfacial resistance and improved overall cycling stability (Figure 10(d1–d5)). That means that these studies predict a much-improved performance and safety for the solid-state batteries using bio-polymer electrolytes that will further the next-generation energy storage technologies [181–190]. The key findings from recent studies on bio-polymer electrolytes are summarized in Table 5.

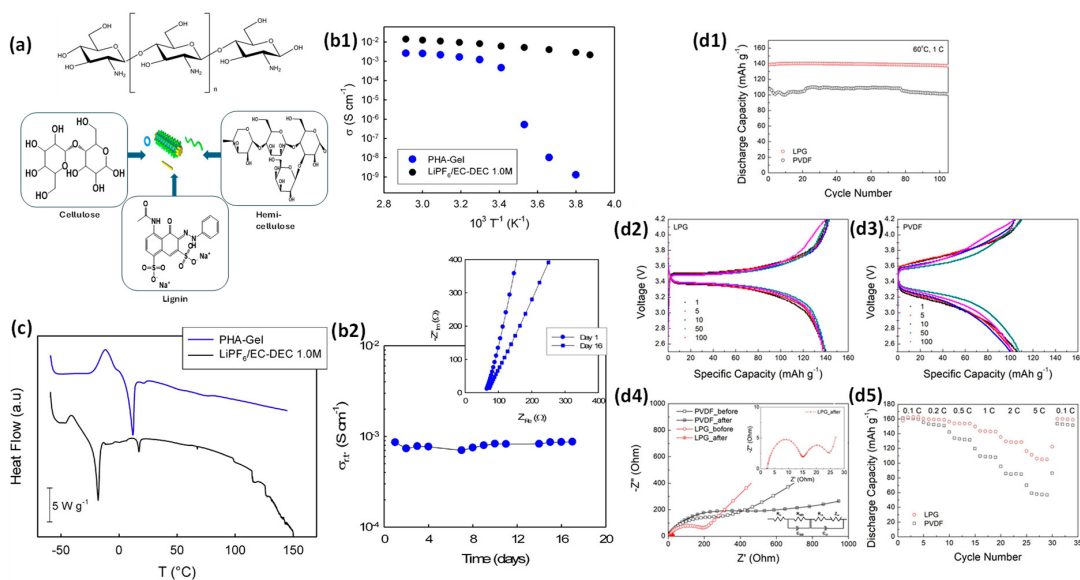


Figure 10. (a) Structure of the lignocellulosic matrix of chitosan. (b1) Conductivity of the P(HB-HV)-based GPE (blue circles) versus 1.0 M LiPF₆-EC/DEC (black circles) as a function of temperature. (b2) Conductivity changes over time for the P(HB-HV) gel electrolyte (blue circles). Adapted with permission from [186]. Copyright 2.017, Elsevier. (c) DSC thermograms of the P(HB-HV) gel electrolyte (blue line) and the commercial 1.0 M LiPF₆-EC/DEC solution (black line). Adapted with permission from [186]. Copyright 2017, Elsevier. (d1) Long-term cycling performance of a Li/Celgard/LiFePO₄ cell at 60 °C, 1C, with LPG or PVDF as the binder. (d2,d3) Voltage-capacity profiles at 1C for cells using LPG and PVDF binders. (d4) Electrochemical impedance spectra before and after 100 cycles at 60 °C, 1C. (d5) Rate capability of cells at 60 °C across various current rates. Adapted with permission from [181]. Copyright 2020, Wiley-VCH Verlag GmbH & Co. KGaA, Weinheim.

Table 5. Overview of results from recent studies on bio-polymer electrolytes.

Monomer	Solvent	Activator	Li ⁺ Salt	Ionic Conductivities (S cm ⁻¹)	Lithium-Ion Transference Number (t_{Li^+})	ESW (V vs. Li/Li ⁺)	Discharge Specific Capacity (mAh g ⁻¹)	Capacity Retention (%/Cycle)	Reference
PPEGMA	ILs	2-bromopropionyl bromide	LiTFSI	8×10^{-5} at 30	-	4.9	140	99/450	[182]
PEO	-	MPEG@LLZTO nanofillers	LiTFSI	1.13×10^{-3} at 55	0.56	-	153.6	92.5/200	[183]
Chitosan and PEO	-	A small amount of LEs	LiTFSI	6.8×10^{-4} at RT	0.74	5	120	-	[191]
Chitosan-lignocellulose composites	-	Plasticizer	LiTFSI	2.89×10^{-3} at RT	0.9	4.8	163.13/0.2 C 152.53/0.5 C 128.45/2 C, and 156.12/0.2 C	161.9 mAh g ⁻¹ /99	[185]

Table 5. Cont.

Monomer	Solvent	Activator	Li^+ Salt	Ionic Conductivities (Scm^{-1})	Lithium-Ion Transference Number (t_{Li^+})	ESW (V vs. Li/Li^+)	Discharge Specific Capacity (mAh g^{-1})	Capacity Retention (%/Cycle)	Reference
PCL	50 wt% glacial acetic acid	Plasticizer	LiTFSI	1.52×10^{-3} at 50	-	5	155/0.05 C	-	[187]
Pectin	-	-	LiClO ₄	5.15×10^{-5} at RT	0.92	-	-	-	[188]
Pectin	Distilled water	EC	LiTFSI	2.43×10^{-4} at RT	-	-	-	-	[189]
Lignin-derived graft polymer (LGP)	THF	PEGDE	LiTFSI	3.33×10^{-3} at 30	-	5	-	98/50	[181]
Cassava starch	-	Li_2SO_4 , LiCl , and CF_3LiSO_3	Li_2SO_4 , LiCl , and CF_3LiSO_3	9.54×10^{-3} at RT	-	-	-	-	[190]
Poly(3-hydroxybutyrate-co-3-hydroxyvalerate) (P3HB-3HV)	EC, and DEC	-	LiPF ₆	8×10^{-4} at RT	-	5	100/3 C	91/20	[186]

4. Synthesis and Performance of PEs

4.1. In Situ Polymerization

In situ polymerization has become a potential method for synthesizing PEs in SSBs, allowing for much-improved interfacial contact and higher efficiency in ionic transport. Generally, the precursor solution contains monomers, Li-salts, and initiators subjected to thermal or photopolymerization. For example, 1,3-dioxolane, using LiTFSI, has shown an ionic conductivity of $1.74 \times 10^{-4} \text{ Scm}^{-1}$. This formulation resulted in excellent capacity retention of 91.9% after 200 cycles (Figure 11a), showing the increase in performance of the batteries by using this method [192]. In addition, PEO and NaFSI improved due to 1% Al_2O_3 nanoparticles, exhibiting an ionic conductivity of $9.52 \times 10^{-4} \text{ Scm}^{-1}$ at 80 °C with a high-capacity retention of 92.8% after 2000 cycles, which exemplifies the improvement in ion transport provided by inorganic fillers [193]. Meanwhile, the CPE-PHCE prepared from PEGMA and LiFSI had a conductivity of $1.2 \times 10^{-4} \text{ Scm}^{-1}$ at RT and enhanced electrochemical performance with a critical current density of 4.5 mA cm^{-2} [194].

This method has the advantage of offering varieties that can optimize the polymer structure for performance in SSBs. Then, the Li/LiCoO₂ tested at 4.2 V showed reduced interfacial resistance, and the capacity retention was 80% after 500 cycles at 0.5 C for the Poly-DOL-40FEC-HDI electrolyte (Figure 11b) [195]. A hybrid crosslinked PE reached an ionic conductivity as high as $2.22 \times 10^{-3} \text{ Scm}^{-1}$ at 30 °C, where a Li^+ transference number (t_{Li^+}) of 0.88 enabled the stable cycling of lithium stripping/plating for more than 1000 h at 1 mAc m^{-2} (Figure 11(c1–c3)) [196]. For example, ring-opening polymerization was employed to create a three-dimensional crosslinking network; the polymer electrolytes had an ionic conductivity of 0.1 mS cm^{-1} with improved thermal stability [197]. In the work, catalyst yttrium-stabilized zirconia (YSZ) was used to improve the ionic conductivity of the composite solid electrolyte to $2.75 \times 10^{-4} \text{ Scm}^{-1}$ [198]. Another work reported a high ionic conductivity of $1.17 \times 10^{-3} \text{ Scm}^{-1}$ due to in situ thermal polymerization in a LAGP framework, which ensured minimal electrolyte leakage [199]. Overall, these works highlight the vital progress of performance and stability achieved by the in situ polymerization method, underscoring its potentially enabling role in high-performance solid-state batteries [200]. Table 6 provides an overview of the ionic conductivity and properties of various PEs developed through in-situ polymerization.

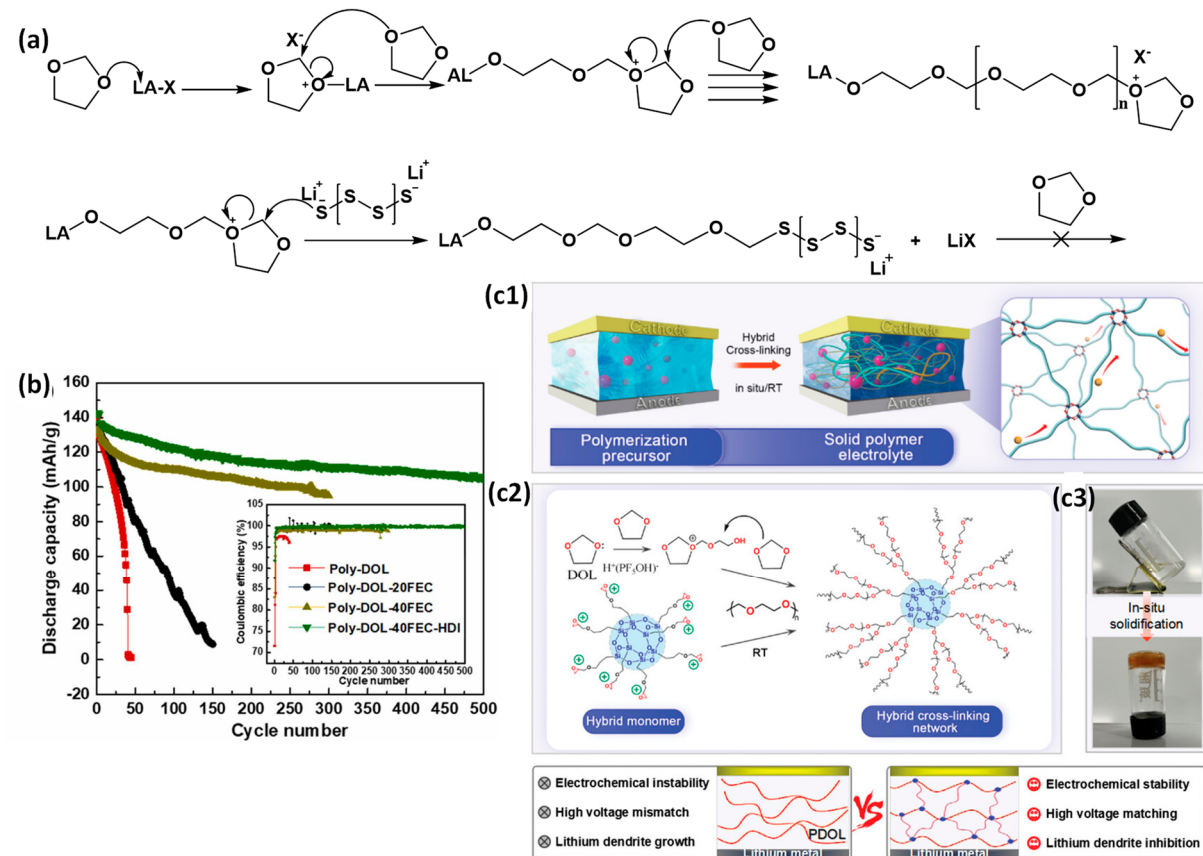


Figure 11. (a) Synthesis of 1,3-dioxolane (DOL) initiated by a Lewis acid (LA). (b) Cycling performance of Li/LiCoO₂ cells using different in situ PEs. Adapted with permission from [195]. Copyright 2021, Elsevier. (c1) Schematic of a hybrid crosslinked SPE made through in situ polymerization. (c2) Illustration of the polymerization process for hybrid crosslinked polymer electrolytes (HCPES). (c3) Image showing the solidification of liquid precursors into SPE. Adapted with permission from [196]. Copyright 2023, Wiley-VCH GmbH.

Table 6. Summary of PEs and their corresponding ionic conductivity values.

Monomer	Li ⁺ Salt	Solvent	Condition (°C)	Ionic Conductivity (S cm ⁻¹)	Lithium-Ion Transference Number (tLi ⁺)	Reference
DEGDA	LiTFSI	Ethylene carbonate (EC)/Diethyl carbonate (DEC)	60	0.141 × 10 ⁻³	0.45	[201]
PEGMA	LiTFSI, LISFI	-	60	0.07 × 10 ⁻³	0.28	[202]
	LiTFSI	-	40/60	0.02 × 10 ⁻³	0.28	[203]
PEGMEA	LiTFSI	Dimethyl carbonate (DMC)/1,2-dimethoxyethane (DME)	60	0.17 × 10 ⁻³	0.47	[204]
	LiTFSI, LiPF6	EC/DMC/Ethyl methyl carbonate(EMC)	60	0.17 × 10 ⁻³	0.42	[205]
VEC	LiTFSI	-	80	1.10 × 10 ⁻³	0.58	[206]
MMA	LiPF6	EC/DEC	70	1 × 10 ⁻³	-	[207]
PEGDA	LiTFSI	-	70	0.14 × 10 ⁻³	0.26	[208]
DOL	LiPF6	MP	-	2.80 × 10 ⁻³	0.61	[209]
DOL	LiTFSI	-	60	2.47 × 10 ⁻³	0.43	[210]
DOL	LiTFSI, LiSF6	DME	-	2.22 × 10 ⁻³	0.88	[196]

Table 6. Cont.

Monomer	Li ⁺ Salt	Solvent	Condition (°C)	Ionic Conductivity (Scm ⁻¹)	Lithium-Ion Transference Number (tLi ⁺)	Reference
Multiple monomers						
DOL, VC	LiTFSI	-	60	1.98×10^{-3}	0.5	[211]
EGDMA/EDT	LiTFSI	-	-	0.03×10^{-3}	0.45	[212]
PEGMEA/Vinylene carbonate	LiTFSI	EC/DMC/DEC	-	0.22×10^{-3}	0.5	[213]
G1S (Glyme-Functionalized Episulfide Monomer)/SGxS (Crosslinking Episulfide)	LiTFSI	DME/DOL	25/60	9.9×10^{-3} Scm ⁻¹ for 20% G1S to 2.9×10^{-3} S cm ⁻¹ for 60%	-	[214]

4.2. Graft Polymerization

The graft polymerization method has shown considerable promise in enhancing the electrochemical performance of PEs for SSBs. Through the strategic attachment of functional side chains to a polymer backbone, researchers have significantly improved ionic conductivity and mechanical properties (Figure 12a,b). For instance, the synthesized polyrotaxane-based polymer electrolyte demonstrates an impressive ionic conductivity of 8.30×10^{-4} Scm⁻¹, showcasing effective ion transport facilitated by lithium salts as well as improved thermal stability and mechanical strength [215]. Another study highlighted an SPE that achieved an ionic conductivity of 0.1 mScm⁻¹ at room temperature, complemented by a high t_{Li⁺} of 0.72, which resulted in stable battery cycling performance even under elevated temperatures [216]. Furthermore, various graft copolymers, such as PHEMA-g-PCL, achieved ionic conductivities of 4.17×10^{-5} Scm⁻¹ at 30 °C, demonstrating superior electrochemical stability and efficient ion transport capabilities [217].

Moreover, innovative formulations like PVNB have yielded ionic conductivities as high as 9.24×10^{-4} Scm⁻¹, with a t_{Li⁺} of 0.86, thereby enhancing the safety and cyclability of LMBs [218]. Other studies have reported ionic conductivities exceeding 10^{-5} S cm⁻¹ at RT for polymer-in-ceramic nanocomposite electrolytes, further emphasizing the benefits of graft polymerization [219]. The combination of effective ionic conduction and enhanced mechanical properties has also been observed in single-ion conductor gel PEs, with a high transference number of 0.97 indicating efficient lithium-ion conduction [220]. Other grafted polymers have also demonstrated improved specific capacitance and energy density in electric double-layer capacitors, showcasing their versatility in energy storage applications [221]. Overall, the application of graft polymerization in the synthesis of PEs has led to substantial advancements in electrochemical performance, representing a significant advancement in developing efficient SSBs (Figure 12(c3–c6)) (Table 7).

Table 7. Recent findings regarding graft PEs.

Monomer	Solvent	Salt	Ionic Conductivity (Scm ⁻¹) at Temperature (°C)	Lithium-Ion Transference Number (t _{Li⁺})	ESW (V vs. Li/Li ⁺)	Discharge Specific Capacity (mAh g ⁻¹)	Capacity Retention (%/Cycle)	Reference
PEG, α -CD	DMF	LiTFSI	8.30×10^{-4} at RT	0.51	-	132.1	99.02/100 78.8/500	[218]
LiDMPA	-	LiTFSI	0.1×10^{-3} at 25	0.72	5	161.1, 86.7, and 54.5 (80, 40, and 25 °C)	98.8/100	[216]
Hydroxyethyl Methacrylate (HEMA), ε -caprolactone	-	-	4.17×10^{-5} at 30	0.74	-	-	-	[217]

Table 7. Cont.

Monomer	Solvent	Salt	Ionic Conductivity (Scm^{-1}) at Temperature ($^{\circ}\text{C}$)	Lithium-Ion Transference Number (t_{Li^+})	ESW (V vs. Li/Li $^{+}$)	Discharge Specific Capacity (mAh g^{-1})	Capacity Retention (%/Cycle)	Reference
PVBN-Organoboron-modified-PEGMA	DMSO	LiTFSI	9.24×10^{-4} at RT	0.86	5	91.4/8 C	90.1/1000	[218]
PEO	Dry ACN	LiTFSI	3.4×10^{-4} at 70	-	-	130/40 120/50	99.5%	[220]
AMPS	EC, and DMC	LiOH.H ₂ O	3.4×10^{-5} at 30	0.97	-	150/0.1 C	99.7/100	[220]
ACN	THF, and MeCN	LiTFSI	1.1×10^{-6} at RT	~0.03	2.7	-	-	[222]
PEO	DMF	LiTFSI	3.1×10^{-5} at 25	0.72	4.97	141.2/0.1 C Highest	85.4/300	[223]
PEGMA	-	LiTFSI	1.82×10^{-5}	0.81	-	142.7/1 C 104.6/2 C	80.3/300	[224]
PLiSSPSI	SiO ₂ NPs	LiTFSI	0.22×10^{-3} at 60	0.77	5.6	140/0.1 C 139/0.2 C 132/0.5 C 121/1 C	80/130	[225]

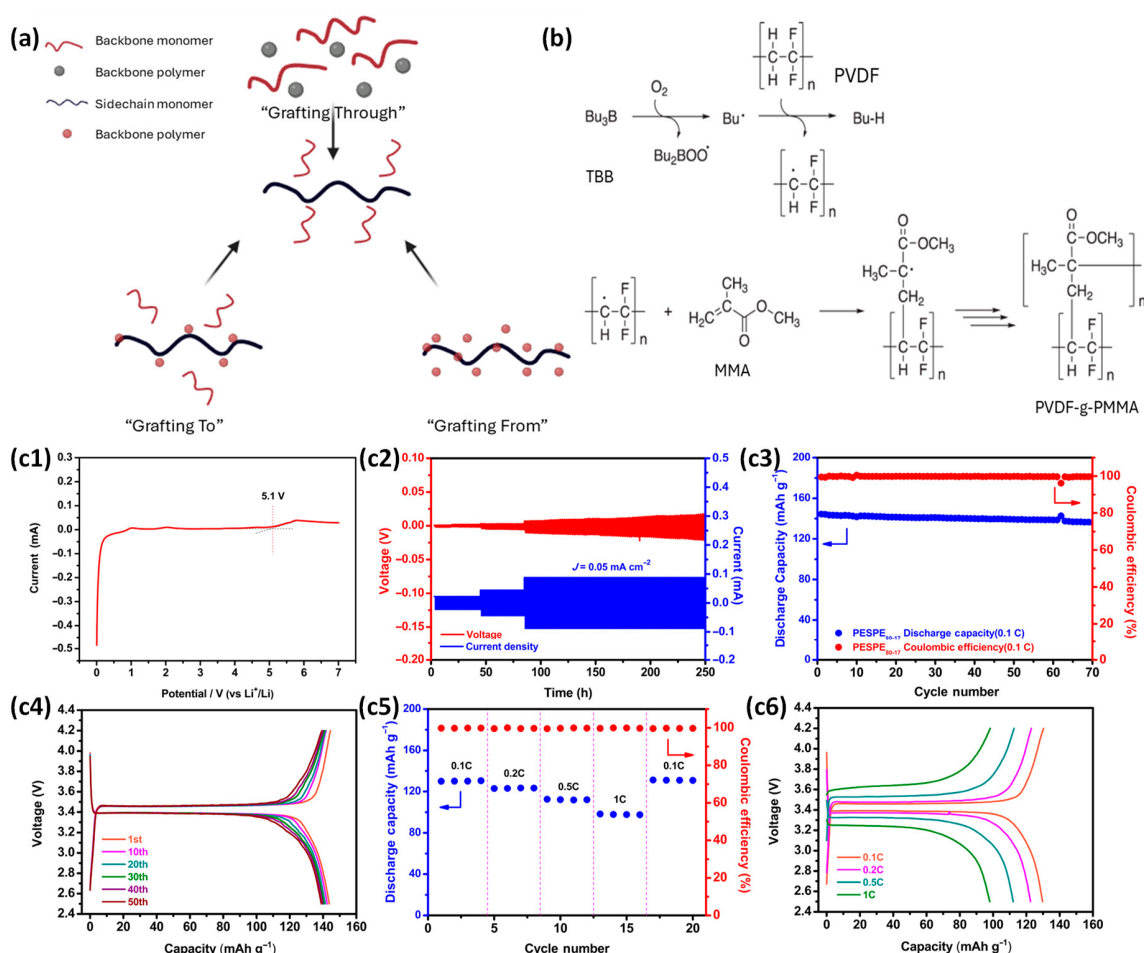


Figure 12. (a) Methods for graft copolymer synthesis: grafting through, grafting from, and grafting to. (b) Graft polymerization of methyl methacrylate on poly (vinylidene fluoride) using tributylborane as the initiator. (c) Electrochemical performance of PESPE80-17: (c1) LSV, (c2) galvanostatic cycling, (c3) long-term cycling, (c4) charge–discharge curves, (c5) performance at varying rates, and (c6) charge–discharge at 0.1 C, 0.2 C, 0.5 C, and 1 C for Li/PESPE80-17/LiFePO₄ cells at 30 °C. Adapted with permission from [217]. Copyright 2021, Chinese Chemical Society.

4.3. Electrospinning Method

Electrospinning is a versatile technique for the fabrication of CPEs, which play the most important role in enhancing the performance of LIBs. The process of electrospinning produces 1D nanostructures like nanofibers that change in solution properties, and electrospinning parameters can be optimized. Figure 13(a1,a2) provides a schematic representation of the electrospinning process, illustrating how polymer solutions are drawn into fibers to create nanostructures. Specifically, CPEs based on a three-dimensional framework of polyimide nanofibers have shown better ionic conductivity of $2.64 \times 10^{-4} \text{ Scm}^{-1}$ and mechanical strength, which affords a stable ESW of 4.6 V and effectively suppresses the growth of lithium dendrites. This new strategy significantly improved the electrochemical performance of the full cells. This can be proven by the $\text{LiCoO}_2 \mid \text{PI-CPE} \mid \text{Li}$ full cell, whose initial discharge capacity is 131.1 mAhg^{-1} and capacity retention rate is 83.3% after 120 cycles (Figure 13b). In addition, the lithiated 2-Acrylamido-2-methylpropanesulfonic acid (AMPS)-grafted PVDF-HFP for the fabrication of porous membranes via the electrospinning process resulted in solid electrolytes with an ionic conductivity of $5.4 \times 10^{-5} \text{ Scm}^{-1}$ at 60°C [226,227]. Several other reports have also evidently suggested that nanofibers produced via electrospinning are crucial for the optimization of the properties of PEs toward next-generation LIBs.

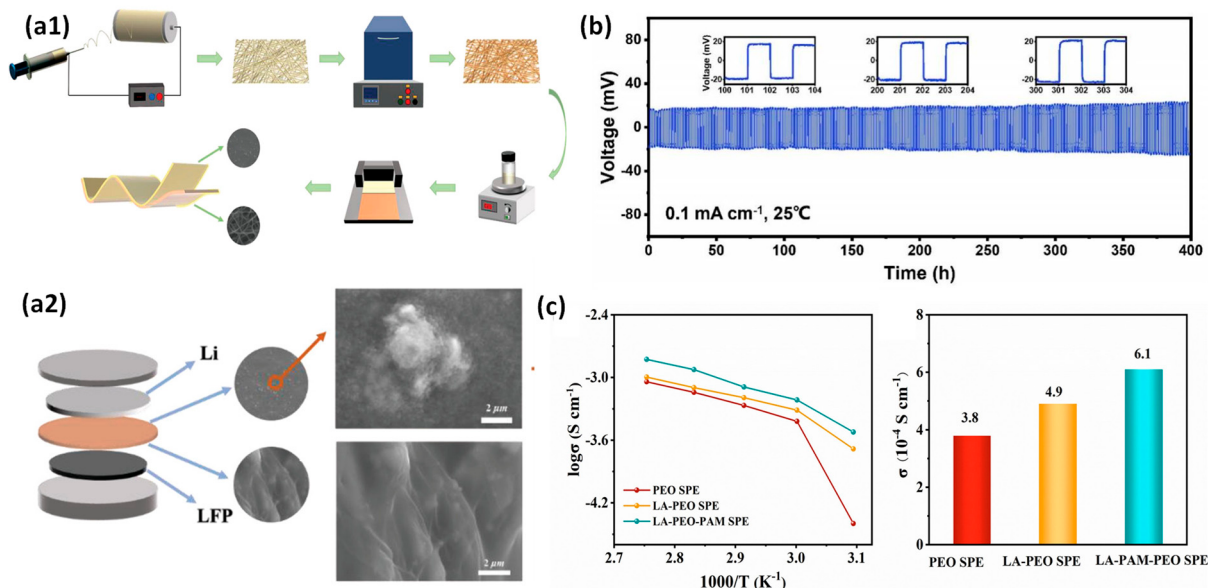


Figure 13. (a1) Schematic representation of the electrospinning process. (a2) Diagram showing the composite electrolyte structure with one side in contact with Li metal and the other with LFP. Adapted with permission from [228]. Copyright 2021, Wiley-VCH GmbH. (b) Cycling performance of the $\text{Li} \mid \text{PI-CPE} \mid \text{Li}$ symmetric cell [226]. (c) Comparison of ionic conductivity for PEO, LA-PEO, and LA-PAM-PEO fiber membranes. Adapted with permission from [229]. Copyright 2024, by Elsevier.

Besides providing improved ionic conduction, the electrospinning method offers immense mechanical stability and cycling performance that is very vital to the reliability of SSBs. For instance, the inclusion of LATTP into a PVdF-HFP matrix led to a composite polymer electrolyte CPE-8 that showed an impressive ionic conductivity of $1.9 \times 10^{-3} \text{ Scm}^{-1}$ at room temperature [230]. Similarly, in the case of a combination of lactic acid, polyacrylamide, and polyethylene oxide, an SPE was obtained that showed a wide ESW of 4.95 V and had a discharge-specific capacity of 135 mAh g^{-1} after 1000 cycles. A comparison of ionic conductivity for PEO, LA-PEO, and LA-PAM-PEO fiber membranes also demonstrated the improved performance of these modified materials (Figure 13c) [229]. Different studies have shown that electrospinning not only can produce high-performance CPEs, but also may be used to tailor mechanical and electrochemical properties for advanced

energy storage applications. Such a new synthesis route holds great promise for the future in SSLMBs, where stability and efficiency during operational conditions need to be ensured. Table 8 highlights the performance metrics of electrospun of PEs in SSBs.

Table 8. Key properties and performance metrics of PEs in SSBs via electrospinning.

Monomer	Solvent	Salt	Ionic Conductivity (Scm^{-1}) at Temperature ($^{\circ}\text{C}$)	Lithium-Ion Transference Number (t_{Li^+})	ESW (V vs. Li/Li $^{+}$)	Discharge Specific Capacity (mAh g^{-1})	Capacity Retention (%/Cycle)	Reference
ODA and PMDA	DMAC	LiTFSI	2.64×10^{-4} at RT	0.76	5.2	131.1	83.3/120/0.2 C	[226]
PVDF-HFP	DMF		5.4×10^{-5} at 60	0.96	-	-	-	[227]
PCL	THF	LiTFSI	2.5×10^{-5} at 25 and 1.6×10^{-4} at 55	-	4.6	136.5	81.6/120	[231]
PEO	ACN	LiTFSI	6.82×10^{-5} at 30	-	-	161.1	Long cycle around 1000 h	
PVDF-HFP	DMF	LiTFSI	8.94×10^{-4} at RT	-	5.2	131	98.7	[232]
PVDF-HFP	DMF	LATTP	1.9×10^{-3} at 30	-	5	130	100/200	[230]
PA6	ACN	LiTFSI	1.26×10^{-3} at 60	0.45	4.3	142	-	[233]
PEO	DMF	LiTFSI	9.3×10^{-4} at 50	-	-	-	96/500	[234]
PAN	DMF	LiTFSI	2.57×10^{-4} at 30	0.6	4.7	-	-	[228]
Ionene oligomer	DMF	LiTFSI	1.01×10^{-3} at 25	0.46	4.61	135-100/0.2	98.5/100	[235]
PAN	DMF	LiClO ₄	7.1×10^{-4} at RT	0.62	5.1	131.9 after 200/0.5	91.1/200	[236]
PAN	DMF	LiTFSI	-	-	-	69.6% after 300/0.3 C	70/500	[237]
Triethylene glycol dimethacrylate	DMF	LiClO ₄	1.60×10^{-3} at 25	-	4.5	110	-	[238]
LA-PAM-PEO	ACN	LiTFSI	6.1×10^{-4} at RT	0.32	4.95	135 after 1000/1 C	93.3/1000	[229]
Polymer-based nanofiber membranes	-	LiTFSI	1.06×10^{-3} at 25	0.82	4.86	99.9%-200/0.5 C	-	[191]

4.4. Sol–Gel Method

Sol–gel is the primary chemical route for synthesizing polymer electrolytes, starting from controlled nanostructures that enhance the properties of the electrolytes for SSLBs. The sol–gel route usually utilizes silane compounds with an alcohol-based solvent by dissolving Li salts. This results in high ionic conductivity at $1.4 \times 10^{-4} \text{ Scm}^{-1}$ and broad electrochemical stability up to 5.0 V. The ionic conductivities of the AP-GPEs membrane were analyzed using electrochemical impedance spectroscopy (EIS), which revealed a conductivity of $0.18 \times 10^{-3} \text{ S cm}^{-1}$ at 20°C , highlighting the need for improvements at lower temperatures (Figure 14a) [239]. The addition of flexible siloxane-based polymers, which are thermally stable, along with nano-filters like zirconia and Al-doped Li₇La₃Zr₂O₁₂, has dramatically improved ionic conduction and mechanical properties that help in the design of high-performance lithium-ion batteries (Figure 14b) [129,240,241]. Further, studies based on gelatin polymers have stated the possibilities of utilizing natural biopolymers in energy fields for sustainability. This results in enhancements in ionic conductivity and electrochromic properties. The SEM image of the sol–gel-synthesized WO₃ thin film indicated a uniform surface and a thickness of 234 nm, both crucial for its electrochromic performance (Figure 14c) [242]. When combined with spin-coating, the sol–gel method facilitates even material distribution and precise control over film thickness, making it particularly suitable for electrochromic applications. Again, using nanoparticles based on cerium–zirconium oxide enhanced lithium-ion transport, improving cycle stability and overall performance [243].

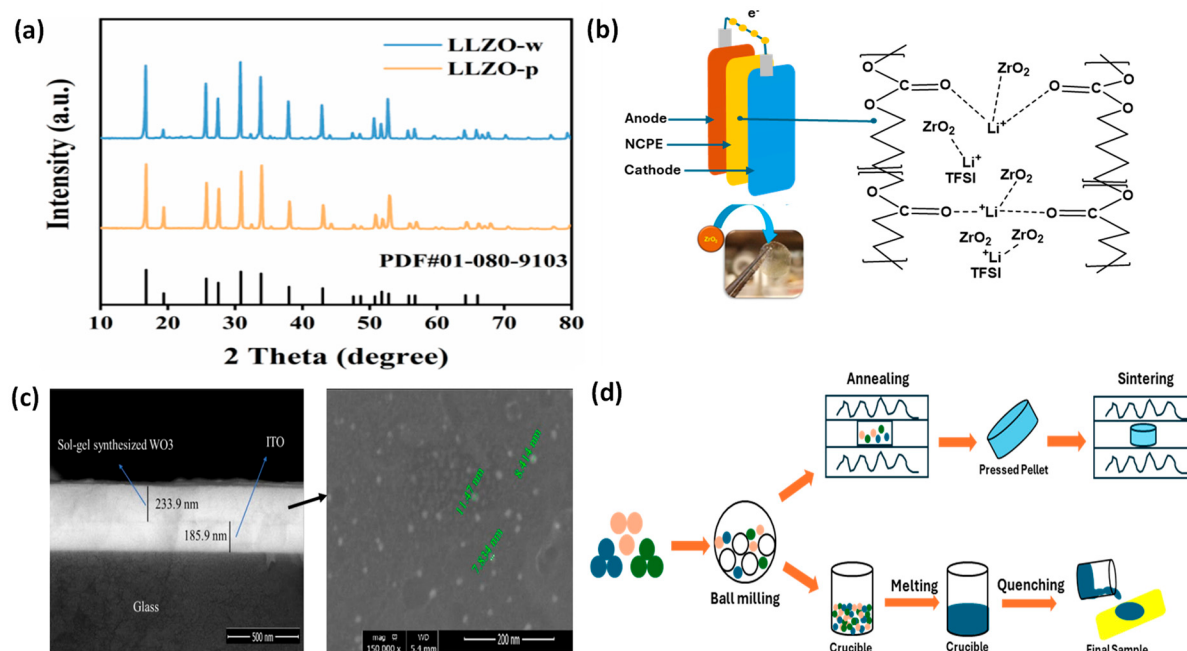


Figure 14. (a) Electrochemical impedance spectroscopy (EIS) profiles for the AP-GPEs membrane at various temperatures. Adapted with permission from [239]. Copyright 2023, Wiley-VCH GmbH. (b) Structure of the polymer electrolyte (NCPE) incorporating zirconia nanoparticles. (c) SEM image showcasing the cross-section of glass/ITO/WO₃, along with the backscattered surface morphology of a sol–gel-synthesized WO₃ thin film. Adapted with permission from [242]. Copyright 2020, Wiley Periodicals LLC. (d) Diagrams illustrating solid-state synthesis methods for NaSICON-type lithium-ion conductors: Solid-state reaction and melt quenching.

Figure 14d illustrates solid-state synthesis methods for NaSICON-type lithium-ion conductors, which enhance ionic conductivity. Recent works prove that the sol–gel route is also very effective for preparing flame-retardant GPEs for Na-ion batteries, with high ionic conductivity of up to 0.91 mScm^{-1} and good cycling stability [244,245]. The role of the filler, such as $\text{Na}_3\text{Zr}_2\text{Si}_2\text{PO}_{12}$, was also critical to improving the ionic conductivity of GPEs up to $2.83 \times 10^{-3} \text{ S cm}^{-1}$ [246]. Novel monomers, like ethoxylated trimethylolpropane triacrylate, have offered better interfacial compatibility with sodium metal anodes and impeded dendrite growth, improving battery performances. Furthermore, the sol–gel method has overcome major concerns about conventional liquid electrolyte safety issues by providing high-purity and controlled composition materials and significantly improved electrochemical properties for high-performance energy storage applications [238,247–250]. In general, the flexibility and efficiency of the sol–gel process are key components in optimizing the performance of electrolytes while encouraging both lithium-ion and sodium-ion battery technologies. Table 9 provides the performance of PEs from recent studies.

Table 9. Performance metrics of various PEs reported by the sol–gel method in recent studies.

Monomer	Solvent	Salt	Ionic Conductivity (Scm^{-1}) at Temperature ($^{\circ}\text{C}$)	Lithium-Ion Transference Number ($t_{\text{Li}^{+}}$)	ESW (V vs. Li/Li^{+})	Discharge Specific Capacity (mAh g^{-1})	Capacity Retention (%/Cycle)	Reference
PEG	-	LiSO_3CF_3	1.4×10^{-4} at 30	-	5	148	94.9/50	[129]
PVDF-HEP with poly(methylmethacrylate) grafted natural rubber (MG49)	-	LiBF_4	2.39×10^{-3} at 30	0.103–0.216	6.9	212 (1st Cycle) 206 (2nd cycle)	98/10	[240]
PEO	-	LiTFSI	4.69×10^{-4} at 25	0.451	5.6	130	89/200	[241]

Table 9. Cont.

Monomer	Solvent	Salt	Ionic Conductivity (Scm^{-1}) at Temperature ($^{\circ}\text{C}$)	Lithium-Ion Transference Number (t_{Li^+})	ESW (V vs. Li/Li $^{+}$)	Discharge Specific Capacity (mAh g $^{-1}$)	Capacity Retention (%/Cycle)	Reference
Gelatin	Formic acid: Acetic acid (1:1)	LiClO ₄	2.25×10^{-7} at 25	-	-	-	-	[242]
PEO	-	LiTFSI	7.3×10^{-5} at 25	0.42	-	150.2/1 C	80	[243]
PEGMA	TEP	NaTFSI	0.91×10^{-3} at RT	0.24 (tNa $^{+}$)	4.8	105.3/0.1 C	91/400	[244]
PEO	-	Na ₃ Zr ₂ Si ₂ PO ₁₂	2.83×10^{-3} at RT	0.33 (tNa $^{+}$)	5.16	92.7/0.5 C	99.2/100	[245]
MMA	Py ₁₃ TFSI	LiTFSI			4.3	146.7/0.1 C 143.3/0.2 C 117.8/0.5 C 105/1 C, and 143.5/0.1 C after cycling.	99.6/70	[246]
PVDF-HFP	TEP, and FEC	LiTFSI	0.42×10^{-3} at 20	-	-	93.3/5 C	87.3/600	[239]
PAN	-	LiPF ₆	1.6×10^{-3} at 25	0.5	4.5	110	-	[238]
VC	-	LiDFOB	1.06×10^{-3} at 25	0.82	4.86	170.7/0.1	99.9/200	[191]
ETPTA	-	NaClO ₄	1.2 to 1.8×10^{-3} at 80	-	4.7	101/1 C	97/1000	[247]
PVDF-HEP	-	LiTFSI	2.14×10^{-4} at RT	-	3–6	103.8/0.1 C	98/50	[248]
Poly(ϵ -caprolactone-co-trimethylene carbonate) (P(CL 80 TMC 20))	ACN	LiTFSI	>10 $^{-5}$ at RT	0.83–0.87	-	0.2 mAh cm $^{-2}$	82/55	[249]
PVDF-HEP	DMF	LiTFSI	4.33×10^{-5} at RT	0.49	0–5.5	115.5/2 C	146.3 mAh g $^{-1}$ /200	[250]

4.5. Crosslinking Polymerization

Crosslinking polymerization is a process where polymer chains are chemically bonded into a three-dimensional network, enhancing the material's mechanical strength, thermal stability, and electrochemical performance. This method is widely used in solid-state batteries to enhance ionic conductivity and suppress lithium dendrite growth, resulting in safer and more efficient electrolytes. Numerous PEs have been synthesized using crosslinking polymerization, yielding improved mechanical properties, ionic conductivity, and electrochemical stability, contributing to higher performance in lithium batteries. Herein, unlike most reported SPEs obtained by radical copolymerization of the different polymers PEO, TEGDMA, and PGMA, different SPEs were obtained utilizing crosslinking, with improved safety and better performance. Those crosslinked networks effectively hinder the growth of lithium dendrites, enhancing mechanical stability and promoting a wide ESW of up to 5.38 V in some cases. In addition, preparation methods without solvent make them even more environmentally friendly and cost-effective. For example, the crosslinked poly(DOL-TTE)-LP electrolyte demonstrated improved ionic conductivity, excellent flexibility, and stable cycling performance, thus becoming suitable for flexible lithium batteries [251–254]. Figure 15a illustrates the crosslinking of DOL and TMPTGE monomers by NaPF₆ to form a gel electrolyte. Moreover, introducing poly(ethylene glycol) diglycidyl ether into GPEs for lithium–sulfur batteries exhibited enhanced ionic conductivity and mechanical strength with a suppressed polysulphide shuttle effect [255,256]. Figure 15b shows the ionic conductivity of crosslinked SPEs versus temperature, highlighting the benefits of crosslinking in enhancing ionic transport.

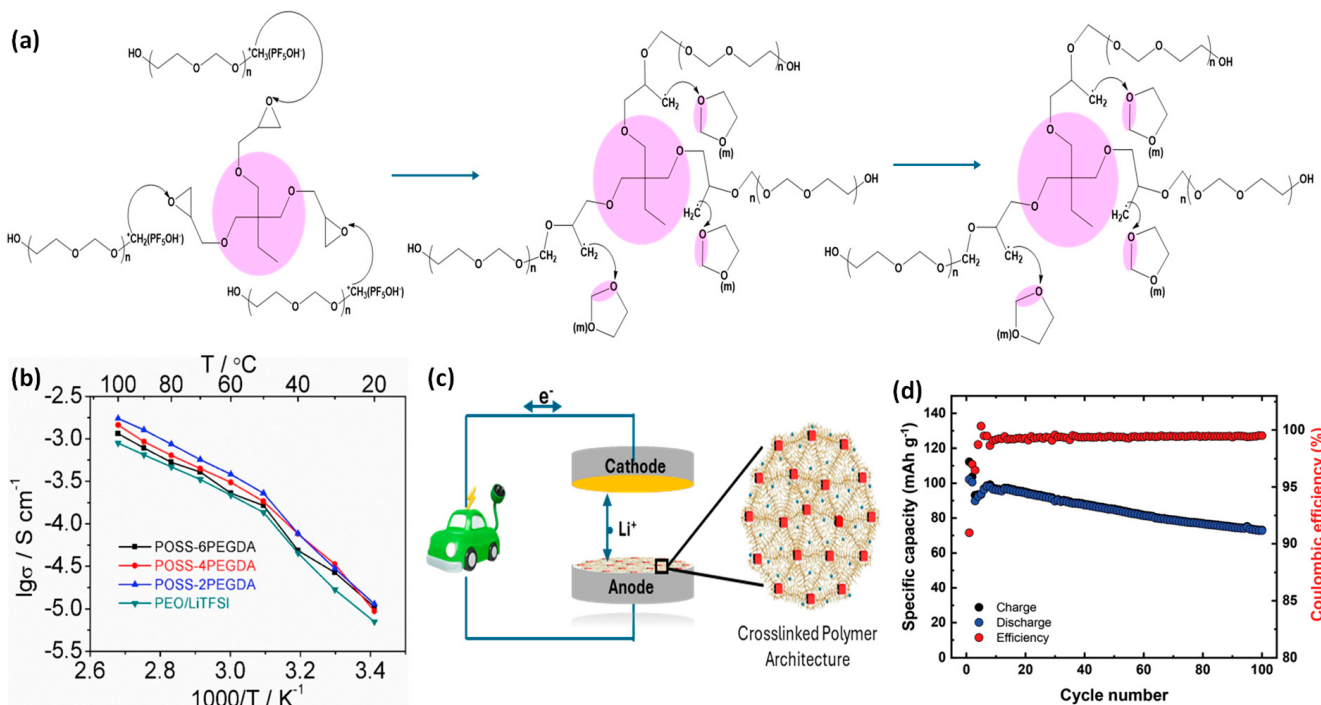


Figure 15. (a) Crosslinking of DOL and TMPTGE monomers by NaPF₆ to form the gel electrolyte. (b) Ionic conductivity of crosslinked SPEs versus temperature. Adapted with permission from [257]. Copyright 2019, Elsevier B.V. (c) Schematic of batteries with ultrathin SSE using crosslinked polymer-brush architecture. (d) Specific capacity vs. cycle number for Li/crosslinked P1 (30 wt% LiTFSI)/LiFePO₄ at 70 °C. Adapted with permission from [258]. Copyright 2021, Royal Society of Chemistry.

In this regard, various crosslinking agents, including VEC and PEGDA, were employed to illustrate the respective promises of their electrolytes in lithium metal and ASSLIBs. For example, CPEs prepared with trifunctional polyether acrylate and silica nano-resin improved ionic conductivity and long-cycling stability. Meanwhile, the double-crosslinked structures with functionalized MOFs greatly enhanced the electrochemical performance of the SSLBs with high areal capacity and capacity retention in the long run (Figure 15c) [212,257,259–263]. Further studies on self-crosslinked polymer electrolytes and polymerized ionic liquid composites have expanded the scope of crosslinking polymerization by showing improved ionic conductivity, transference numbers, and stability in high-performance battery applications [258,264–266] (Figure 15d). These advances highlight the flexibility and power of crosslinking polymerization to mitigate the key challenges in solid-state battery electrolytes: dendrite suppression, high ionic conductivity, and long-term cycling stability. Recent performance findings of PEs from crosslinking polymerization are summarized in Table 10.

Table 10. Evaluated performance metrics of various crosslinked PEs in SSB applications.

Monomers	Solvent	Salt	Ionic Conductivity (S cm ⁻¹) at Temperature (°C)	Lithium-Ion Transference Number (t_{Li^+})	ESW (V vs. Li/Li ⁺)	Discharge Specific Capacity (mAh g ⁻¹)	Capacity Retention (%/Cycle)	Reference
PEO-TEGDMA	-	LiTFSI	0.27×10^{-3} at 24	0.56	6	160/0.5 C	60 mAh g ⁻¹ /100	[251]
TGIC-NPEG	-	LiTFSI	1.15×10^{-4} at 60	0.32	0–5.1	161.1	94.5/100	[252]
Poly (DOL-TTE)-LP	-	LiTFSI, and LiBF ₄	3×10^{-4} at RT	0.35, and 0.26 without LP	1–7	152	80/200	[253]

Table 10. *Cont.*

Monomers	Solvent	Salt	Ionic Conductivity (S cm^{-1}) at Temperature ($^{\circ}\text{C}$)	Lithium-Ion Transference Number (t_{Li^+})	ESW (V vs. Li/Li $^{+}$)	Discharge Specific Capacity (mAh g^{-1})	Capacity Retention (%/Cycle)	Reference
PGMA-PEG	-	LiTFSI	1.3×10^{-4} at 40, and 1.22×10^{-4} at 90	0.150–0.234	5.3	160	80/50	[255]
PEI-PEGDE	-	LiTFSI	0.830×10^{-3} at 25, and 1.557×10^{-4} at 85	0.674	-	940/0.2 C	80/180	[256]
Poly(ethylene glycol dimethacrylate-1,2-ethane dithiol) (P-(EGDMA-EDT))	-	LiTFSI	3.02×10^{-5} at AT	0.45	4.5	150.1/0.05 C, 145.1/0.1 C, and 137.5/0.2 C	96.2/100	[212]
VEC-OFHDODA	-	LiTFSI	1.37×10^{-3} at 25	-	5.08	164.19/0.5 C	90/200	[259]
PVEC-NR20	-	-	1.65×10^{-4} at 25	0.63	5.3	95/2 C	79.4/200	[260]
PEGDGE-polyoxypropylenediamine (D2000)	-	LiTFSI	2.55×10^{-5} at RT, and 2.55×10^{-4} at 75	0.11	4.03	150/0.05 C	99.95/100	[261]
POSS-PEGDA	-	LITFSI	-	-	5.3	138.6	92.7/42	[257]
SH-PEG-SH-PEGDA	-	-	5.8×10^{-5} at RT	0.46	4.1	1.43 mAh cm^{-2}	81/1000	[262]
PEO-POSS	THF	LiTFSI	0.23×10^{-3} at RT	-	-	161/10 C, and 147/2 C	92/500	[263]
CMC-CA	-	LiClO ₄	1.24×10^{-7} at RT	-	2.15	-	-	[264]
SPPG-LiBOB	PC	LiBOB	2.6×10^{-4} at RT	0.65	4.7	132/0.5 C, and 120/2 C	83/500	[265]
1-vinyl-3-ethylimidazolium bis(trifluoromethanesulfonyl)imide ([VEIm][TFSI])-PIL	-	LiTFSI	7.78×10^{-5} at 30, and 5.92×10^{-4} at 60	0.21	-	138.4	90/250	[266]

4.6. Block Copolymerization

It is a synthesis technique that covalently bonds different polymer blocks to eventually form a copolymer with tailored properties, hence improving the performance of PEs for LMBs. This technique has become one of the most promising ways of synthesizing polymer electrolytes with enhanced ionic conductivity and mechanical stability. So far, several works have prepared different polymer architectures, such as ABA triblock copolymers and diblock copolymers with combined ionic and non-ionic blocks. Among them, some examples of the former category, including poly(styrene) and poly(ethylene oxide), achieved remarkable enhancements in ionic conduction and cycling performance, while fluorine-containing block copolymers such as PFMA-b-PEO-b-PFMA (Figure 16a,b), broad electrochemical stability, and high capacity retention after long-time cycling have been reported [267–269]. More importantly, the paradigmatic examples of block copolymer systems like polyvinyl benzyl methoxy polyethylene oxide ether-block-polystyrene and polyethylene oxide-based materials have also underlined the balance between ionic conductivity and mechanical integrity and opened further directions for advanced electrolyte materials (Figure 16c) [270–272].

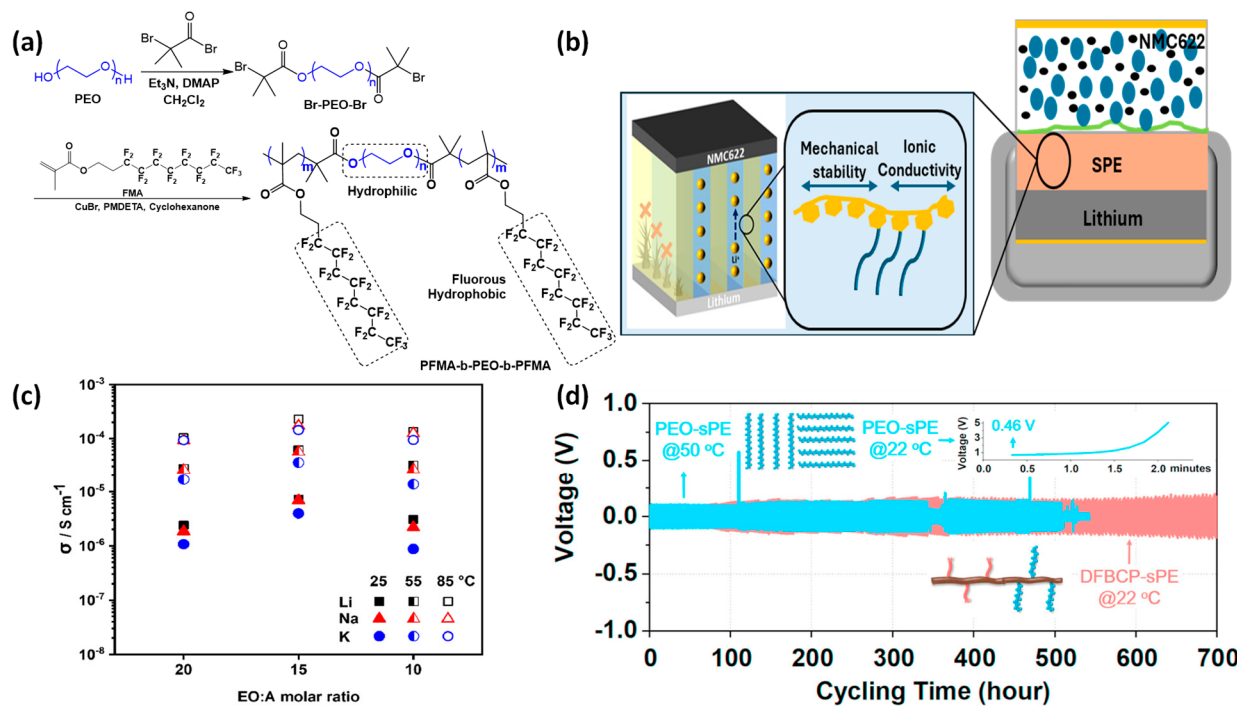


Figure 16. (a) The formation process of FBCPs. (b) Illustration showing how microphase separation in block copolymers inhibits dendrite growth. (c) Influence of the EO molar ratio on ionic conductivity (measured via EIS from 1 MHz to 500 mHz) in BPE15-ATFSI1 (A = Li, Na, or K) at temperatures of 25, 55, and 85 °C [271]. (d) Cycling stability comparison between Li/DFBCP-sPE/Li cells. Adapted with permission from [273]. Copyright 2020, Elsevier B.V.

Innovative methods have been developed to achieve improved properties for the SPEs by using block copolymerization techniques, as in the case of polycarbonate and CO₂ derivatives, furthering the ionic conductivity to improve the Li-ion transference numbers [274]. The addition of flexible polymer segments, such as poly(propylene carbonate) and polystyrene–butadiene–styrene, dramatically enhances composite solid electrolytes' mechanical strength and cycling stability [269,275]. These advancements have highlighted the contribution of block copolymerization in the design of high-performance PEs that are suitable for the next generation of lithium batteries, pointing out the crucial role that tailored polymer structures can play in improving electrochemical performances and operational stability (Figure 16d) [147,273,276,277]. Recent findings of PEs from block copolymerization are summarized in Table 11.

Table 11. Performance metrics of block copolymer electrolytes in SSBs.

Monomers	Solvent	Salt	Ionic Conductivity (S cm ⁻¹) at Temperature (°C)	Lithium-Ion Transference Number (<i>t</i> _{Li+})	ESW (V vs. Li/Li ⁺)	Discharge Specific Capacity (mAh g ⁻¹)	Capacity Retention (%/Cycle)	Reference
Polystyrene-poly(styrene-b-1-((2-acryloyloxy)ethyl)-3-butylimidazolium bis(tri-fluoromethanesulfonyl)imide)	EC	LiFSI	4×10^{-5} at 50	0.56	-	161	97.4/125	
PFMA-b-PEO-b-PFMA	-	LiTFSI	2.68×10^{-4} at 70	0.41	4.9	162/0.1 C, 160/0.2 C, 157/0.5 C, 150/1 C, and 144/2 C	95.8/250	[268]
Styrene-PEO	-	LiTFSI	1.6×10^{-2} at 25	0.13	4.75	-	80/100	[275]
PCL-PPC-PCL	-	LiTFSI	1.6×10^{-5} at 30	0.4	5	161/0.1 C	90/100	[269]

Table 11. *Cont.*

Monomers	Solvent	Salt	Ionic Conductivity (Scm^{-1}) at Temperature ($^{\circ}\text{C}$)	Lithium-Ion Transference Number (t_{Li^+})	ESW (V vs. Li/Li $^{+}$)	Discharge Specific Capacity (mAh g^{-1})	Capacity Retention (%/Cycle)	Reference
P(HOEA-co-MA)-PEG	THF	LiTFSI	0.6×10^{-3} at 30	0.35	4	-	-	[273]
Pebax-PEGDE (P-P)	-	LiTFSI	4.47×10^{-4} at 60	-	-	162/0.1 C	99.3/900	[270]
PVBmPEO-b-PS	-	LiTFSI	1×10^{-3} at 40	0.127	-	-	-	[276]
PEGMA-PEO	CH_3OH	LiTFSI	0.22×10^{-3} at RT	0.63	5	165	94/100	[278]
PVBmPEO-b-PS	-	TFSI	7.20×10^{-6} at 25	0.13–0.18	-	140, and 105 (Na, and K-based cells)	73–94/100	[271]
PEO-b-vCHO	-	LiTFSI	9.1×10^{-3} at 60	0.3–0.62	4	-	86/200	[274]
PVDF-b-PTFE	-	LiPF_6	6.4×10^{-4} at RT	0.56	5.1	170.1/0.1 C, 164.5/0.2 C, 149.3/0.5 C, and 109.8/1 C.	72.7/150	[272]
Styrene-butadiene-Styrene	-	LPSCl	1.3×10^{-1} at RT			123.2/0.1 C	72.9/100, and 42.7/500	[279]
Poly(lithium 1-[3-(methacryloyloxy)-propylsulfonyl]-1-(trifluoromethylsulfonyl)imide) and poly(ethylene glycol) methyl ether methacrylate	-	LiTFSI	10^{-4} at 60	0.8	-	-	-	[147]
PFPEMA-b-PEO	-	-	7.462×10^{-1} at RT	0.56	5	143.9	90/100	[277]

5. PEs: Film Casting, Characterization Techniques, Modifications, and Battery Fabrication

5.1. Solution Casting Method

Solution casting is a traditional technique for making films and gels of PEs. In this process, definite quantities of polymer and complexing salts are separately dissolved in a common solvent and combined to ensure effective complexation. Micro- or nano-sized fillers are added to composite PE films. The mixture is cast onto a Petri dish to enable gradual evaporation of the solvent, followed by vacuum drying to obtain a film of uniform thickness. This method is preferred because it is easier and cheaper; moreover, it allows for homogeneous thickness and distribution of additives, improving the final product's mechanical and functional properties. Regarding solid-state lithium batteries, solution casting plays a vital role in developing SPEs that can avoid lithium dendrite growth for improved safety. By adding lithium salts and functional materials, the resulting material's ionic conductivity and mechanical strength can be further enhanced, and copolymerization and grafting techniques can optimize the polymer design. On the contrary, inappropriate solvent choices and incomplete evaporation processes might give rise to some defects due to poor environmental control. Even so, solution casting is a versatile and widely adopted route in fabricating polymer materials (Figure 17a) [280].

This technique has found a notable application in the synthesis of SPEs, as narrated by Ali et al. [281]. In the referenced work, the authors used the solution casting technique to develop SPEs by synthesizing nanofillers of cerium oxide from cerium nitrates through a hydrothermal method. Accordingly, an equimolar ratio of cerium nitrate was mixed with excess water and ethanol, adding excess carbamide. Then, the mixture was autoclaved for 12 h at a temperature of 180°C , followed by calcination at 300°C for two hours to yield the yellow powder. A mix of 68% PEO, 16% PEG, and 11% lithium perchlorate with 0%, 1%, 3%, and 7% cerium oxide nanofiller was mixed. The resultant mixture was dried in a Petri dish under a vacuum to obtain the SPE film. Other works used similar approaches with PEO and different dopants. As an example, one SPE prepared by PEO (10%), LiClO_4 (5%), and TiO_2 in acetonitrile showed an enhanced ionic conductivity of $1.4 \times 10^{-4} \text{ Scm}^{-1}$ [282]. In another case, almost the same kind of ionic conductivity was found at $2.62 \times 10^{-4} \text{ Scm}^{-1}$ when PEO (20%) and NaClO_4 (5%) were doped with TiO_2 [283]. The maximum conductivity

of $5.05 \times 10^{-5} \text{ Scm}^{-1}$ was obtained for the membrane based on PEO doped with LiTFSI in the presence of acetonitrile and PEG. Substitution of nanofillers by graphite powder, prepared by Hummer's method, resulted in lower conductivity, equal to $3.4 \times 10^{-5} \text{ Scm}^{-1}$, which testifies to a minor effect of graphite [284]. Generally, amorphous materials are characterized by higher ionic conductivity compared to crystalline ones [285], which may explain the lower melting temperature and wider melting endotherm of amorphous species. Finally, ionic transport number measurements can provide information on the extent to which ionic conductivity contributes to the overall conductivity, a pertinent issue when a superionic electrolyte or mixed-conducting cathode material is to be selected for battery applications. SPEs of low melting point would yield better ionic conductivity [286].

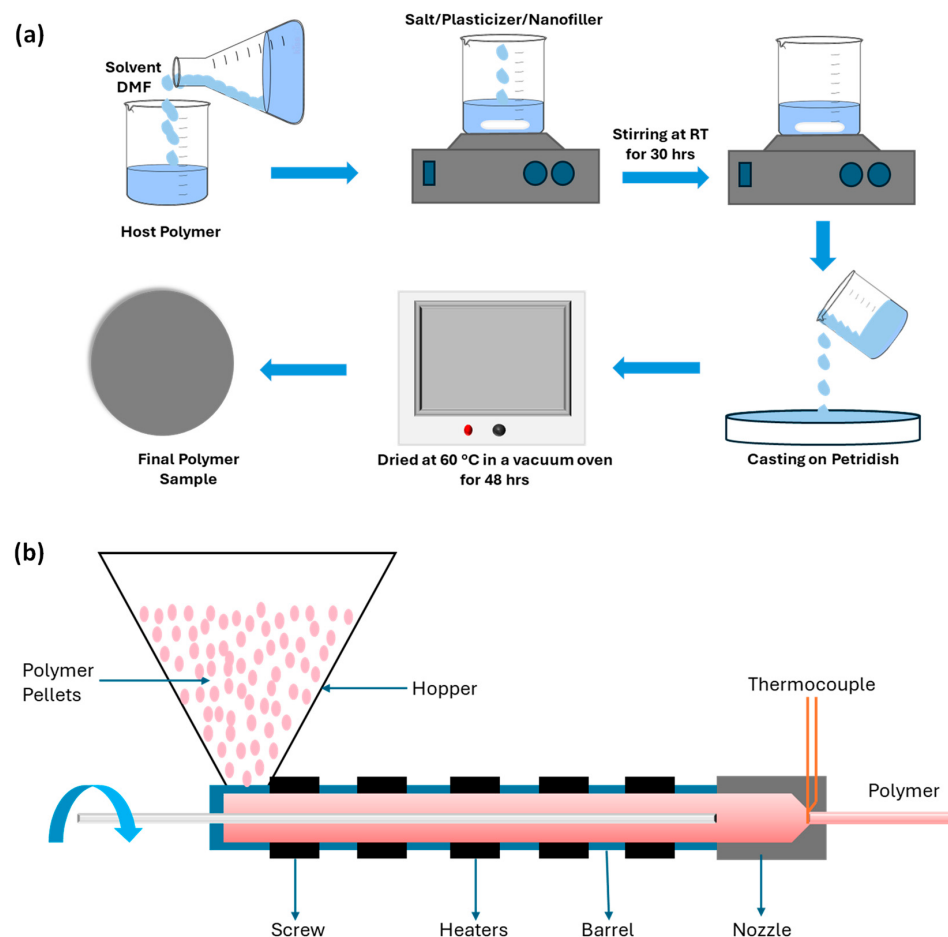


Figure 17. (a) The picture depicts the solution-casting method. (b) Schematic of hot-press method.

5.2. Hot Press (Extrusion) Technique

This technique was first reported and has since been employed by many research groups with minor modifications. The superiority of this technique compared with the conventional solution casting method is relatively significant. It presents one of the fastest, cheapest, and driest processes for preparing PE films. In this process, dry powders of polymer and complexing salt are combined in the appropriate ratios for conventional SPEs. In contrast, a mixture of polymer, complex salt, and micro-/nano-sized filler particles is used for CPE films. The homogeneous powder mixture is subsequently heated near the melting point of the host polymer while stirring continuously to accomplish the complete complexation of the salt. As a result of the heating process, a soft slurry is produced. Then, this soft slurry is pressed between two cold metal plates or rollers to make a flat, uniform polymer electrolyte film roughly μm thick (Figure 17b).

In this respect, hot-press casting is an efficient, cost-effective, and environmentally friendly technique that has been tried for the fabrication of PE films. For example, Deka et al. [287] employed this technique with PEO as the polymer matrix, silver triflate as the dopant, and Al_2O_3 as the nanofiller. In their work, PEO and silver triflate were mixed in a 90:10 ratio and heated to just below the melting point for an hour while being stirred continuously. Then, Al_2O_3 filler was added and stirred continued for another hour until solid lumps were absent from the mixture. This was then pressed between two cold stainless-steel plates to yield a SPE film in the thickness range of 100 to 150 μm [288]. The ionic conductivity of the resultant SPE was $7.12 \times 10^{-7} \text{ Scm}^{-1}$ at ambient temperature, with excellent mechanical stability. When zinc triflate was used as a dopant instead of silver triflate, ionic conductivity increased to $1.09 \times 10^{-6} \text{ Scm}^{-1}$. This can be attributed to efficient complexation or dissolution of the salt in the PEO matrix, along with a decrease in crystallinity and a rise in the amorphous nature of the polymer, as evidenced by XRD studies that indicated the disappearance of peaks. Hot-press casting is, therefore, one of the promising techniques for the preparation of advanced polymer electrolytes for energy storage applications.

5.3. Characterization Techniques

These analytical techniques include FTIR, Raman spectroscopy, XRD, and extended X-ray absorption fine structure (EXAFS) studies on the material properties of PE films in salt complexation and distribution of fillers. These techniques, together with nuclear magnetic resonance (NMR), scanning electron microscopy (SEM), and thermal analysis (DTA and DSC), provide information about structural features, including crystallinity, amorphous content, glass transition temperature (T_g), and melting point (T_m). For ion transport property evaluation, some of the key parameters are ionic conductivity (σ), ionic mobility (μ), mobile ion concentration (n), ionic drift velocity (v_d), and ionic transference number (t^+). Impedance spectroscopy (IS) is a technique for measuring conductivity based on an investigation by impedance, both real and imaginary parts in a wide frequency range from MHz to MHz. This yields a complex impedance plot that differentiates between resistive contributions due to bulk and interfacial resistance. Furthermore, the value of ionic mobility and transference number can be measured by various methods, including direct and transient ionic currents.

Studying additive effects on SPEs is impossible without XRD analysis; however, this technique often fails to indicate crystalline peaks in many polymeric materials. It is assumed that doping PEO with nanofillers such as alumina, silica, and titania below a 10% concentration level results in a particle size of less than 100 nm. For example, lithium silver triflate with alumina (less than 50 nm) complexation produced membranes from 100 to 150 μm . These peaks at 2θ values of 19.5° and 24° shifted to lower values upon salt complexation, as confirmed by FT-IR spectroscopy [289]. This doping type enhances the amorphous phase, favoring ionic conduction, and DSC analysis indicates a lowering of the T_g [290].

In CPEs prepared by PEO, lithium perchlorate, and titanium oxide, 10% lithium perchlorate and 5% titanium oxide doping (3.7 nm) helped with fast lithium-ion migration due to the interactions with the PEO chain [282,291]. The other works showed that, in PEO combined with LiTFSI and nickel phosphate (VSB-5), the shift from semi-crystalline to amorphous structures enhanced ionic conductivity. The nanorods improved the Li^+ mobility by interacting with the TFSI anion and affecting PEO crystallinity. FTIR spectra confirmed this through peak shifts. SEM revealed smooth surfaces of SPEs where the thickness ranged between 30 and 50 μm (Figure 18a–d) [292]. XRD analyses revealed that NMPC and NMPC-OMPk polymer electrolytes were essentially amorphous or semi-crystalline. OMPk enhanced membrane crystallinity [293]. Adding CuS to PVA matrices and clay-modified methyl methacrylate into PVDF also increased the amorphous nature of the polymer electrolyte. Investigations into PVDF-co-HFP finally indicated the addition

of clay nanoparticles, yielding a transition toward an amorphous structure and, hence, flexibility in the electrolyte.

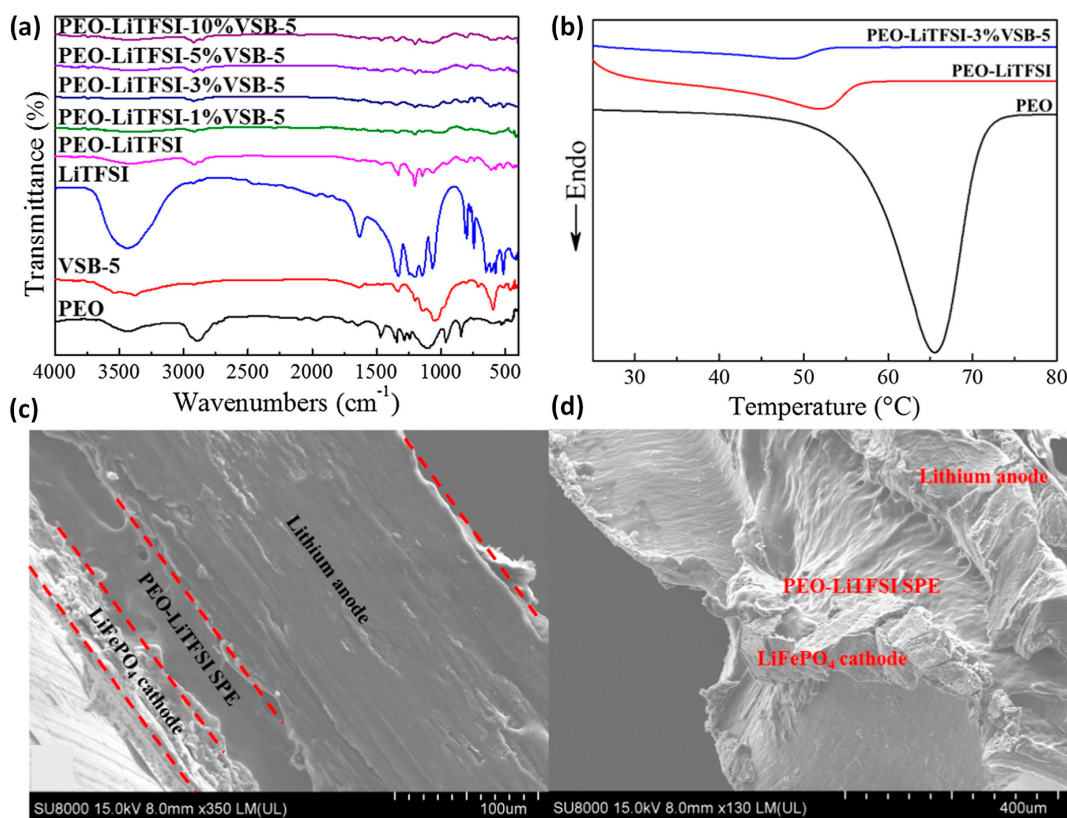


Figure 18. (a) Schematic illustrating Li^{+} migration in VSB-5-enhanced composite SPEs. (b) DSC analysis of PEO, PEO-LiTFSI, and PEO-LiTFSI-3%VSB-5. (c,d) Cross-sectional and interface images of the LiFePO₄/PEO-LiTFSI/Li battery post-rate cycling test. Adapted with permission from [292]. Copyright 2020, Elsevier.

5.4. Electrochemical Properties

5.4.1. Impedance Spectroscopy

Impedance spectroscopy: The following techniques are used in the ion conduction study of electrolytes. In impedance plots, the semicircle at a high frequency represents the resistive nature; the spike obtained at a low frequency reflects the capacitive nature. From the semicircle, the x-axis intercept yields the bulk resistance, which can be expressed as $Z^* = Z' + Z''$. With increasing frequency points, higher impedance values decrease owing to the effects of electrode polarization, and the dotted line denotes the point of frequency where the influence of electrode polarization becomes negligible. The direct current ionic conductivity ($\sigma_{dc} = A/R_{bt}$), relaxation times ($\tau_s = 1/2\pi f$), and transport numbers for electrons and ions can be calculated from their respective current ratios. While ZnO nanofillers yield shorter relaxation times due to their higher interaction with the polymer chains, SiO₂ nanofillers yield higher ion transport numbers since their ions are more mobile [294].

Recent research has indicated that the variation in salt concentration greatly affects the ionic conductivity of PEs. Among them, the addition of succinonitrile to the PE4 polymer electrolyte system resulted in the highest ionic conductivity of $1.92 \times 10^{-5} \text{ Scm}^{-1}$ due to reduced crystallinity and enhanced mobility of cations, which was confirmed by XRD analysis [295]. Kalim Deshmukh et al. [296], noticed for the PVA/PVP/Li₂CO₃ polymer blend that the ionic conductivity passed through a maximum at 20 wt% Li₂CO₃ with a value of $1.15 \times 10^{-5} \text{ Scm}^{-1}$, and then decreased with further increasing salt concentration due

to ion aggregation. On the other hand, polymer electrolytes based on PVC exhibited low ionic conductivity. The highest ionic conductivity value, 5.57×10^{-5} S/cm, was obtained when the addition of NH₄I salt reached 10 wt.%. Such a low ionic conductivity is mainly due to partial complexation between NH₄ cations with the main chain of PVC, which impedes cation transport [297]. Also, it could be observed that the ionic conductivity of the PVC-based electrolytes increased with the salt content up to 20 wt% and then decreased due to the immobilization of the polymer chain. The impedance plot also indicated a decrease in charge transfer resistance upon increasing NH₄SCN content [298].

5.4.2. AC Conductivity

The AC conductivity follows Jonscher's power law and depicts three clear regions in the frequency-dependent conductivity curve, i.e., a low-frequency, a high-frequency, and a frequency-independent region. The low-frequency region corresponds to the polarization of charges at the electrode/electrolyte interface, which reduces the ionic conductivity by accumulating charges. Maximum conductivity is found at 1% CeO₂, and further addition of filler reduces conductivity dispersion. The bulk relaxation, on the contrary, corresponds to the high-frequency region, where higher-mobility lithium ions take responsibility for higher conductivity even at temperatures below the melting temperature of PEO/PEG [281,299].

The recent works illustrated that the AC conductivity of PVA/PVP/Li₂CO₃ polymer blend electrolytes increased considerably upon the addition of Li₂CO₃, reaching the maximum value of 1.15×10^{-5} S cm⁻¹ at 20 wt% due to the enhancement in ionic mobility and charge transfer complex formation, particularly in the amorphous regions [295]. Temperature, in turn, enhanced the hopping of ions, confirming the suitability of the blend in SSBs [296]. On the other hand, the addition of salt NH₄I to PVC-based electrolytes led to only a slight improvement in DC conductivity due to its restricted ion motion, since strong interactions between NH₄ cations and the PVC backbone limit the free-ion concentration, thus offering material with high resistance [297]. Though it was not explicitly discussed, AC conductivity probably exhibited similar trends to that of the ionic conductivities, since it also would have been at a maximum at 20 wt% NH₄SCN due to the increased ionic mobility through the dissolution of ions and the increased segmental motion of the polymer matrix [298].

5.4.3. Dielectric Properties

The dielectric characteristics are expressed as $\epsilon^* = \epsilon' - j\epsilon'$, where the real part, ϵ' , gives the stored electric energy, the dielectric constant for an increase in the content of TiO₂. It was increased at a low frequency due to polarization and decreased at a higher frequency due to the relaxation mechanism. The dielectric loss also showed the same trend as the increasing peaks, which were associated with more heightened amorphous characteristics that gave rise to easier transport charges. The effective Lewis acid–base interactions improved ion mobility in CeO₂-containing electrolytes, while the low-frequency polarization enhanced the dielectric constant in PMMA/ENR 50-filled HCl-SiO₂ electrolytes (Figure 19a,b) [300–302].

Recent research has demonstrated the remarkable dielectric properties of PE systems. The highest dielectric constant was recorded for the PE4 PEs system, thereby corresponding to its highly conductive ionic conductivity, reflecting its excellent capacity for charge storage. Most importantly, the dielectric loss decreased with increasing frequency; hence, this signifies lower diffusivity of ions, while on the other hand, an increased dielectric constant represents an increase in charge carriers in the system [295]. In the other work, the dielectric constant of the PVA/PVP/Li₂CO₃ polymer blend electrolyte was as high as 1200 at a low frequency. It increased further with an increase in temperature, hence enhancing ion mobility. Its dielectric loss with 25 wt% Li₂CO₃ was less than 4 at 50 Hz, showing efficient energy storage and suitability for SSBs [296]. On the other hand, PVC-based PEs showed, by dielectric measurements, an inverse relation of dielectric constant with NH₄I variation; hence, they could be useful in microelectronic applications where

the requirement for low dielectric material is essential [297]. The non-Debye nature of relaxation in the Argand plot proved that complex relaxation processes were occurring, indicating suitability for insulation applications. Among other things, the dielectric analysis showed that the dielectric constant and loss fell with frequency; the highest value of the dielectric constant was recorded in the PVCNH electrolyte system, reflecting a greater charge carrier density [298].

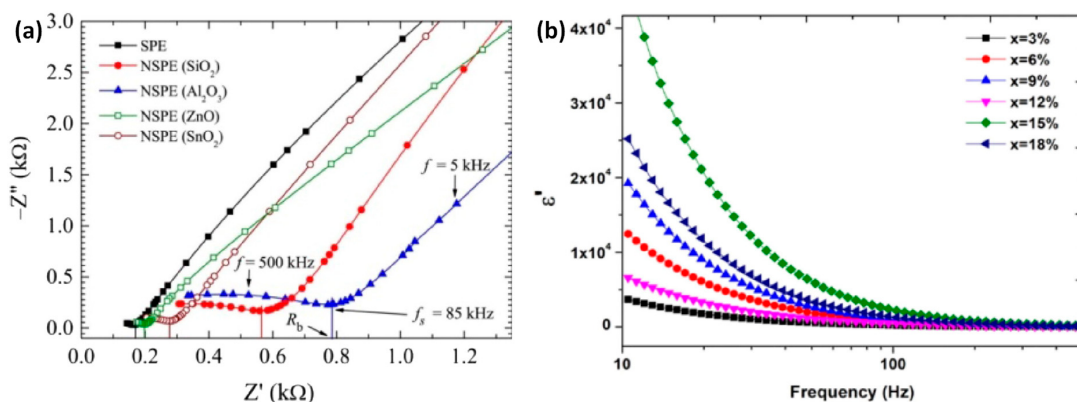


Figure 19. (a) Complex impedance plane plots of SPEs based on (PEO–PMMA)–LiClO₄, with and without 3 wt% of SiO₂, Al₂O₃, ZnO, or SnO₂. Adapted with permission from [294]. Copyright 2018, Elsevier. (b) Real parts of the complex permittivity for (80%, 20% PEO, PVDF) films containing 7.5 wt% NaClO₄ and varying wt% of TiO₂ NCPE at room temperature. Adapted with permission from [300]. Copyright 2021, Springer Nature.

5.5. Modifications of PEs

Many methods have been developed to functionalize PEs in order to achieve an optimized performance of SSBs. Among them, adding nanofillers such as SiO₂, Al₂O₃, and TiO₂ mainly enhances ionic conductivity and thermal stability and suppresses crystallinity [303,304]. Piezoelectric ceramics, such as LiNbO₃ and BaTiO₃, as well as superacid-conducting zeolites, further improve ion transport and electrochemical stability [6]. Another effective strategy involves the modification of polymer networks through crosslinking. For example, adding DEBA and PEGDE into the matrix greatly enhances mechanical strength and ionic conductivity [305]. In addition, incorporating α -CD into PEO-based electrolytes and novel structural design in nerve network-inspired SPEs improves conductivity and avoids problems such as lithium dendrite growth [306–308].

Resulting from this, several modification strategies have taken the direction of developing PEO-based electrolytes. Although PEO's polar -O- groups can allow for Li-ion transport in their amorphous regions, the crystalline nature inhibits long-term conductivity. Accordingly, additives such as LiAsF₆ create cylindrical channels that enhance Li⁺ transport. Substitution of ions, adding ionic liquids, or plasticizing agents such as tetraglyme or succinonitrile have also been applied to improve ionic conductivity and interfacial resistance [102,309,310]. Copolymerization is another modification method; various polymers, such as poly(styrene-ethylene oxide) of PS-b-PEO, by copolymerizing with lithium salts, yield mechanically strong membranes with great electrochemical performance [311,312]. The emergence of more complex systems such as SICs and PISSEs has thus been to improve further the selectivity, conductivity, and energy storage performance.

The realization of plasticized polymer electrolytes, GPEs, and hybrid ceramic–polymer systems represents several innovative approaches to the area in general. Such systems make bridges between liquid and solid electrolytes, enhancing ionic transport, mechanical strength, and thermal stability, which enables one, in several instances, to approach the dendrite formation concerns [313]. Plasticizers like PEG or crown ethers increase free volume and reduce crystallinity, hence enhancing ionic conductivity [314,315]. Besides that, hybrid systems, particularly with organometallic components like methylalumoxane

(MAO), grant safety and stability by not releasing toxic by-products upon decomposition. All these preparation methods result in increased conductivity and cycling behavior and provide thermal stability, where all hybrid and PISSE systems obtain room temperature conductivity of more than 10^{-6} Scm $^{-1}$, and hybrid ceramic systems offer improved thermal stability of at least more than 50 °C.

5.6. Battery Fabrication

The development of rechargeable battery technology has accelerated, particularly in lithium-ion conducting SPEs. These materials provide an opportunity for high energy density due to a wide electrochemical window for lithium-based systems. Employing lithium metal as an anode is highly challenging due to its fundamental characteristics of high reactivity and environmental sensitivity, hence raising safety concerns. More recent work has targeted the elimination of these deficiencies with intercalating and layered cathode and anode materials. Commercially important cathodes include LiCoO₂, LiMn₂O₄, and LiFePO₄, while laboratory development of the anodes focuses on LiC₆, SnO₂, and Li₃Sb. All these electrode active materials are processed into thin solid films deposited on metal foils, usually with polymer binders and electron-conducting additives such as carbon black, to enhance their conductivity. The transition to more benign, stable electrode materials has allowed lithium-ion batteries to retain a high capacity while delivering significant improvement in safety and efficiency (Figure 20).

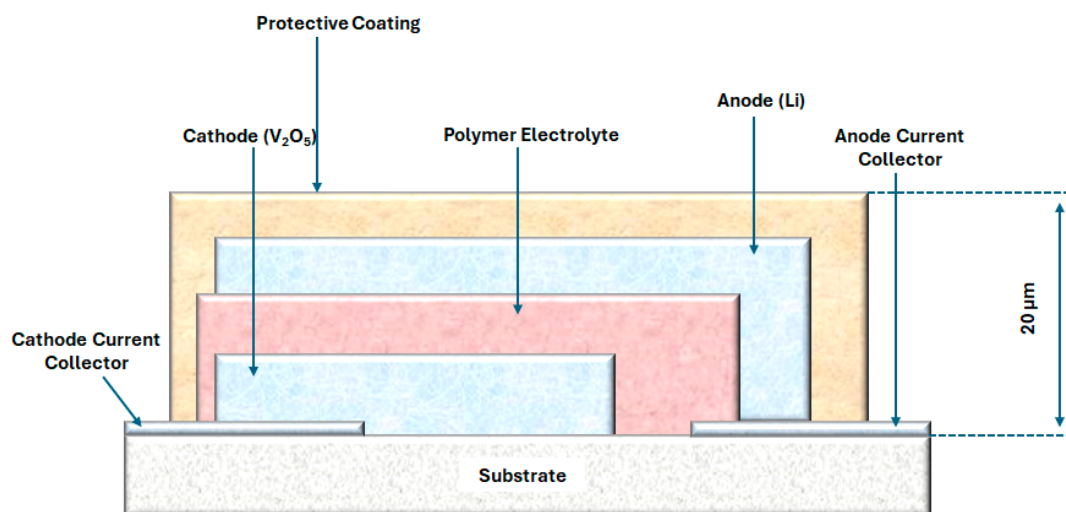


Figure 20. The picture depicts the cross-sectional view of a thin-film Li-micro battery.

Research into LPEBs has opened up exciting vistas for the future of energy storage systems. The advances in materials science drive the fabrication of a lightweight, flexible, high-energy-density, and fully solid-state battery that could revolutionize the whole energy scenario. Examples include all SSLBs of a laminated design with a Li⁺-conducting polymer membrane sandwiched between composite anode and cathode films. Such designs reveal interesting perspectives for innovative battery shapes and configurations and even safer and more efficient batteries for electric vehicles and other high-demand applications. The principal techniques to characterize their performance are cyclic voltammetry, charge-discharge cycling at different loads, and thermal analysis. The tools enable the optimization of key battery characteristics, such as critical cycle life, safety, and overall efficiency, that will allow for commercialization and further innovations in energy storage [316,317].

6. Li-Ion Solvation and Desolvation of PEs

Solvation within the PEs refers to the interaction of Li⁺ ions with a polymer matrix, usually assisted by some kind of solvent or plasticizer. This is a vital route for ion transport in LIBs, since it activates the dissolution of lithium salts and builds up a conductive

medium through which ions can pass between electrodes. This enhances its ionic conductivity and, therefore, the battery's general performance [318,319]. This also directly affects the interaction sites of a polymer to solvate lithium ions, considering the nature of the polar functional groups in the polymer structure. The higher the polar functionalities in the polymer are, the higher the solvation efficiency and the smoother the transport of ions. Besides the polymer structure, the properties of the solvent or plasticizer are very influential on solvation. Generally, the higher the dielectric constant of a solvent and the lower its viscosity, the better it is at solvating lithium ions, increasing their mobility throughout the electrolyte. Optimal performance can only be achieved if an optimal solvation structure for Li-ion diffusion exists, specifically under extreme conditions such as fast charge and low temperature. Nevertheless, striking a good balance between the degree of solvation and desolvation remains the key challenge to overcome in designing PEs. The strong solvation enhances ion mobility, but over-solvation worsens the other crucial process, which is desolvation for lithium-ion intercalation into an electrode. In most cases, desolvation includes an unavoidable energy barrier that might limit the ion transfer rate [320,321]. It proceeds only when all the solvent molecules near the electrode surface are effectively removed from Li. Therefore, optimizing the solvation–desolvation balance is highly important given the realization of high-performance lithium-ion batteries; it ensures efficient ion transport with minimal energy losses and various other performance improvements under a wide range of operating conditions (Figure 21) [322,323].

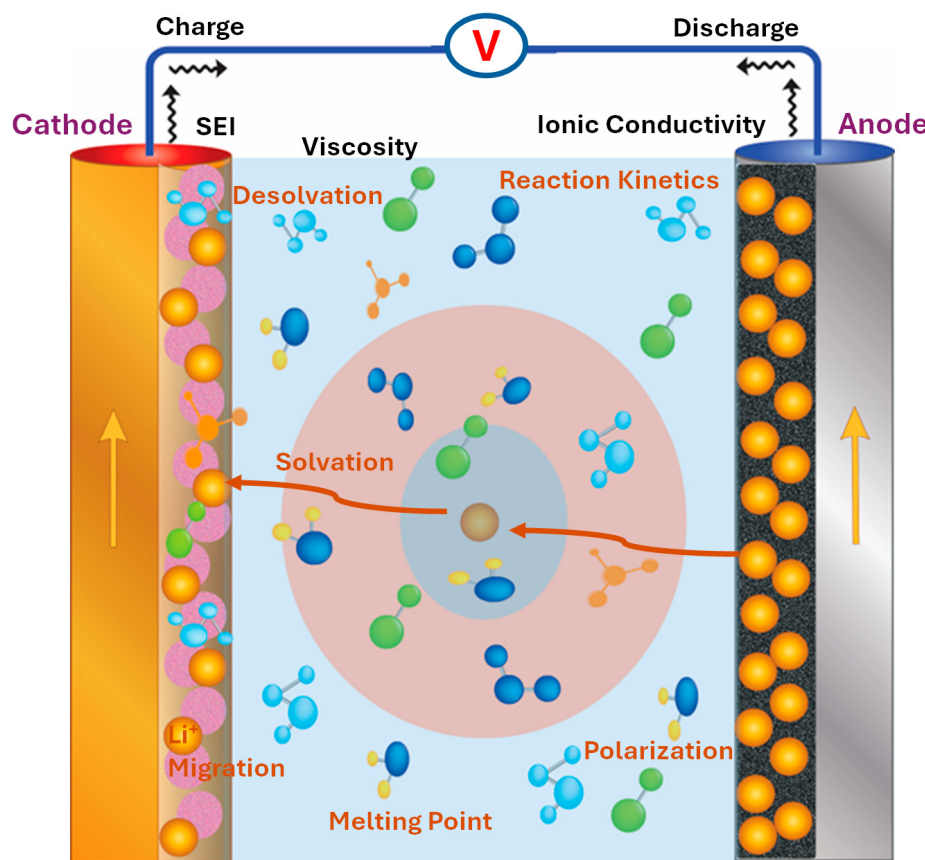


Figure 21. Illustration of Li-ion solvation and desolvation in PEs, showing ion transport through the polymer matrix and interactions with solvents or plasticizers.

Recent efforts in LIBs have focused on optimizing the solvation–desolvation processes of PEs, demonstrating outstanding performance in recent studies. For example, one recent study employed weakly solvated electrolytes composed of LiFSI, acetonitrile, and fluorobenzene to enable ultrafast lithium-ion intercalation into graphite with capacities of 370 mAh g^{-1} at 0.2 C and 302.7 mAh g^{-1} at 8 C . The addition of vinylene carbonate

yielded further improvement in cycling stability: it resulted in 80% capacity retention after 500 cycles at 5 C, a very effective electrolyte combination for fast charge and low-temperature applications [324]. Another study pointed out that the solvation structure of organic electrolytes, particularly those containing ethylene carbonate and ethyl methyl carbonate, determines lithium-ion mobility. The tighter solvation in EC reduces the diffusivity, whereas the weaker solvation in EMC promotes the faster transportation of ions; this suggests that optimization in the strength of the solvation of PEs plays an essential role in applying it to fast charging [325]. Regarding the study of dual-ion batteries, the key points have involved a dual-ion battery with an anion-permselective PE which weakens the interactions between PF_6^- and solvents, enhances anion desolvation, and provides oxidative stability. This structure allows for a cut-off potential of 5.4V and maintains 87.1% of its capacity after 2000 cycles, thereby showing the potential of the electrolyte to improve its performance and lifetime [326]. Furthermore, the critical role played by the solvation environments is hugely responsible for interfacial resistance in polymer electrolytes. Optimizing the solvation conditions by means of quantum chemical modeling and NMR studies increased the transfer of lithium ions at the interface between the electrolyte and the electrode. Further, it improved the battery's overall performance [327].

Other works have explored weak solutions for the development of more efficient batteries. A work concerning polyacetal electrolytes, for example, described how weaker coordination to lithium ions strengthens desolvation, greatly minimizing dendrite formation and extending cycling life for over 1300 h [328]. It also studied the effect of functional groups on solvation, where the cyano (-CN) groups increase the concentration of free lithium ions to offer fast desolvation, while fluorine (-F) groups contribute to constructing a stable SEI for enhanced cycling stability [329]. Other works involving the study of PEs with incorporated PEO and lithium poly(4-styrenesulfonyl(trifluoromethylsulfonyl)imide) (PSTFSI) have demonstrated how such a design optimizes both lithium-ion solvation and conduction for single-ion conduction along with anion migration suppression [90]. The investigation of polymer-in-salt systems has shown that the type of polymer used in solvation affects the stability of the system, with PEO improving the dynamics of ligand exchange and poly(butyl acrylate) offering better lithium-ion transport owing to its lower glass transition temperature [330]. In another study on covalent organic frameworks, specifically TpPa-2, it was found to effectively control both the solvation and desolvation processes, lowering the energy barrier towards desolvation significantly and further enhancing the stability of SEI [331]. It was reported that the special three-dimensional structure of GPEs decreased the activation energy for lithium-ion desolvation, offering high ionic conductivity of 5.73 mScm^{-1} at 25°C and guaranteeing an effective process of ion transport, especially in fast charging at low-temperature conditions [332]. Other attempts toward enhancing ionic conductivity have included blending rigid lithium salt homopolymers with flexible polymers such as PEO. This approach overcomes problems with strong electrostatic interactions between anions and cations, eventually providing stable battery performances with discharge capacities maintained over 100 cycles [333]. Some studies have emphasized the role of solvation complexes formed between lithium ions and glyme molecules within different polymer matrices, underscoring the fact that stable solvation improves ionic conductivity and thermal stability [334]. The introduction of a weak solvation strategy by 1,4-diiodotetrafluorobenzene (1,4-DITFB) significantly enhances lithium-ion mobility in PEO-based electrolytes. It promotes the formation of a stable Li_2O -rich SEI layer, hence offering overall improvements in cycling stability and superior performances of batteries [334]. These findings underlined how the optimization of PEs for advanced LIBs depends on their dynamic interplay with processes of solvation and desolvation.

7. Potential Applications and Advances of PEs in Li-Based Batteries and Beyond

The unique advantages of PEs have garnered much interest in relation to lithium-based batteries. Their main advantage is their enhanced safety since they are not flammable, un-

like LEs, thereby reducing the possibility of burning batteries at times of higher stress while working, such as in EVs or portable devices. Their flexibility also opens up opportunities for innovative battery designs, including in flexible and wearable electronics, where batteries must be shaped around irregular forms. Although liquid electrolytes are still lagging, improvements in recent years have made their performance serviceable in portable devices and supported higher voltages that boost energy density. They can inhibit the growth of lithium dendrite to a great degree and, hence, avoid a short circuit, thereby prolonging the life cycle of batteries. Most PEs are prepared from sustainable feedstock to go “green” in energy storage. However, a few drawbacks can be overcome, such as the lower ionic conductivity, a narrow operating temperature range, complicated fabrication processes, thermal instability at high temperatures, and compatibility issues that raise manufacturing costs. Considering the obstacles mentioned earlier, further research promises to realize the full potential of PEs, whose central role is played within energy storage technology.

PEs provide a way for solid-state cells in LIBs to avoid using flammable LEs and to allow for the usage of high-energy-density electrode materials. Advanced systems like Li-air, Li-sulfur, and SSLBs also look promising. Several different lithium salts could be incorporated into plasticizers and fillers within PEs; this provides methods for their customization and optimization of their performance. The potential of PEs across wide areas in the energy industry is furthered by this adaptability, which now drives innovation in next-generation energy storage solutions.

7.1. Lithium-Ion Polymer Batteries

In the case of LIPBs, however, the PEs are in solid or gel forms, and such batteries have very flexible designs, thus being suitable for use in wearable gadgets and smartphones. Lee et al. [335] studied the effect of unreacted monomers in LIPBs. The work has shown that, the higher the amount of unreacted monomers, the lower the discharge capacity, particularly at low temperatures and high discharge rates, due to a significant increase in interfacial resistance caused by the formation of a resistive layer at the surface of an electrode during charging. A further study explored preparing PEs with LiODFB, LiBOB, ionic liquids, sulfolane (TMS), and PVDF using the casting method; the optimization for battery performance was carried out by combining quaternary lithium salt, ionic liquids, and TMS [336].

7.2. Lithium-Ion Solid-State Batteries

The SPEs employed in LISSBs replace the highly flammable LEs in LIBs, improving safety by allowing higher energy densities and longer cycle lives, especially in applications for electric vehicles and grid energy storage. One of the recent important works reported recently by Wang et al. [337] was the preparation of a new SPE by electrospinning through incorporating bio-polyamide with an N-substituted pyrrolidone ring, IBD, and PEO/Li bis(trifluoromethane sulfonyl)imide. In this combination, it exhibited outstanding affinity to Li^+ ions, which improved the ion transport properties and reached an outstanding ionic conductivity of $4.26 \times 10^{-4} \text{ Scm}^{-1}$ at 50°C . Zhu et al. [338]. It also introduced a new structure for the inorganic polymer gel electrolyte in quasi-solid-state LIBs by adding helical mesoporous silica nanofibers (HMSFs) into a P(VDF-HFP) matrix. This novel methodology achieved great thermal stability up to 372°C , with a wide electrochemical stability window of 5.30 V and an impressive ionic conductivity of $1.2 \times 10^{-3} \text{ Scm}^{-1}$ at room temperature. These breakthroughs indicate immense possibilities with SSBs, which can transform energy storage technologies into even safer, more effective, and diverse applications for various industries.

7.3. Lithium–Sulfur Batteries

The combination of PES with LSBs is also obvious, particularly in their sulfur-based cathodes. This has been considered in pursuits toward achieving higher energy density for electric vehicles, storage of renewable energies, and portable electronics. In this

regard, Li et al. [339] developed a cathode material and an additive called poly(sulfur-1,3-diisopropenylbenzene) (PSD) from organosulfide incorporated into P(VDF-HFP) polymer electrolyte. The obtained composite, P(VDF-HFP)-10% PSD, showed good ionic conductivity (2.27×10^{-3} S cm $^{-1}$ at RT), which was higher than LEs. Another study prepared a flame-retardant PE to improve lithium-ion conduction and to ensure all-around battery safety [340]. Another group of authors developed a non-flammable polyether electrolyte for Li-S@pPAN batteries by using an in situ electrochemical polymerization. This newly developed approach greatly improved lithium compatibility to more than 3000 h and modified the cathode interphase to improve reaction kinetics. The polyether-rich interphase obtained in this way resulted in excellent battery performance, including a high capacity of 1645.3 mAh g $^{-1}$ based on sulfur, fast charging up to 10 °C, and exceptional cycling stability (99.5%/400 cycles). It also showed an excellent average coulombic efficiency of more than 99%, indicating very small irreversible reaction consumption at the cathode and a high sulfur utilization rate of 91.2% with capacity retention of 84.6% after 60 cycles. A novel SPE obtained through in situ polymerization of DOL with indium phthalocyanine largely improved ionic conductivity, suppressed the shuttle effect, and favored uniform lithium deposition at the interface (Figure 22a,b) [341]. These mentioned developments highlight the capability of PEs to bring disruptive technology change to LSB technology and offer a route to effective, safe energy storage.

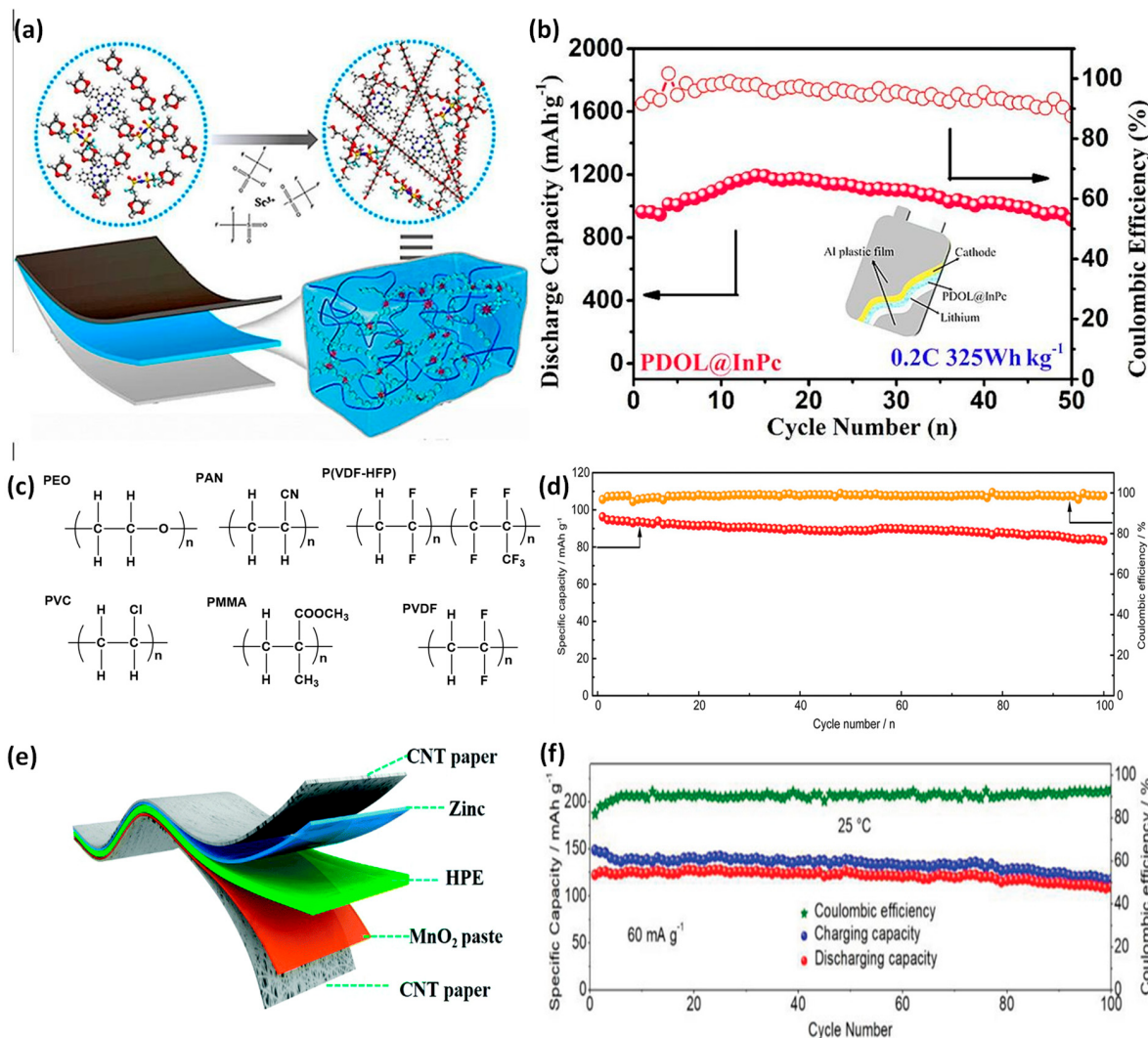


Figure 22. (a,b) Diagram of a gel electrolyte modified with InPc through in situ polymerization for high-loading Li-sulfur batteries and its electrochemical performance. Adapted with permission

from [341]. Copyright 2023, Elsevier B.V. (c) Chemical structures of typical polymer matrices. (d) Na | CESS | NVP cell operating at 0.5 C. Adapted with permission from [342]. Copyright 2020, WILEY-VCH Verlag GmbH & Co. KGaA, Weinheim. (e) Illustration of the solid-state ZIB architecture. Adapted with permission from [343]. Copyright 2018, Royal Society of Chemistry. (f) Cycle stability performance of the solid-state AIB at 60 mA g⁻¹. Adapted with permission from [344]. Copyright 2018, WILEY-VCH Verlag GmbH & Co. KGaA, Weinheim.

7.4. Lithium-Metal Batteries

LMBs are a very advanced class of energy storage systems using lithium metal as an anode; this allows for the achievement of exceedingly high energy densities. However, serious safety-related issues, like dendrite growth, are still in progress. In that respect, developing PEs and solid-state architectures will mitigate the safety issue and improve performance. Xie et al. [345] prepared the AT11-GF electrolyte based on the non-flammable compound ADN, which greatly conducted Li⁺ ions and demonstrated a huge ionic conductivity of 1.724×10^{-3} Scm⁻¹ with an electrochemical window as high as 5.75V. Fluoroethylene carbonate reduced some unwanted reactions on the lithium anode surface. In addition, a novel family of single-ion conductive block copolymers was prepared that exhibited high ionic conductivity and stability within LMB prototypes with up to 130 mAh g⁻¹ capacities. PEs were further developed by Porcarelli et al. [61] through controlled polymerization, where all-solid lithium-based cells exhibited excellent cycling performance, impressive ionic conductivity above 0.1 mS cm⁻¹, and pronounced resistance to the growth of lithium dendrites; hence, they could be the main candidates for application in next-generation batteries.

7.5. "Beyond Li" Pes-Based Batteries

7.5.1. Sodium-Based Batteries

In recent years, great interest has been focused on SBBs due to the abundance of raw materials, lower cost, and competitive electrochemical performances compared to lithium batteries [346]. Sodium metal has an even lower redox potential (-2.714 V vs. SHE) with a high theoretical capacity of 1165 mAh g⁻¹. Therefore, it becomes a very attractive alternative in searching for anode materials. Organic liquid electrolytes have practical applications that leak or run the risk of combustion. Accordingly, polymer electrolytes possess excellent stability and offer great resistance to the growth of sodium dendrites (Figure 22c). PEO-based polymers have been deemed practical candidates for sodium-ion battery applications since 1988; for example, K. West et al. [347] prepared a PEO-NaClO₄ film with an ionic conductivity of 3.1×10^{-6} Scm⁻¹ at 60 °C. Further development has yielded various species of sodium salts, such as NaPF₆ and NaTFSI, that improve conductivity [348,349]. PEO-based electrolytes, in the early history of their study, suffered from poor ionic conductivity and high crystallinity; however, great achievements have been made by blending or copolymerization with other polymers such as PAN and PVDF. For example, a crosslinked SPE network showed a conductivity of 2.56×10^{-4} Scm⁻¹ at 80 °C due to reduced crystallinity [350]. Although modified SPEs seldom surpassed 10^{-3} Scm⁻¹, liquid plasticizer-containing GPEs have demonstrated superior ionic conductivity. Besides this, Zhou et al. [351] synthesized a hierarchical poly(ionic liquid)-based solid electrolyte that exhibited ionic conductivity above 10^{-1} Scm⁻¹ at RT. In addition, CPEs containing materials such as SiO₂ and TiO₂ have also been developed to optimize high ionic conductivity with mechanical strength; one example is the CPE based on NaTFSI/PEO, which exhibited an ionic conductivity of 2.8×10^{-3} Scm⁻¹ at 80 °C [352]. More recently, flexible organic/inorganic CPEs with interpenetrating network structures have been developed, exhibiting conductivity above 10^{-4} S cm⁻¹ at 60 °C, effectively inhibiting dendrite formation and maintaining mechanical stability (Figure 22d) [342].

7.5.2. Potassium-Based Batteries

Despite possessing similar resource abundance and a higher Fermi level than sodium, potassium-based batteries have similarly received less attention due to similar safety

concerns over flammable nonaqueous electrolytes. The recent development of polymer electrolytes has created a promising pathway for developing solid-state potassium batteries that show competitive electrochemical properties. In 2013, a KBr-complexed PVC-PEO polymer blend electrolyte showed an enhanced ionic conductivity of $2.56 \times 10^{-5} \text{ Scm}^{-1}$ at RT, demonstrating that KBr doping enhances the electrochemical performance of the PE [353]. More recently, a potassium battery with a crosslinked PMMA-based GPE delivers high energy density alongside excellent cycling stability. The GPE also exhibited a stable electrochemical window up to 4.9 V vs. K^+/K , making it suitable for most potassium battery cathodes [354]. Additionally, PEO-based electrolytes have been one of the most explored materials for KIBs because of their enhanced ionic conductivity upon doping with potassium salts. For example, it was reported that the optimum conductivity of a PEO-KBr SPE film at a PEO/KBr ratio of 70:30 was about $5.0 \times 10^{-7} \text{ Scm}^{-1}$. At the same time, with increasing concentrations of KBr, the material exhibited conductivity that was lower and brittle [355]. Further modification via blending and copolymerization techniques, such as the comb polymer PECH-g-POEM complexed with KI, yielded even higher room-temperature ionic conductivity of $3.7 \times 10^{-5} \text{ Scm}^{-1}$ [356]. More importantly, a full cell using PEO-based SPE with KFSI salt showed a reversible capacity of 312 mAh g^{-1} with 98% capacity retention after 100 cycles, which proved its practical applicability [357]. Compared to traditional organic electrolytes, PEO-based electrolytes could have better safety and cycling performance. For example, PEO-CH₃COOK SPE showed an ionic conductivity of $2.74 \times 10^{-7} \text{ Scm}^{-1}$ at a 95:5 PEO/CH₃COOK ratio [358]. These developments epitomize the capability of polymer electrolytes to improve the performance and safety of potassium solid-state batteries, rendering them one of the most promising future energy storage research frontiers.

7.5.3. Zinc-Based Batteries

ZBBs have been gaining increasing interest as one of the most promising energy storage technologies due to their Zn metal anode, which possesses an unprecedented theoretical capacity of 820 mAh g^{-1} in combination with a low electrochemical redox potential of -0.76 V vs. SHE, high energy density, and low toxicity [359]. Nevertheless, such batteries suffer from disadvantages such as undesired reactions and dissolution of cathode active materials in aqueous electrolytes, which reduce battery efficiencies and excessively consume the electrolyte. Conductive PEs that could reduce the dissolution of active materials are being developed to overcome these issues. Among nonaqueous or aqueous liquid hydrogel and gel electrolytes, organic carbonates, oligomeric polyethers, and ionic liquids are some of the promising ones. The PEs using PEO, PVA, PVDF, and PAM are some of the most attractive ones for flexible ZBBs [360]. Most notably, Li et al. [361] have developed a flexible, wearable, and safe solid-state Zn battery based on a novel PAM-based hierarchical colloidal PE with high room-temperature ionic conductivity ($1.76 \times 10^{-2} \text{ Scm}^{-1}$). The hierarchical electrolyte, enabled by grafting PAM onto the PAN membrane, allowed for the design of a wearable ZB-powered smart insole that could track sports data, such as exercise duration and calorie consumption, and wirelessly transmit such information to a mobile application through Bluetooth. The present invention is one of the first highly safe, wearable, and rechargeable solid-state Zn batteries, which demonstrates very promising applications for practical applications. Secondly, large anion zinc salts enhance the polymer matrix's solubility, enhancing ionic conductivity much better than the conventional process [362].

Recent works based on these developments continued the design improvement using PEs for ZBBs (Figure 22e). The polymer gel electrolyte significantly mitigates major challenges like zinc dendrite formation and water-induced side reactions, offering improved electrochemical stability and performance [363]. It also contains hydrogen bonding and hydroxyl groups that allow some self-healing GPEs, such as those from PVA, to self-repair the gel upon its damage to improve battery lifetimes [343]. Improved cycling performance was also reported, with certain zinc-ion batteries sustaining 100% capacity over 3300 cycles and up to 93% over 4000 cycles [364]. These gels are suitable for flexible electronic devices due

to their flexibility and water-elastic properties [365]. Their ability to lock water molecules and reduce nucleation of ice crystals ensures effectiveness at low temperatures [366]. Great contact with the electrodes and good ion mobility are created through a combination of the mechanical strength of solid electrolytes with liquid electrolyte ion transport characteristics. Organic and inorganic additives have further improved ionic conductivity and helped to inhibit zinc dendrite growth, assuring more stability for superior electrochemical performance. These recent advances have put polymer electrolytes at the forefront and core of developing viable and scaled-up energy storage systems, primarily for ZBBs [363].

7.5.4. Aluminum-Based Batteries

In contrast, rechargeable ABBs have gained promise for energy storage systems after lithium, especially because of the much higher volumetric capacity of Al-metal (8040 mAh cm^{-3}) than that of lithium (2046 mAh cm^{-3}). The strongest obstacle lies in the very slow migration of Al^{3+} ions in the conventional electrolytes at ambient temperature owing to the strong solvation effect [367]. Cycle stability performance of the solid-state AIB at 60 mA g^{-1} was reported (Figure 22f) [344]. However, their work confirmed the reversible intercalation of Al^{3+} into V_2O_5 nanowires, an important step for ABBs [368]. Traditional liquid electrolytes suffer from many disadvantages, such as gas generation, moisture sensitivity, and safety risks, which seriously affect the cycling stability and coulombic efficiency of ABBs [369,370]. Furthermore, traditional polymer matrices like PEO, PAN, and PVDF have limited functionality in Al-based ionic liquids owing to the undesired coordination between the EO group of PEO and active Al_2Cl_7^- species [371]. Recent research has focused on the synthesis of solid-state polymers facilitating salt dissociation and thereby increasing ionic conductivity, one of the prime requirements for Al-based batteries. In 2018, the first solid polymer electrolyte for AIBs demonstrated an ionic conductivity of $2.86 \times 10^{-5} \text{ S cm}^{-1}$ with several aluminum salts, thus opening a road for future applications of polymers in this area [372]. Later, Yu et al. [344] synthesized mechanically self-standing GPE with acrylamide and AlCl_3 , which can effectively suppress gas generation and enhance the coulombic efficiency of AIBs. Plasticization of PEO chains by SiO_2 nanoparticles and imidazole ionic liquids yielded an impressively increased ionic conductivity of $9.6 \times 10^{-4} \text{ Scm}^{-1}$ and a superior electrochemical performance of ABBs [373]. Infiltration of chloroaluminate-based ionic liquids into polymer matrices has also been used to mitigate moisture sensitivity for further protection and to promote the development of ABBs.

8. Conclusions and Perspective

PEs are a significant area of potential growth in the development of SSBs because most hold high potential for mitigating key challenges traditionally seen with LEs, such as flammability and poor stability. Among those, various in situ polymerizations, grafting techniques, sol-gel methods, and electrospinning techniques have greatly improved the performances of SPE, GPE, and CPE. An improvement in ionic conductivity, particularly at room temperature, as well as electrochemical stability and mechanical robustness, has been achieved with such developments, making them potential candidates for batteries in the new generation. However, realizing high ionic conductivity with good mechanical strength is the main challenge. Developing new concepts such as nanocomposite structures, blending of polymers, and crosslinking techniques to optimize ion transport without giving up the structural integrity of PEs is ongoing. While much progress has been made so far, challenges remain in the direction of long-term stability and compatibility in different components of the solid-state system. Overcoming these limitations is crucial for achieving efficient battery performance with a longer cycle life, which is essential for the practical implementation of energy storage applications.

Therefore, the future of PEs in SSBs is bright, and it is bound to find a place in applications requiring high safety, such as EVs, portable electronics, and large-scale energy storage. As the research progresses, the aim will be to develop polymers with better ionic

transport and stability even in harsh operational conditions. The development of green and bio-based polymers, which is of growing interest, will also drive innovation toward sustainable solutions in battery technology. In addition, composite and hybrid polymer electrolytes that take advantage of organic and inorganic materials will also be indispensable to achieving high energy density and performance in commercial applications. Since such PEs can contribute to energy density and safety in batteries, especially for all SSBs, they are considered one of the most critical topics to pursue in the near future. Continued materials science and design improvements will enable the full exploitation of the potential for PEs to contribute to the global drive for cleaner, more efficient means of energy storage.

Author Contributions: N.G.N. wrote the review manuscript and produced the graphics. A.K.M.R.R. and K.Z. designed the structure of the review, collected the papers related to the topic of the review, and completed the language corrections, with all authors contributing equally. All authors have read and agreed to the published version of the manuscript.

Funding: The research was funded by Concordia University.

Acknowledgments: The authors would like to thank the Government of Quebec (MEIE) for its financial support.

Conflicts of Interest: The authors declare no conflicts of interest.

Acronyms

ABBs	Aluminum-based batteries
ACN	Acetonitrile
AMPS	2-Acrylamido-2-methylpropanesulfonic acid
ASSBs	All-solid-state batteries
ASSLBs	All-solid-state lithium batteries
ASSLIBs	All-solid-state lithium-ion batteries
CPEs	Composite polymer electrolytes
DEBA	Diethylbenzylamine
DEC	Diethyl carbonate
DEGDA	Diethylene glycol diacrylate
DMAC	Dimethylacetamide
DMC	Dimethyl carbonate
DME	1, 2-dimethoxyethane
DMF	Dimethylformamide
DMSO	Dimethyl Sulfoxide
DOL	1,3-dioxolane
DSPEs	Dry solid polymer electrolytes
EC	Ethylene carbonate
EDT	1,2-ethane dithiol
EGDMA	Ethylene glycol dimethacrylate
EMC	Ethyl methyl carbonate
ESW	Electrochemical stability window
FEC	Fluoroethylene carbonate
GPEs	Gel polymer electrolytes
HOMO	Highly occupied molecular orbitals
ILs	Ionic liquids
LATP	Lithium aluminum titanium phosphate
LEs	Liquid electrolytes
LFP	Lithium iron phosphate

LiBOB	Lithium bis(oxalate)borate
LIBs	Lithium-ion batteries
LiCTFPB	Lithium tetrakis(4-(chloromethyl)-2,3,5,6-tetrafluorophenyl)borate
LiDFOB	Lithium difluoroxalate borate
LiDMPA	Lithium dimethylol propionic acid
LiFSI	Lithium Bis(fluorosulfonyl)imide
LiODFB	Lithium difluoro(oxalato)borate
LIPBs	Lithium-ion polymer batteries
LiPCSI	Lithiated poly[(cyano)(4-styrenesulfonyl)imide]
LiPhTFSI	Lithium phenylsulfonyl(trifluoromethanesulfonyl)imide
LiPON	Lithium phosphorus oxynitride
LISSBs	Lithium-ion solid-state batteries
LiTFSI	Lithium Bis(trifluoromethanesulfonyl)imide
LLTO	Lanthanum titanium oxide
LLZO	Lithium lanthanum zirconium oxide
LLZTO	Lithium lanthanum zirconate
LMBs	Lithium metal batteries
LPEBs	Lithium-polymer electrolyte batteries
LPO	Lithium phosphate oxide
LSBs	Lithium–sulfur batteries
LUMO	Lower unoccupied molecular orbitals
MMA	Methyl methacrylate
NaFSI	Sodium bis(fluorosulfonyl)imide
NASICON	Sodium super ionic conductor
NMC	Nickel manganese cobalt oxide
NMP	N-Methyl-2-pyrrolidone
ODA	4,4'-oxybisbenzenamine
P3HB-3HV	Poly(3-hydroxybutyrate-co-3-hydroxyvalerate)
PA6	Polyamide 6
PAM	Polyacrylamide
PAN	Polyacrylonitrile
PBBs	Potassium-based batteries
PBSEs	Polymer-based solid electrolytes
PCL	Poly(ϵ -caprolactone)
PEG	Poly(ethylene glycol)
PEG, α -CD	Polyethylene glycol, α -Cyclodextrin
PEGDA	Poly(ethylene glycol) Diacrylate
PEGDE	Poly(ethylene glycol) Diacrylate
PEGDME	Poly(ethylene glycol) dimethyl ether
PEGM	Poly(ethylene glycol) methyl ether
PEGMA	Poly(ethylene glycol)methyl ether methacrylate
PEGMEA	Poly(ethylene glycol)methyl ether acrylate
PEO	Poly(ethylene oxide)
PEs	Polymer electrolytes
PISEs	Polymer-in-salt electrolytes
PliSS	Poly(lithium 4-styrene sulfonate)
PLiSSPSI	Poly(lithium (4-styrenesulfonyl)(phenylsulfonyl) imide)
PMDA	1,2,4,5-benzenetetracarboxylic anhydride
PMMA	Polymethyl methacrylate
PPEGMA	Poly(poly(ethylene glycol) methyl ether methacrylate
PVA	Polyvinyl alcohol
PVBN	Polyvinylbenzylamine
PVDF	Poly(vinylidene fluoride)
PVP	Polyvinyl pyrrolidone
SBBs	Sodium-based batteries
SEI	Solid electrolyte interphase
SEs	Solid electrolytes
SICPEs	Single-ion-conducting polymer electrolytes

SPEs	Solid polymer electrolytes
SSBs	Solid-state batteries
SSEBs	Solid-state electrolyte batteries
SSEs	Solid-state electrolytes
SSLBs	Solid-state lithium batteries
SSLPBs	Solid-state lithium polymer batteries
TEGDMA	Triethylene glycol dimethacrylate
TEGDME	Tetraethylene glycol dimethyl ether
TEP	Triethyl phosphate
TFSI	bis(trifluoromethanesulfonyl)imide
THF	Tetrahydrofuran
TFSI	bis(trifluoromethanesulfonyl)imide
THF	Tetrahydrofuran
VC	Vinylene carbonate
VEC	Vinyl ethylene carbonate
ZBBs	Zinc-based batteries

References

1. Zhai, D.; Lau, K.C.; Wang, H.-H.; Wen, J.; Miller, D.J.; Lu, J.; Kang, F.; Li, B.; Yang, W.; Gao, J.; et al. Interfacial Effects on Lithium Superoxide Disproportionation in Li-O₂ Batteries. *Nano Lett.* **2015**, *15*, 1041–1046. [[CrossRef](#)] [[PubMed](#)]
2. Elia, G.A.; Hassoun, J. A Polymer Lithium-Oxygen Battery. *Sci. Rep.* **2015**, *5*, 12307. [[CrossRef](#)] [[PubMed](#)]
3. Li, Y.; Bai, Y.; Bi, X.; Qian, J.; Ma, L.; Tian, J.; Wu, C.; Wu, F.; Lu, J.; Amine, K. An Effectively Activated Hierarchical Nano-/Microspherical Li_{1.2}Ni_{0.2}Mn_{0.6}O₂ Cathode for Long-Life and High-Rate Lithium-Ion Batteries. *ChemSusChem* **2016**, *9*, 728–735. [[CrossRef](#)]
4. Tarascon, J.-M.; Armand, M. Issues and Challenges Facing Rechargeable Lithium Batteries. *Nature* **2001**, *414*, 359–367. [[CrossRef](#)]
5. Mauger, A.; Julien, C.M.; Paoletta, A.; Armand, M.; Zaghib, K. Building Better Batteries in the Solid State: A Review. *Materials* **2019**, *12*, 3892. [[CrossRef](#)] [[PubMed](#)]
6. Quartarone, E.; Mustarelli, P. Electrolytes for Solid-State Lithium Rechargeable Batteries: Recent Advances and Perspectives. *Chem. Soc. Rev.* **2011**, *40*, 2525. [[CrossRef](#)]
7. Zhao, Y.; Wu, C.; Peng, G.; Chen, X.; Yao, X.; Bai, Y.; Wu, F.; Chen, S.; Xu, X. A New Solid Polymer Electrolyte Incorporating Li₁₀GeP₂S₁₂ into a Polyethylene Oxide Matrix for All-Solid-State Lithium Batteries. *J. Power Sources* **2016**, *301*, 47–53. [[CrossRef](#)]
8. Kato, Y.; Hori, S.; Saito, T.; Suzuki, K.; Hirayama, M.; Mitsui, A.; Yonemura, M.; Iba, H.; Kanno, R. High-Power All-Solid-State Batteries Using Sulfide Superionic Conductors. *Nat. Energy* **2016**, *1*, 16030. [[CrossRef](#)]
9. Goodenough, J.B.; Park, K.-S. The Li-Ion Rechargeable Battery: A Perspective. *J. Am. Chem. Soc.* **2013**, *135*, 1167–1176. [[CrossRef](#)]
10. Yue, L.; Ma, J.; Zhang, J.; Zhao, J.; Dong, S.; Liu, Z.; Cui, G.; Chen, L. All Solid-State Polymer Electrolytes for High-Performance Lithium Ion Batteries. *Energy Storage Mater.* **2016**, *5*, 139–164. [[CrossRef](#)]
11. Fu, K.; Gong, Y.; Liu, B.; Zhu, Y.; Xu, S.; Yao, Y.; Luo, W.; Wang, C.; Lacey, S.D.; Dai, J.; et al. Toward Garnet Electrolyte-Based Li Metal Batteries: An Ultrathin, Highly Effective, Artificial Solid-State Electrolyte/Metallic Li Interface. *Sci. Adv.* **2017**, *3*, e1601659. [[CrossRef](#)]
12. Homann, G.; Meister, P.; Stolz, L.; Brinkmann, J.P.; Kulisch, J.; Adermann, T.; Winter, M.; Kasnatscheew, J. High-Voltage All-Solid-State Lithium Battery with Sulfide-Based Electrolyte: Challenges for the Construction of a Bipolar Multicell Stack and How to Overcome Them. *ACS Appl. Energy Mater.* **2020**, *3*, 3162–3168. [[CrossRef](#)]
13. Méry, A.; Rousselot, S.; Lepage, D.; Dollé, M. A Critical Review for an Accurate Electrochemical Stability Window Measurement of Solid Polymer and Composite Electrolytes. *Materials* **2021**, *14*, 3840. [[CrossRef](#)]
14. Che, H.; Chen, S.; Xie, Y.; Wang, H.; Amine, K.; Liao, X.-Z.; Ma, Z.-F. Electrolyte Design Strategies and Research Progress for Room-Temperature Sodium-Ion Batteries. *Energy Environ. Sci.* **2017**, *10*, 1075–1101. [[CrossRef](#)]
15. Kim, J.; Yoon, K.; Park, I.; Kang, K. Progress in the Development of Sodium-Ion Solid Electrolytes. *Small Methods* **2017**, *1*, 1700219. [[CrossRef](#)]
16. Fan, L.; Wei, S.; Li, S.; Li, Q.; Lu, Y. Recent Progress of the Solid-State Electrolytes for High-Energy Metal-Based Batteries. *Adv. Energy Mater.* **2018**, *8*, 1702657. [[CrossRef](#)]
17. Manthiram, A.; Yu, X.; Wang, S. Lithium Battery Chemistries Enabled by Solid-State Electrolytes. *Nat. Rev. Mater.* **2017**, *2*, 16103. [[CrossRef](#)]
18. Hou, H.; Xu, Q.; Pang, Y.; Li, L.; Wang, J.; Zhang, C.; Sun, C. Efficient Storing Energy Harvested by Triboelectric Nanogenerators Using a Safe and Durable All-Solid-State Sodium-Ion Battery. *Adv. Sci.* **2017**, *4*, 1700072. [[CrossRef](#)] [[PubMed](#)]
19. Lanjan, A.; Ghalami Choobar, B.; Amjad-Iranagh, S. Promoting Lithium-Ion Battery Performance by Application of Crystalline Cathodes Li_xMn_{1-x}Fe_zPO₄. *J. Solid State Electrochem.* **2020**, *24*, 157–171. [[CrossRef](#)]
20. Experimental Researches on Electricity, Third Series. *Proc. R. Soc. Lond.* **1837**, *3*, 161–163. [[CrossRef](#)]
21. Scrosati, B. Recent Advances in Lithium Solid State Batteries. *J. Appl. Electrochem.* **1972**, *2*, 231–238. [[CrossRef](#)]

22. Lehovec, K.; Broder, J. Semiconductors as Solid Electrolytes in Electrochemical Systems. *J. Electrochem. Soc.* **1954**, *101*, 208. [[CrossRef](#)]
23. Diaz, G.; Peckler, L.; Sampurno, Y.; Philipossian, A. Communication—Tribology of Retaining Rings in Chemical Mechanical Planarization. *ECS J. Solid State Sci. Technol.* **2018**, *7*, P266–P268. [[CrossRef](#)]
24. Jin, Y.; Liu, K.; Lang, J.; Jiang, X.; Zheng, Z.; Su, Q.; Huang, Z.; Long, Y.; Wang, C.; Wu, H.; et al. High-Energy-Density Solid-Electrolyte-Based Liquid Li-S and Li-Se Batteries. *Joule* **2020**, *4*, 262–274. [[CrossRef](#)]
25. Liang, C.C.; Epstein, J.; Boyle, G.H. A High-Voltage, Solid-State Battery System. II. Fabrication of Thin-Film Cells. *J. Electrochem. Soc.* **1969**, *116*, 1452. [[CrossRef](#)]
26. Liang, C.C.; Bro, P. A High-Voltage, Solid-State Battery System. I. Design Considerations. *J. Electrochem. Soc.* **1969**, *116*, 1322. [[CrossRef](#)]
27. Liang, C.C. Conduction Characteristics of the Lithium Iodide-Aluminum Oxide Solid Electrolytes. *J. Electrochem. Soc.* **1973**, *120*, 1289. [[CrossRef](#)]
28. Voropaeva, D.Y.; Stenina, I.A.; Yaroslavtsev, A.B. Solid-State Electrolytes: A Way to Increase the Power of Lithium-Ion Batteries. *Russ. Chem. Rev.* **2024**, *93*, RCR5126. [[CrossRef](#)]
29. Owens, B.B. Solid State Electrolytes: Overview of Materials and Applications during the Last Third of the Twentieth Century. *J. Power Sources* **2000**, *90*, 2–8. [[CrossRef](#)]
30. Aono, H.; Sugimoto, E.; Sadaoka, Y.; Imanaka, N.; Adachi, G.-Y. Ionic Conductivity and Sinterability of Lithium Titanium Phosphate System. *Solid State Ion.* **1990**, *40–41*, 38–42. [[CrossRef](#)]
31. Inaguma, Y.; Liquan, C.; Itoh, M.; Nakamura, T.; Uchida, T.; Ikuta, H.; Wakihara, M. High Ionic Conductivity in Lithium Lanthanum Titanate. *Solid State Commun.* **1993**, *86*, 689–693. [[CrossRef](#)]
32. Murugan, R.; Thangadurai, V.; Weppner, W. Fast Lithium Ion Conduction in Garnet-Type $\text{Li}_7\text{La}_3\text{Zr}_2\text{O}_{12}$. *Angew. Chem. Int. Ed.* **2007**, *46*, 7778–7781. [[CrossRef](#)]
33. Birke, P. A First Approach to a Monolithic All Solid State Inorganic Lithium Battery. *Solid State Ion.* **1999**, *118*, 149–157. [[CrossRef](#)]
34. Ribes, M.; Barrau, B.; Souquet, J.L. Sulfide Glasses: Glass Forming Region, Structure and Ionic Conduction of Glasses in $\text{Na}_2\text{S}-\text{XS}_2$ ($X = \text{Si}; \text{Ge}$), $\text{Na}_2\text{S}-\text{P}_2\text{S}_5$ and $\text{Li}_2\text{S}-\text{GeS}_2$ Systems. *J. Non-Cryst. Solids* **1980**, *38–39*, 271–276. [[CrossRef](#)]
35. Kamaya, N.; Homma, K.; Yamakawa, Y.; Hirayama, M.; Kanno, R.; Yonemura, M.; Kamiyama, T.; Kato, Y.; Hama, S.; Kawamoto, K.; et al. A Lithium Superionic Conductor. *Nat. Mater.* **2011**, *10*, 682–686. [[CrossRef](#)] [[PubMed](#)]
36. Wang, S.; Xu, H.; Li, W.; Dolocan, A.; Manthiram, A. Interfacial Chemistry in Solid-State Batteries: Formation of Interphase and Its Consequences. *J. Am. Chem. Soc.* **2018**, *140*, 250–257. [[CrossRef](#)]
37. Strauss, F.; Teo, J.H.; Maibach, J.; Kim, A.-Y.; Mazilkin, A.; Janek, J.; Brezesinski, T. Li_2ZrO_3 -Coated NCM622 for Application in Inorganic Solid-State Batteries: Role of Surface Carbonates in the Cycling Performance. *ACS Appl. Mater. Interfaces* **2020**, *12*, 57146–57154. [[CrossRef](#)]
38. Sastre, J.; Futscher, M.H.; Pompizi, L.; Aribia, A.; Priebe, A.; Overbeck, J.; Stiefel, M.; Tiwari, A.N.; Romanyuk, Y.E. Blocking Lithium Dendrite Growth in Solid-State Batteries with an Ultrathin Amorphous Li-La-Zr-O Solid Electrolyte. *Commun. Mater.* **2021**, *2*, 76. [[CrossRef](#)]
39. Okur, F.; Zhang, H.; Karabay, D.T.; Muench, K.; Parrilli, A.; Neels, A.; Dachraoui, W.; Rossell, M.D.; Cancellieri, C.; Jeurgens, L.P.H.; et al. Intermediate-Stage Sintered LLZO Scaffolds for Li-Garnet Solid-State Batteries. *Adv. Energy Mater.* **2023**, *13*, 2203509. [[CrossRef](#)]
40. Meng, Y.S. Lithium Metal Anode—Advanced Characterization, Slides from the Web Seminar by Dr. Y. Shirley Meng 2020. Available online: <https://osf.io/preprints/ecstarxiv/6fr7c> (accessed on 18 December 2024).
41. Feng, X.; Ouyang, M.; Liu, X.; Lu, L.; Xia, Y.; He, X. Thermal Runaway Mechanism of Lithium Ion Battery for Electric Vehicles: A Review. *Energy Storage Mater.* **2018**, *10*, 246–267. [[CrossRef](#)]
42. Wang, Q.; Ping, P.; Zhao, X.; Chu, G.; Sun, J.; Chen, C. Thermal Runaway Caused Fire and Explosion of Lithium Ion Battery. *J. Power Sources* **2012**, *208*, 210–224. [[CrossRef](#)]
43. Iturronobeitia, A.; Aguesse, F.; Genies, S.; Waldmann, T.; Kasper, M.; Ghanbari, N.; Wohlfahrt-Mehrens, M.; Bekaert, E. Post-Mortem Analysis of Calendar-Aged 16 Ah NMC/Graphite Pouch Cells for EV Application. *J. Phys. Chem. C* **2017**, *121*, 21865–21876. [[CrossRef](#)]
44. Perea, A.; Dontigny, M.; Zaghib, K. Safety of Solid-State Li Metal Battery: Solid Polymer versus Liquid Electrolyte. *J. Power Sources* **2017**, *359*, 182–185. [[CrossRef](#)]
45. Zhang, W.; Nie, J.; Li, F.; Wang, Z.L.; Sun, C. A Durable and Safe Solid-State Lithium Battery with a Hybrid Electrolyte Membrane. *Nano Energy* **2018**, *45*, 413–419. [[CrossRef](#)]
46. Janek, J.; Zeier, W.G. A Solid Future for Battery Development. *Nat. Energy* **2016**, *1*, 16141. [[CrossRef](#)]
47. Gutiérrez-Pardo, A.; Pitillas Martinez, A.I.; Otaegui, L.; Schneider, M.; Roters, A.; Llordés, A.; Aguesse, F.; Buannic, L. Will the Competitive Future of Solid State Li Metal Batteries Rely on a Ceramic or a Composite Electrolyte? *Sustain. Energy Fuels* **2018**, *2*, 2325–2334. [[CrossRef](#)]
48. Julien, C.; Nazri, G.-A. *Solid State Batteries: Materials Design and Optimization*; The Kluwer International Series in Engineering and Computer Science; Springer US: Boston, MA, USA, 1994; Volume 271, ISBN 978-0-7923-9460-0.
49. Solid State Batteries. *Volume 1: Emerging Materials and Applications*; Gupta, R.K., Ed.; ACS symposium series; American Chemical Society: Washington, DC, USA, 2022; ISBN 978-0-8412-9768-5.

50. Grady, Z.A.; Wilkinson, C.J.; Randall, C.A.; Mauro, J.C. Emerging Role of Non-Crystalline Electrolytes in Solid-State Battery Research. *Front. Energy Res.* **2020**, *8*, 218. [[CrossRef](#)]
51. Nanda, J.; Wang, C.; Liu, P. Frontiers of Solid-State Batteries. *MRS Bull.* **2018**, *43*, 740–745. [[CrossRef](#)]
52. Zhang, Z.; Shao, Y.; Lotsch, B.; Hu, Y.-S.; Li, H.; Janek, J.; Nazar, L.F.; Nan, C.-W.; Maier, J.; Armand, M.; et al. New Horizons for Inorganic Solid State Ion Conductors. *Energy Environ. Sci.* **2018**, *11*, 1945–1976. [[CrossRef](#)]
53. Zhao, C.; Liu, L.; Qi, X.; Lu, Y.; Wu, F.; Zhao, J.; Yu, Y.; Hu, Y.; Chen, L. Solid-State Sodium Batteries. *Adv. Energy Mater.* **2018**, *8*, 1703012. [[CrossRef](#)]
54. Han, X.; Gong, Y.; Fu, K.; He, X.; Hitz, G.T.; Dai, J.; Pearse, A.; Liu, B.; Wang, H.; Rubloff, G.; et al. Negating Interfacial Impedance in Garnet-Based Solid-State Li Metal Batteries. *Nat. Mater.* **2017**, *16*, 572–579. [[CrossRef](#)] [[PubMed](#)]
55. Famprikis, T.; Canepa, P.; Dawson, J.A.; Islam, M.S.; Masquelier, C. Fundamentals of Inorganic Solid-State Electrolytes for Batteries. *Nat. Mater.* **2019**, *18*, 1278–1291. [[CrossRef](#)] [[PubMed](#)]
56. Kerman, K.; Luntz, A.; Viswanathan, V.; Chiang, Y.-M.; Chen, Z. Review—Practical Challenges Hindering the Development of Solid State Li Ion Batteries. *J. Electrochem. Soc.* **2017**, *164*, A1731–A1744. [[CrossRef](#)]
57. Strauss, F.; Bartsch, T.; De Biasi, L.; Kim, A.-Y.; Janek, J.; Hartmann, P.; Brezesinski, T. Impact of Cathode Material Particle Size on the Capacity of Bulk-Type All-Solid-State Batteries. *ACS Energy Lett.* **2018**, *3*, 992–996. [[CrossRef](#)]
58. Zhang, Q.; Liu, K.; Ding, F.; Liu, X. Recent Advances in Solid Polymer Electrolytes for Lithium Batteries. *Nano Res.* **2017**, *10*, 4139–4174. [[CrossRef](#)]
59. Zhu, X.; Wang, K.; Xu, Y.; Zhang, G.; Li, S.; Li, C.; Zhang, X.; Sun, X.; Ge, X.; Ma, Y. Strategies to Boost Ionic Conductivity and Interface Compatibility of Inorganic—Organic Solid Composite Electrolytes. *Energy Storage Mater.* **2021**, *36*, 291–308. [[CrossRef](#)]
60. Wang, Y.; Fan, F.; Agapov, A.L.; Saito, T.; Yang, J.; Yu, X.; Hong, K.; Mays, J.; Sokolov, A.P. Examination of the Fundamental Relation between Ionic Transport and Segmental Relaxation in Polymer Electrolytes. *Polymer* **2014**, *55*, 4067–4076. [[CrossRef](#)]
61. Porcarelli, L.; Gerbaldi, C.; Bella, F.; Nair, J.R. Super Soft All-Ethylene Oxide Polymer Electrolyte for Safe All-Solid Lithium Batteries. *Sci. Rep.* **2016**, *6*, 19892. [[CrossRef](#)] [[PubMed](#)]
62. Fenton, D.E.; Parker, J.M.; Wright, P.V. Complexes of Alkali Metal Ions with Poly(Ethylene Oxide). *Polymer* **1973**, *14*, 589. [[CrossRef](#)]
63. Berthier, C.; Gorecki, W.; Minier, M.; Armand, M.B.; Chabagno, J.M.; Rigaud, P. Microscopic Investigation of Ionic Conductivity in Alkali Metal Salts-Poly(Ethylene Oxide) Adducts. *Solid State Ion.* **1983**, *11*, 91–95. [[CrossRef](#)]
64. Gao, H.; Zhou, W.; Park, K.; Goodenough, J.B. A Sodium-Ion Battery with a Low-Cost Cross-Linked Gel-Polymer Electrolyte. *Adv. Energy Mater.* **2016**, *6*, 1600467. [[CrossRef](#)]
65. Osman, Z.; Md Isa, K.B.; Ahmad, A.; Othman, L. A Comparative Study of Lithium and Sodium Salts in PAN-Based Ion Conducting Polymer Electrolytes. *Ionics* **2010**, *16*, 431–435. [[CrossRef](#)]
66. Feuillade, G.; Perche, P. Ion-Conductive Macromolecular Gels and Membranes for Solid Lithium Cells. *J. Appl. Electrochem.* **1975**, *5*, 63–69. [[CrossRef](#)]
67. Cui, Y.; Liang, X.; Chai, J.; Cui, Z.; Wang, Q.; He, W.; Liu, X.; Liu, Z.; Cui, G.; Feng, J. High Performance Solid Polymer Electrolytes for Rechargeable Batteries: A Self-Catalyzed Strategy toward Facile Synthesis. *Adv. Sci.* **2017**, *4*, 1700174. [[CrossRef](#)] [[PubMed](#)]
68. Long, L.; Wang, S.; Xiao, M.; Meng, Y. Polymer Electrolytes for Lithium Polymer Batteries. *J. Mater. Chem. A* **2016**, *4*, 10038–10069. [[CrossRef](#)]
69. Sun, C.; Liu, J.; Gong, Y.; Wilkinson, D.P.; Zhang, J. Recent Advances in All-Solid-State Rechargeable Lithium Batteries. *Nano Energy* **2017**, *33*, 363–386. [[CrossRef](#)]
70. Hu, Y.; Xie, X.; Li, W.; Huang, Q.; Huang, H.; Hao, S.-M.; Fan, L.-Z.; Zhou, W. Recent Progress of Polymer Electrolytes for Solid-State Lithium Batteries. *ACS Sustain. Chem. Eng.* **2023**, *11*, 1253–1277. [[CrossRef](#)]
71. Vasudevan, S.; Dwivedi, S.; Balaya, P. Overview and Perspectives of Solid Electrolytes for Sodium Batteries. *Int. J. Appl. Ceram. Tech.* **2023**, *20*, 563–584. [[CrossRef](#)]
72. Zhu, Q.; Ye, C.; Mao, D. Solid-State Electrolytes for Lithium–Sulfur Batteries: Challenges, Progress, and Strategies. *Nanomaterials* **2022**, *12*, 3612. [[CrossRef](#)] [[PubMed](#)]
73. Botros, M.; Janek, J. Embracing Disorder in Solid-State Batteries. *Science* **2022**, *378*, 1273–1274. [[CrossRef](#)]
74. Huo, S.; Sheng, L.; Xue, W.; Wang, L.; Xu, H.; Zhang, H.; He, X. Challenges of Polymer Electrolyte with Wide Electrochemical Window for High Energy Solid-state Lithium Batteries. *InfoMat* **2023**, *5*, e12394. [[CrossRef](#)]
75. Xue, Z.; He, D.; Xie, X. Poly(Ethylene Oxide)-Based Electrolytes for Lithium-Ion Batteries. *J. Mater. Chem. A* **2015**, *3*, 19218–19253. [[CrossRef](#)]
76. Doyle, E.S.; Mirmira, P.; Ma, P.; Vu, M.C.; Hixson-Wells, T.; Kumar, R.; Amanchukwu, C.V. Phase Morphology Dependence of Ionic Conductivity and Oxidative Stability in Fluorinated Ether Solid-State Electrolytes. *Chem. Mater.* **2024**, *36*, 5063–5076. [[CrossRef](#)]
77. Cheng, X.-B.; Zhang, R.; Zhao, C.-Z.; Zhang, Q. Toward Safe Lithium Metal Anode in Rechargeable Batteries: A Review. *Chem. Rev.* **2017**, *117*, 10403–10473. [[CrossRef](#)] [[PubMed](#)]
78. Wan, J.; Xie, J.; Kong, X.; Liu, Z.; Liu, K.; Shi, F.; Pei, A.; Chen, H.; Chen, W.; Chen, J.; et al. Ultrathin, Flexible, Solid Polymer Composite Electrolyte Enabled with Aligned Nanoporous Host for Lithium Batteries. *Nat. Nanotechnol.* **2019**, *14*, 705–711. [[CrossRef](#)] [[PubMed](#)]

79. Yang, X.; Jiang, M.; Gao, X.; Bao, D.; Sun, Q.; Holmes, N.; Duan, H.; Mukherjee, S.; Adair, K.; Zhao, C.; et al. Determining the Limiting Factor of the Electrochemical Stability Window for PEO-Based Solid Polymer Electrolytes: Main Chain or Terminal –OH Group? *Energy Environ. Sci.* **2020**, *13*, 1318–1325. [[CrossRef](#)]
80. Pala, R.G.; Kankani, K.; Chakraborty, P. Phase-Field Modeling of Electrolyte Transport Properties and Elasticity Modulus in Suppression of Dendrite Growth in Solid-State-Lithium-Ion-Batteries. *Electrochim. Soc. Meet. Abstr.* **2024**. [[CrossRef](#)]
81. Yi, T.; Zhao, E.; He, Y.; Liang, T.; Wang, H. Quantification and Visualization of Spatial Distribution of Dendrites in Solid Polymer Electrolytes. *eScience* **2024**, *4*, 100182. [[CrossRef](#)]
82. Krauskopf, T.; Richter, F.H.; Zeier, W.G.; Janek, J. Physicochemical Concepts of the Lithium Metal Anode in Solid-State Batteries. *Chem. Rev.* **2020**, *120*, 7745–7794. [[CrossRef](#)] [[PubMed](#)]
83. Um, J.H.; Kim, K.; Park, J.; Sung, Y.-E.; Yu, S.-H. Revisiting the Strategies for Stabilizing Lithium Metal Anodes. *J. Mater. Chem. A* **2020**, *8*, 13874–13895. [[CrossRef](#)]
84. Yao, P.; Yu, H.; Ding, Z.; Liu, Y.; Lu, J.; Lavorgna, M.; Wu, J.; Liu, X. Review on Polymer-Based Composite Electrolytes for Lithium Batteries. *Front. Chem.* **2019**, *7*, 522. [[CrossRef](#)] [[PubMed](#)]
85. Li, Z.; Yu, R.; Weng, S.; Zhang, Q.; Wang, X.; Guo, X. Tailoring Polymer Electrolyte for High-Voltage Solid-State Li Metal Batteries Working at Ultra-Low Temperatures. *Res. Sq.* **2022**. [[CrossRef](#)]
86. Ren, Y.; Hatzell, K.B. Elasticity-Oriented Design of Solid-State Batteries: Challenges and Perspectives. *J. Mater. Chem. A* **2021**, *9*, 13804–13821. [[CrossRef](#)]
87. Yu, X.; Manthiram, A. Electrode–Electrolyte Interfaces in Lithium–Sulfur Batteries with Liquid or Inorganic Solid Electrolytes. *Acc. Chem. Res.* **2017**, *50*, 2653–2660. [[CrossRef](#)]
88. Agrawal, R.C.; Pandey, G.P. Solid Polymer Electrolytes: Materials Designing and All-Solid-State Battery Applications: An Overview. *J. Phys. D Appl. Phys.* **2008**, *41*, 223001. [[CrossRef](#)]
89. Sun, Y.-Z.; Huang, J.-Q.; Zhao, C.-Z.; Zhang, Q. A Review of Solid Electrolytes for Safe Lithium-Sulfur Batteries. *Sci. China Chem.* **2017**, *60*, 1508–1526. [[CrossRef](#)]
90. Meziane, R.; Bonnet, J.-P.; Courty, M.; Djellab, K.; Armand, M. Single-Ion Polymer Electrolytes Based on a Delocalized Polyanion for Lithium Batteries. *Electrochim. Acta* **2011**, *57*, 14–19. [[CrossRef](#)]
91. Zhu, Y.S.; Gao, X.W.; Wang, X.J.; Hou, Y.Y.; Liu, L.L.; Wu, Y.P. A Single-Ion Polymer Electrolyte Based on Boronate for Lithium Ion Batteries. *Electrochim. Commun.* **2012**, *22*, 29–32. [[CrossRef](#)]
92. Zhu, Y.S.; Wang, X.J.; Hou, Y.Y.; Gao, X.W.; Liu, L.L.; Wu, Y.P.; Shimizu, M. A New Single-Ion Polymer Electrolyte Based on Polyvinyl Alcohol for Lithium Ion Batteries. *Electrochim. Acta* **2013**, *87*, 113–118. [[CrossRef](#)]
93. Mitra, S. Electrical Conductivity Studies on the Plasticised PEO–DBP–CdX (X = Cl; SO₄) Polymer Electrolytes. *Solid State Ion.* **2002**, *154–155*, 37–43. [[CrossRef](#)]
94. Diederichsen, K.M.; McShane, E.J.; McCloskey, B.D. Promising Routes to a High Li⁺ Transference Number Electrolyte for Lithium Ion Batteries. *ACS Energy Lett.* **2017**, *2*, 2563–2575. [[CrossRef](#)]
95. Hao, S.-M.; Liang, S.; Sewell, C.D.; Li, Z.; Zhu, C.; Xu, J.; Lin, Z. Lithium-Conducting Branched Polymers: New Paradigm of Solid-State Electrolytes for Batteries. *Nano Lett.* **2021**, *21*, 7435–7447. [[CrossRef](#)]
96. Lafont, U.; Anastasopol, A.; Garcia-Tamayo, E.; Kelder, E. Electrostatic Spray Pyrolysis of LiNi_{0.5}Mn_{1.5}O₄ Films for 3D Li-Ion Microbatteries. *Thin Solid Film.* **2012**, *520*, 3464–3471. [[CrossRef](#)]
97. Yu, X.; Manthiram, A. A Review of Composite Polymer-Ceramic Electrolytes for Lithium Batteries. *Energy Storage Mater.* **2021**, *34*, 282–300. [[CrossRef](#)]
98. Stoeva, Z.; Martin-Litas, I.; Staunton, E.; Andreev, Y.G.; Bruce, P.G. Ionic Conductivity in the Crystalline Polymer Electrolytes PEO₆:LiXF₆, X = P, As, Sb. *J. Am. Chem. Soc.* **2003**, *125*, 4619–4626. [[CrossRef](#)]
99. Sun, J.; Liao, X.; Minor, A.M.; Balsara, N.P.; Zuckermann, R.N. Morphology-Conductivity Relationship in Crystalline and Amorphous Sequence-Defined Peptoid Block Copolymer Electrolytes. *J. Am. Chem. Soc.* **2014**, *136*, 14990–14997. [[CrossRef](#)] [[PubMed](#)]
100. Borodin, O.; Smith, G.D. Mechanism of Ion Transport in Amorphous Poly(Ethylene Oxide)/LiTFSI from Molecular Dynamics Simulations. *Macromolecules* **2006**, *39*, 1620–1629. [[CrossRef](#)]
101. Young, W.; Kuan, W.; Epps, T.H. Block Copolymer Electrolytes for Rechargeable Lithium Batteries. *J. Polym. Sci. B Polym. Phys.* **2014**, *52*, 1–16. [[CrossRef](#)]
102. Christie, A.M.; Lilley, S.J.; Staunton, E.; Andreev, Y.G.; Bruce, P.G. Increasing the Conductivity of Crystalline Polymer Electrolytes. *Nature* **2005**, *433*, 50–53. [[CrossRef](#)] [[PubMed](#)]
103. MacGlashan, G.S.; Andreev, Y.G.; Bruce, P.G. Structure of the Polymer Electrolyte Poly(Ethylene Oxide)₆:LiAsF₆. *Nature* **1999**, *398*, 792–794. [[CrossRef](#)]
104. Gadjourova, Z.; Andreev, Y.G.; Tunstall, D.P.; Bruce, P.G. Ionic Conductivity in Crystalline Polymer Electrolytes. *Nature* **2001**, *412*, 520–523. [[CrossRef](#)]
105. Zhang, C.; Staunton, E.; Andreev, Y.G.; Bruce, P.G. Raising the Conductivity of Crystalline Polymer Electrolytes by Aliovalent Doping. *J. Am. Chem. Soc.* **2005**, *127*, 18305–18308. [[CrossRef](#)] [[PubMed](#)]
106. Lilley, S.J.; Andreev, Y.G.; Bruce, P.G. Ionic Conductivity in Crystalline PEO₆:Li(AsF₆)_{1-x}(SbF₆)_x. *J. Am. Chem. Soc.* **2006**, *128*, 12036–12037. [[CrossRef](#)]

107. Prasanth, R.; Shubha, N.; Hng, H.H.; Srinivasan, M. Effect of Poly(Ethylene Oxide) on Ionic Conductivity and Electrochemical Properties of Poly(Vinylidenefluoride) Based Polymer Gel Electrolytes Prepared by Electrospinning for Lithium Ion Batteries. *J. Power Sources* **2014**, *245*, 283–291. [[CrossRef](#)]
108. Fan, L.; Li, M.; Li, X.; Xiao, W.; Chen, Z.; Lu, J. Interlayer Material Selection for Lithium-Sulfur Batteries. *Joule* **2019**, *3*, 361–386. [[CrossRef](#)]
109. Li, C.; Huang, Y.; Feng, X.; Zhang, Z.; Liu, P. High Electrochemical Performance Poly(Ethylene Oxide)/2,4-Toluene Diisocyanate/Polyethylene Glycol as Electrolytes for All-Solid-State Lithium Batteries. *J. Membr. Sci.* **2019**, *587*, 117179. [[CrossRef](#)]
110. Liang, J.; Sun, Q.; Zhao, Y.; Sun, Y.; Wang, C.; Li, W.; Li, M.; Wang, D.; Li, X.; Liu, Y.; et al. Stabilization of All-Solid-State Li–S Batteries with a Polymer–Ceramic Sandwich Electrolyte by Atomic Layer Deposition. *J. Mater. Chem. A* **2018**, *6*, 23712–23719. [[CrossRef](#)]
111. Nie, K.; Hong, Y.; Qiu, J.; Li, Q.; Yu, X.; Li, H.; Chen, L. Interfaces Between Cathode and Electrolyte in Solid State Lithium Batteries: Challenges and Perspectives. *Front. Chem.* **2018**, *6*, 616. [[CrossRef](#)]
112. Goodenough, J.B. Electrochemical Energy Storage in a Sustainable Modern Society. *Energy Environ. Sci.* **2014**, *7*, 14–18. [[CrossRef](#)]
113. Wu, F.; Zhu, N.; Bai, Y.; Liu, L.; Zhou, H.; Wu, C. Highly Safe Ionic Liquid Electrolytes for Sodium-Ion Battery: Wide Electrochemical Window and Good Thermal Stability. *ACS Appl. Mater. Interfaces* **2016**, *8*, 21381–21386. [[CrossRef](#)] [[PubMed](#)]
114. Fang, Z.; Luo, Y.; Liu, H.; Hong, Z.; Wu, H.; Zhao, F.; Liu, P.; Li, Q.; Fan, S.; Duan, W.; et al. Boosting the Oxidative Potential of Polyethylene Glycol-Based Polymer Electrolyte to 4.36 V by Spatially Restricting Hydroxyl Groups for High-Voltage Flexible Lithium-Ion Battery Applications. *Adv. Sci.* **2021**, *8*, 2100736. [[CrossRef](#)]
115. Marchiori, C.F.N.; Carvalho, R.P.; Ebadi, M.; Brandell, D.; Araujo, C.M. Understanding the Electrochemical Stability Window of Polymer Electrolytes in Solid-State Batteries from Atomic-Scale Modeling: The Role of Li-Ion Salts. *Chem. Mater.* **2020**, *32*, 7237–7246. [[CrossRef](#)]
116. Li, Q.; Takeda, Y.; Imanish, N.; Yang, J.; Sun, H.Y.; Yamamoto, O. Cycling Performances and Interfacial Properties of a Li/PEO-Li(CF₃SO₂)₂N-Ceramic Filler/LiNi_{0.8}Co_{0.2}O₂ Cell. *J. Power Sources* **2001**, *97–98*, 795–797. [[CrossRef](#)]
117. Seki, S.; Kobayashi, Y.; Miyashiro, H.; Yamanaka, A.; Mita, Y.; Iwahori, T. Degradation Mechanism Analysis of All-Solid-State Lithium Polymer Secondary Batteries by Using the Impedance Measurement. *J. Power Sources* **2005**, *146*, 741–744. [[CrossRef](#)]
118. Sasaki, Y.; Handa, M.; Kurashima, K.; Tonuma, T.; Usami, K. Application of Lithium Organoborate with Salicylic Ligand to Lithium Battery Electrolyte. *J. Electrochem. Soc.* **2001**, *148*, A999. [[CrossRef](#)]
119. Shimonishi, Y.; Zhang, T.; Imanishi, N.; Im, D.; Lee, D.J.; Hirano, A.; Takeda, Y.; Yamamoto, O.; Sammes, N. A Study on Lithium/Air Secondary Batteries—Stability of the NASICON-Type Lithium Ion Conducting Solid Electrolyte in Alkaline Aqueous Solutions. *J. Power Sources* **2011**, *196*, 5128–5132. [[CrossRef](#)]
120. Dashjav, E.; Ma, Q.; Xu, Q.; Tsai, C.-L.; Giarola, M.; Mariotto, G.; Tietz, F. The Influence of Water on the Electrical Conductivity of Aluminum-Substituted Lithium Titanium Phosphates. *Solid State Ion.* **2018**, *321*, 83–90. [[CrossRef](#)]
121. Xia, Y.; Fujieda, T.; Tatsumi, K.; Prosini, P.P.; Sakai, T. Thermal and Electrochemical Stability of Cathode Materials in Solid Polymer Electrolyte. *J. Power Sources* **2001**, *92*, 234–243. [[CrossRef](#)]
122. Zhao, Y.; Huang, Z.; Chen, S.; Chen, B.; Yang, J.; Zhang, Q.; Ding, F.; Chen, Y.; Xu, X. A Promising PEO/LAGP Hybrid Electrolyte Prepared by a Simple Method for All-Solid-State Lithium Batteries. *Solid State Ion.* **2016**, *295*, 65–71. [[CrossRef](#)]
123. Jiang, Y.; Yan, X.; Ma, Z.; Mei, P.; Xiao, W.; You, Q.; Zhang, Y. Development of the PEO Based Solid Polymer Electrolytes for All-Solid State Lithium Ion Batteries. *Polymers* **2018**, *10*, 1237. [[CrossRef](#)] [[PubMed](#)]
124. He, Z.; Chen, L.; Zhang, B.; Liu, Y.; Fan, L.-Z. Flexible Poly(Ethylene Carbonate)/Garnet Composite Solid Electrolyte Reinforced by Poly(Vinylidene Fluoride-Hexafluoropropylene) for Lithium Metal Batteries. *J. Power Sources* **2018**, *392*, 232–238. [[CrossRef](#)]
125. Vignarooban, K.; Kushagra, R.; Elango, A.; Badami, P.; Mellander, B.-E.; Xu, X.; Tucker, T.G.; Nam, C.; Kannan, A.M. Current Trends and Future Challenges of Electrolytes for Sodium-Ion Batteries. *Int. J. Hydrogen Energy* **2016**, *41*, 2829–2846. [[CrossRef](#)]
126. Karatas, Y.; Banhatti, R.D.; Kaskhedikar, N.; Burjanadze, M.; Funke, K.; Wiemhöfer, H.-D. Synthesis and Modeling of Polysiloxane-Based Salt-in-Polymer Electrolytes with Various Additives. *J. Phys. Chem. B* **2009**, *113*, 15473–15484. [[CrossRef](#)] [[PubMed](#)]
127. Paulsdorf, J. Ionic Conductivity in Polyphosphazene Polymer Electrolytes Prepared by the Living Cationic Polymerization. *Solid. State Ion.* **2004**, *169*, 25–33. [[CrossRef](#)]
128. Tominaga, Y.; Ohno, H. Lithium Ion Conduction in Linear- and Network-Type Polymers of PEO/Sulfonamide Salt Hybrid. *Electrochim. Acta* **2000**, *45*, 3081–3086. [[CrossRef](#)]
129. Wang, Q.; Zhang, H.; Cui, Z.; Zhou, Q.; Shangguan, X.; Tian, S.; Zhou, X.; Cui, G. Siloxane-Based Polymer Electrolytes for Solid-State Lithium Batteries. *Energy Storage Mater.* **2019**, *23*, 466–490. [[CrossRef](#)]
130. Wang, Q.; Cui, Z.; Zhou, Q.; Shangguan, X.; Du, X.; Dong, S.; Qiao, L.; Huang, S.; Liu, X.; Tang, K.; et al. A Supramolecular Interaction Strategy Enabling High-Performance All Solid State Electrolyte of Lithium Metal Batteries. *Energy Storage Mater.* **2020**, *25*, 756–763. [[CrossRef](#)]
131. Zhang, J.; Yang, J.; Dong, T.; Zhang, M.; Chai, J.; Dong, S.; Wu, T.; Zhou, X.; Cui, G. Aliphatic Polycarbonate-Based Solid-State Polymer Electrolytes for Advanced Lithium Batteries: Advances and Perspective. *Small* **2018**, *14*, 1800821. [[CrossRef](#)]
132. Rolland, J.; Brassinne, J.; Bourgeois, J.-P.; Poggi, E.; Vlad, A.; Gohy, J.-F. Chemically Anchored Liquid-PEO Based Block Copolymer Electrolytes for Solid-State Lithium-Ion Batteries. *J. Mater. Chem. A* **2014**, *2*, 11839–11846. [[CrossRef](#)]
133. Kondou, S.; Abdullah, M.; Popov, I.; Martins, M.L.; O'Dell, L.A.; Ueda, H.; Makhlooghiazad, F.; Nakanishi, A.; Sudoh, T.; Ueno, K.; et al. Poly(Ionic Liquid) Electrolytes at an Extreme Salt Concentration for Solid-State Batteries. *J. Am. Chem. Soc.* **2024**. [[CrossRef](#)]

134. Zhang, J.; Zeng, Y.; Li, Q.; Tang, Z.; Sun, D.; Huang, D.; Zhao, L.; Tang, Y.; Wang, H. Polymer-in-Salt Electrolyte Enables Ultrahigh Ionic Conductivity for Advanced Solid-State Lithium Metal Batteries. *Energy Storage Mater.* **2023**, *54*, 440–449. [[CrossRef](#)]
135. Wu, H.; Gao, P.; Jia, H.; Zou, L.; Zhang, L.; Cao, X.; Engelhard, M.H.; Bowden, M.E.; Ding, M.S.; Hu, J.; et al. A Polymer-in-Salt Electrolyte with Enhanced Oxidative Stability for Lithium Metal Polymer Batteries. *ACS Appl. Mater. Interfaces* **2021**, *13*, 31583–31593. [[CrossRef](#)]
136. Sun, M.; Zeng, Z.; Zhong, W.; Han, Z.; Peng, L.; Yu, C.; Cheng, S.; Xie, J. *In Situ* Prepared “Polymer-in-Salt” Electrolytes Enabling High-Voltage Lithium Metal Batteries. *J. Mater. Chem. A* **2022**, *10*, 11732–11741. [[CrossRef](#)]
137. Yan, K.; Fan, Y.; Hu, F.; Li, G.; Yang, X.; Wang, X.; Li, X.; Peng, C.; Wang, W.; Fan, H.; et al. A “Polymer-in-Salt” Solid Electrolyte Enabled by Fast Phase Transition Route for Stable Zn Batteries. *Adv. Funct. Mater.* **2024**, *34*, 2307740. [[CrossRef](#)]
138. Xie, J.; Xu, H.; Wang, Q.; Ke, R.; Han, B.; Chang, J.; Wang, J.; Deng, Y. A Polymer-in-Salt Electrolyte Enables Room Temperature Lithium Metal Batteries. *J. Electrochem. Soc.* **2022**, *169*, 040562. [[CrossRef](#)]
139. Bai, S.; Zhang, X.; Chen, Z.; Lin, J.; Wang, Q.; Zhang, Y. Design of Polymer-in-Salt Electrolyte for Solid State Lithium Battery with Wide Working Temperature Range. *ChemistrySelect* **2022**, *7*, e202201571. [[CrossRef](#)]
140. Zhang, J.; Cui, C.; Wang, P.-F.; Li, Q.; Chen, L.; Han, F.; Jin, T.; Liu, S.; Choudhary, H.; Raghavan, S.R.; et al. “Water-in-Salt” Polymer Electrolyte for Li-Ion Batteries. *Energy Environ. Sci.* **2020**, *13*, 2878–2887. [[CrossRef](#)]
141. Yang, J.; Li, R.; Zhang, P.; Zhang, J.; Meng, J.; Li, L.; Li, Z.; Pu, X. Crosslinked Polymer-in-Salt Solid Electrolyte with Multiple Ion Transport Paths for Solid-State Lithium Metal Batteries. *Energy Storage Mater.* **2024**, *64*, 103088. [[CrossRef](#)]
142. Yang, J.; Chu, Y.; Zhang, X.; Li, Y.; Cui, X.; Pan, Q. Realizing Highly Conductive “Polymer in Salt” Electrolytes through Li-Ion-Highway for Room Temperature All-Solid-State Li-S Batteries. *J. Energy Storage* **2024**, *96*, 112539. [[CrossRef](#)]
143. Liu, W.; Yi, C.; Li, L.; Liu, S.; Gui, Q.; Ba, D.; Li, Y.; Peng, D.; Liu, J. Designing Polymer-in-Salt Electrolyte and Fully Infiltrated 3D Electrode for Integrated Solid-State Lithium Batteries. *Angew. Chem.* **2021**, *133*, 13041–13050. [[CrossRef](#)]
144. Li, H.; Du, Y.; Wu, X.; Xie, J.; Lian, F. Developing “Polymer-in-Salt” High Voltage Electrolyte Based on Composite Lithium Salts for Solid-State Li Metal Batteries. *Adv. Funct. Mater.* **2021**, *31*, 2103049. [[CrossRef](#)]
145. Nguyen, M.L.; Nguyen, V.-C.; Lee, Y.-L.; Jan, J.-S.; Teng, H. Synergistic Combination of Ether-Linkage and Polymer-in-Salt for Electrolytes with Facile Li⁺ Conducting and High Stability in Solid-State Lithium Batteries. *Energy Storage Mater.* **2024**, *65*, 103178. [[CrossRef](#)]
146. Pan, L.; Feng, S.; Sun, H.; Liu, X.X.; Yuan, P.; Cao, M.; Gao, M.; Wang, Y.; Sun, Z. Ultrathin, Mechanically Durable, and Scalable Polymer-in-Salt Solid Electrolyte for High-Rate Lithium Metal Batteries. *Small* **2024**, *20*, 2400272. [[CrossRef](#)]
147. Zhu, J.; Zhang, Z.; Zhao, S.; Westover, A.S.; Belharouak, I.; Cao, P. Single-Ion Conducting Polymer Electrolytes for Solid-State Lithium–Metal Batteries: Design, Performance, and Challenges. *Adv. Energy Mater.* **2021**, *11*, 2003836. [[CrossRef](#)]
148. Yang, M.; Epps, T.H. Solid-State, Single-Ion Conducting, Polymer Blend Electrolytes with Enhanced Li⁺ Conduction, Electrochemical Stability, and Limiting Current Density. *Chem. Mater.* **2024**, *36*, 1855–1869. [[CrossRef](#)]
149. Fraile-Insagurbe, D.; Boaretto, N.; Aldalur, I.; Raposo, I.; Bonilla, F.J.; Armand, M.; Martínez-Ibañez, M. Novel Single-Ion Conducting Polymer Electrolytes with High Toughness and High Resistance against Lithium Dendrites. *Nano Res.* **2023**, *16*, 8457–8468. [[CrossRef](#)]
150. Zhang, J.; Zhu, J.; Zhao, R.; Liu, J.; Song, X.; Xu, N.; Liu, Y.; Zhang, H.; Wan, X.; Ma, Y.; et al. An All-in-One Free-Standing Single-Ion Conducting Semi-Solid Polymer Electrolyte for High-Performance Practical Li Metal Batteries. *Energy Environ. Sci.* **2024**, *17*, 7119–7128. [[CrossRef](#)]
151. Yuan, H.; Luan, J.; Yang, Z.; Zhang, J.; Wu, Y.; Lu, Z.; Liu, H. Single Lithium-Ion Conducting Solid Polymer Electrolyte with Superior Electrochemical Stability and Interfacial Compatibility for Solid-State Lithium Metal Batteries. *ACS Appl. Mater. Interfaces* **2020**, *12*, 7249–7256. [[CrossRef](#)] [[PubMed](#)]
152. Li, H.; Du, Y.; Zhang, Q.; Zhao, Y.; Lian, F. A Single-Ion Conducting Network as Rationally Coordinating Polymer Electrolyte for Solid-State Li Metal Batteries. *Adv. Energy Mater.* **2022**, *12*, 2103530. [[CrossRef](#)]
153. Li, Z.; Liu, F.; Chen, S.; Zhai, F.; Li, Y.; Feng, Y.; Feng, W. Single Li Ion Conducting Solid-State Polymer Electrolytes Based on Carbon Quantum Dots for Li-Metal Batteries. *Nano Energy* **2021**, *82*, 105698. [[CrossRef](#)]
154. Lingua, G.; Grysar, P.; Vlasov, P.S.; Verge, P.; Shaplov, A.S.; Gerbaldi, C. Unique Carbonate-Based Single Ion Conducting Block Copolymers Enabling High-Voltage, All-Solid-State Lithium Metal Batteries. *Macromolecules* **2021**, *54*, 6911–6924. [[CrossRef](#)] [[PubMed](#)]
155. Liang, H.; Zarrabeitia, M.; Chen, Z.; Jovanovic, S.; Merz, S.; Granwehr, J.; Passerini, S.; Bresser, D. Polysiloxane-Based Single-Ion Conducting Polymer Blend Electrolyte Comprising Small-Molecule Organic Carbonates for High-Energy and High-Power Lithium-Metal Batteries. *Adv. Energy Mater.* **2022**, *12*, 2200013. [[CrossRef](#)]
156. He, Y.; Li, H.; Huo, S.; Chen, Y.; Zhang, Y.; Wang, Y.; Cai, W.; Zeng, D.; Li, C.; Cheng, H. Enabling Interfacial Stability via 3D Networking Single Ion Conducting Nano Fiber Electrolyte for High Performance Lithium Metal Batteries. *J. Power Sources* **2021**, *490*, 229545. [[CrossRef](#)]
157. Zhou, M.; Liu, R.; Jia, D.; Cui, Y.; Liu, Q.; Liu, S.; Wu, D. Ultrathin Yet Robust Single Lithium-Ion Conducting Quasi-Solid-State Polymer-Brush Electrolytes Enable Ultralong-Life and Dendrite-Free Lithium-Metal Batteries. *Adv. Mater.* **2021**, *33*, 2100943. [[CrossRef](#)] [[PubMed](#)]
158. Zhou, X.; Zhou, Y.; Yu, L.; Qi, L.; Oh, K.-S.; Hu, P.; Lee, S.-Y.; Chen, C. Gel Polymer Electrolytes for Rechargeable Batteries toward Wide-Temperature Applications. *Chem. Soc. Rev.* **2024**, *53*, 5291–5337. [[CrossRef](#)]

159. Aruchamy, K.; Ramasundaram, S.; Divya, S.; Chandran, M.; Yun, K.; Oh, T.H. Gel Polymer Electrolytes: Advancing Solid-State Batteries for High-Performance Applications. *Gels* **2023**, *9*, 585. [[CrossRef](#)]
160. Castillo, J.; Santiago, A.; Judez, X.; Garbayo, I.; Coca Clemente, J.A.; Morant-Miñana, M.C.; Villaverde, A.; González-Marcos, J.A.; Zhang, H.; Armand, M.; et al. Safe, Flexible, and High-Performing Gel-Polymer Electrolyte for Rechargeable Lithium Metal Batteries. *Chem. Mater.* **2021**, *33*, 8812–8821. [[CrossRef](#)]
161. Wang, H.; Sheng, L.; Yasin, G.; Wang, L.; Xu, H.; He, X. Reviewing the Current Status and Development of Polymer Electrolytes for Solid-State Lithium Batteries. *Energy Storage Mater.* **2020**, *33*, 188–215. [[CrossRef](#)]
162. Liu, X.; Xin, X.; Shen, L.; Gu, Z.; Wu, J.; Yao, X. Poly(Methyl Methacrylate)-Based Gel Polymer Electrolyte for High-Performance Solid State Li-O₂ Battery with Enhanced Cycling Stability. *ACS Appl. Energy Mater.* **2021**, *4*, 3975–3982. [[CrossRef](#)]
163. Celik, M.; Kizilaslan, A.; Can, M.; Cetinkaya, T.; Akbulut, H. Electrochemical Investigation of PVDF: HFP Gel Polymer Electrolytes for Quasi-Solid-State Li-O₂ Batteries: Effect of Lithium Salt Type and Concentration. *Electrochim. Acta* **2021**, *371*, 137824. [[CrossRef](#)]
164. Jia, D.; Cui, Y.; Liu, Q.; Zhou, M.; Huang, J.; Liu, R.; Liu, S.; Zheng, B.; Zhu, Y.; Wu, D. Multifunctional Polymer Bottlebrush-Based Gel Polymer Electrolytes for Lithium Metal Batteries. *Mater. Today Nano* **2021**, *15*, 100128. [[CrossRef](#)]
165. Ma, C.; Cui, W.; Liu, X.; Ding, Y.; Wang, Y. In Situ Preparation of Gel Polymer Electrolyte for Lithium Batteries: Progress and Perspectives. *InfoMat* **2022**, *4*, e12232. [[CrossRef](#)]
166. Poiana, R.; Lufrano, E.; Tsurumaki, A.; Simari, C.; Nicotera, I.; Navarra, M.A. Safe Gel Polymer Electrolytes for High Voltage Li-Batteries. *Electrochim. Acta* **2022**, *401*, 139470. [[CrossRef](#)]
167. Long, M.-C.; Wu, G.; Wang, X.-L.; Wang, Y.-Z. Self-Adaptable Gel Polymer Electrolytes Enable High-Performance and All-Round Safety Lithium Ion Batteries. *Energy Storage Mater.* **2022**, *53*, 62–71. [[CrossRef](#)]
168. Ren, W.; Ding, C.; Fu, X.; Huang, Y. Advanced Gel Polymer Electrolytes for Safe and Durable Lithium Metal Batteries: Challenges, Strategies, and Perspectives. *Energy Storage Mater.* **2021**, *34*, 515–535. [[CrossRef](#)]
169. Liu, S.; Liu, W.; Ba, D.; Zhao, Y.; Ye, Y.; Li, Y.; Liu, J. Filler-Integrated Composite Polymer Electrolyte for Solid-State Lithium Batteries. *Adv. Mater.* **2023**, *35*, 2110423. [[CrossRef](#)] [[PubMed](#)]
170. Yu, Q.; Jiang, K.; Yu, C.; Chen, X.; Zhang, C.; Yao, Y.; Jiang, B.; Long, H. Recent Progress of Composite Solid Polymer Electrolytes for All-Solid-State Lithium Metal Batteries. *Chin. Chem. Lett.* **2021**, *32*, 2659–2678. [[CrossRef](#)]
171. Li, S.; Zhang, S.; Shen, L.; Liu, Q.; Ma, J.; Lv, W.; He, Y.; Yang, Q. Progress and Perspective of Ceramic/Polymer Composite Solid Electrolytes for Lithium Batteries. *Adv. Sci.* **2020**, *7*, 1903088. [[CrossRef](#)]
172. Dirican, M.; Yan, C.; Zhu, P.; Zhang, X. Composite Solid Electrolytes for All-Solid-State Lithium Batteries. *Mater. Sci. Eng. R Rep.* **2019**, *136*, 27–46. [[CrossRef](#)]
173. Li, B.; Su, Q.; Yu, L.; Wang, D.; Ding, S.; Zhang, M.; Du, G.; Xu, B. Li_{0.35}La_{0.55}TiO₃ Nanofibers Enhanced Poly(Vinylidene Fluoride)-Based Composite Polymer Electrolytes for All-Solid-State Batteries. *ACS Appl. Mater. Interfaces* **2019**, *11*, 42206–42213. [[CrossRef](#)]
174. Zheng, J.; Hu, Y.-Y. New Insights into the Compositional Dependence of Li-Ion Transport in Polymer–Ceramic Composite Electrolytes. *ACS Appl. Mater. Interfaces* **2018**, *10*, 4113–4120. [[CrossRef](#)]
175. Fan, P.; Liu, H.; Marosz, V.; Samuels, N.T.; Suib, S.L.; Sun, L.; Liao, L. High Performance Composite Polymer Electrolytes for Lithium-Ion Batteries. *Adv. Funct. Mater.* **2021**, *31*, 2101380. [[CrossRef](#)]
176. Xu, L.; Li, J.; Shuai, H.; Luo, Z.; Wang, B.; Fang, S.; Zou, G.; Hou, H.; Peng, H.; Ji, X. Recent Advances of Composite Electrolytes for Solid-State Li Batteries. *J. Energy Chem.* **2022**, *67*, 524–548. [[CrossRef](#)]
177. Tang, S.; Guo, W.; Fu, Y. Advances in Composite Polymer Electrolytes for Lithium Batteries and Beyond. *Adv. Energy Mater.* **2021**, *11*, 2000802. [[CrossRef](#)]
178. Tran, H.K.; Wu, Y.-S.; Chien, W.-C.; Wu, S.; Jose, R.; Lue, S.J.; Yang, C.-C. Composite Polymer Electrolytes Based on PVA/PAN for All-Solid-State Lithium Metal Batteries Operated at Room Temperature. *ACS Appl. Energy Mater.* **2020**, *3*, 11024–11035. [[CrossRef](#)]
179. Qiu, Z.; Liu, C.; Xin, J.; Wang, Q.; Wu, J.; Wang, W.; Zhou, J.; Liu, Y.; Guo, B.; Shi, S. High Conductive Composite Polymer Electrolyte via in Situ UV-Curing for All-Solid-State Lithium Ion Batteries. *ACS Sustain. Chem. Eng.* **2019**, *7*, 9875–9880. [[CrossRef](#)]
180. Zhang, D.; Xu, X.; Qin, Y.; Ji, S.; Huo, Y.; Wang, Z.; Liu, Z.; Shen, J.; Liu, J. Recent Progress in Organic–Inorganic Composite Solid Electrolytes for All-Solid-State Lithium Batteries. *Chem. A Eur. J.* **2020**, *26*, 1720–1736. [[CrossRef](#)] [[PubMed](#)]
181. Jeong, D.; Shim, J.; Shin, H.; Lee, J. Sustainable Lignin-Derived Cross-Linked Graft Polymers as Electrolyte and Binder Materials for Lithium Metal Batteries. *ChemSusChem* **2020**, *13*, 2642–2649. [[CrossRef](#)] [[PubMed](#)]
182. Wang, S.; Zhang, L.; Zeng, Q.; Liu, X.; Lai, W.-Y.; Zhang, L. Cellulose Microcrystals with Brush-Like Architectures as Flexible All-Solid-State Polymer Electrolyte for Lithium-Ion Battery. *ACS Sustain. Chem. Eng.* **2020**, *8*, 3200–3207. [[CrossRef](#)]
183. Zhou, K.; Zhang, M.; Zhang, X.; Wang, T.; Wang, H.; Wang, Z.; Tang, X.; Bai, M.; Li, S.; Wang, Z.; et al. A Cellulose Reinforced Polymer Composite Electrolyte for the Wide-Temperature-Range Solid Lithium Batteries. *Chem. Eng. J.* **2023**, *464*, 142537. [[CrossRef](#)]
184. Ai, S.; Wang, T.; Li, T.; Wan, Y.; Xu, X.; Lu, H.; Qu, T.; Luo, S.; Jiang, J.; Yu, X.; et al. A Chitosan/Poly(Ethylene Oxide)-Based Hybrid Polymer Composite Electrolyte Suitable for Solid-State Lithium Metal Batteries. *ChemistrySelect* **2020**, *5*, 2878–2885. [[CrossRef](#)]
185. Han, J.; Huang, Y.; Chen, Y.; Song, A.; Deng, X.; Liu, B.; Li, X.; Wang, M. High-Performance Gel Polymer Electrolyte Based on Chitosan-Lignocellulose for Lithium-Ion Batteries. *ChemElectroChem* **2020**, *7*, 1213–1224. [[CrossRef](#)]
186. Dall’Asta, V.; Berbenni, V.; Mustarelli, P.; Ravelli, D.; Samorì, C.; Quartarone, E. A Biomass-Derived Polyhydroxyalkanoate Biopolymer as Safe and Environmental-Friendly Skeleton in Highly Efficient Gel Electrolytes for Lithium Batteries. *Electrochim. Acta* **2017**, *247*, 63–70. [[CrossRef](#)]

187. Zhou, L.; Liu, S.; Li, W.; Song, H.; Du, L.; Cui, Z. Highly Conductive Poly(ϵ -Caprolactone) and Chitosan Based Polymer Electrolyte for Lithium Metal Battery. *J. Power Sources* **2023**, *553*, 232271. [[CrossRef](#)]
188. Perumal, P.; Christopher Selvin, P.; Selvasekarapandian, S.; Sivaraj, P. Structural and Electrical Properties of Bio-Polymer Pectin with LiClO₄ Solid Electrolytes for Lithium Ion Polymer Batteries. *Mater. Today Proc.* **2019**, *8*, 196–202. [[CrossRef](#)]
189. Rajendran, S.; Saratha, R. An Evaluation of Solid-State Electrolyte Based on Pectin and Lithium Bis (Trifluoromethanesulphonyl)Imide for Lithium-Ion Batteries. *Mater. Today Proc.* **2021**, *47*, 819–824. [[CrossRef](#)]
190. Arrieta, A.A.; Calabokis, O.P.; Mendoza, J.M. Effect of Lithium Salts on the Properties of Cassava Starch Solid Biopolymer Electrolytes. *Polymers* **2023**, *15*, 4150. [[CrossRef](#)] [[PubMed](#)]
191. Jin, Y.; Zong, X.; Zhang, X.; Jia, Z.; Xie, H.; Xiong, Y. Constructing 3D Li⁺-Percolated Transport Network in Composite Polymer Electrolytes for Rechargeable Quasi-Solid-State Lithium Batteries. *Energy Storage Mater.* **2022**, *49*, 433–444. [[CrossRef](#)]
192. Zou, S.; Yang, Y.; Wang, J.; Zhou, X.; Wan, X.; Zhu, M.; Liu, J. In Situ Polymerization of Solid-State Polymer Electrolytes for Lithium Metal Batteries: A Review. *Energy Environ. Sci.* **2024**, *17*, 4426–4460. [[CrossRef](#)]
193. Liu, L.; Qi, X.; Yin, S.; Zhang, Q.; Liu, X.; Suo, L.; Li, H.; Chen, L.; Hu, Y.-S. In Situ Formation of a Stable Interface in Solid-State Batteries. *ACS Energy Lett.* **2019**, *4*, 1650–1657. [[CrossRef](#)]
194. Deng, T.; Cao, L.; He, X.; Li, A.-M.; Li, D.; Xu, J.; Liu, S.; Bai, P.; Jin, T.; Ma, L.; et al. In Situ Formation of Polymer-Inorganic Solid-Electrolyte Interphase for Stable Polymeric Solid-State Lithium-Metal Batteries. *Chem.* **2021**, *7*, 3052–3068. [[CrossRef](#)]
195. Geng, Z.; Huang, Y.; Sun, G.; Chen, R.; Cao, W.; Zheng, J.; Li, H. In-Situ Polymerized Solid-State Electrolytes with Stable Cycling for Li/LiCoO₂ Batteries. *Nano Energy* **2022**, *91*, 106679. [[CrossRef](#)]
196. Mu, K.; Wang, D.; Dong, W.; Liu, Q.; Song, Z.; Xu, W.; Yao, P.; Chen, Y.; Yang, B.; Li, C.; et al. Hybrid Crosslinked Solid Polymer Electrolyte via In-Situ Solidification Enables High-Performance Solid-State Lithium Metal Batteries. *Adv. Mater.* **2023**, *35*, 2304686. [[CrossRef](#)]
197. Grewal, M.S.; Tanaka, M.; Kawakami, H. Bifunctional Poly(Ethylene Glycol) Based Crosslinked Network Polymers as Electrolytes for All-solid-state Lithium Ion Batteries. *Polym. Int.* **2019**, *68*, 684–693. [[CrossRef](#)]
198. Yang, H.; Zhang, B.; Jing, M.; Shen, X.; Wang, L.; Xu, H.; Yan, X.; He, X. In Situ Catalytic Polymerization of a Highly Homogeneous PDOL Composite Electrolyte for Long-Cycle High-Voltage Solid-State Lithium Batteries. *Adv. Energy Mater.* **2022**, *12*, 2201762. [[CrossRef](#)]
199. Zha, W.; Li, W.; Ruan, Y.; Wang, J.; Wen, Z. In Situ Fabricated Ceramic/Polymer Hybrid Electrolyte with Vertically Aligned Structure for Solid-State Lithium Batteries. *Energy Storage Mater.* **2021**, *36*, 171–178. [[CrossRef](#)]
200. Hao, Q.; Yan, J.; Gao, Y.; Chen, F.; Chen, X.; Qi, Y.; Li, N. In Situ Formed Gel Polymer Electrolytes Enable Stable Solid Electrolyte Interface for High-Performance Lithium Metal Batteries. *ACS Appl. Mater. Interfaces* **2024**, *16*, 44689–44696. [[CrossRef](#)]
201. Lin, W.; Zheng, X.; Ma, S.; Ji, K.; Wang, C.; Chen, M. Quasi-Solid Polymer Electrolyte with Multiple Lithium-Ion Transport Pathways by In Situ Thermal-Initiating Polymerization. *ACS Appl. Mater. Interfaces* **2023**, *15*, 8128–8137. [[CrossRef](#)]
202. Wu, M.; Liu, D.; Qu, D.; Lei, J.; Zhang, X.; Chen, H.; Tang, H. In-Situ Polymerized Composite Polymer Electrolyte with Cesium-Ion Additive Enables Dual-Interfacial Compatibility in All-Solid-State Lithium-Metal Batteries. *J. Colloid. Interface Sci.* **2022**, *615*, 627–635. [[CrossRef](#)] [[PubMed](#)]
203. Xu, Y.; Zhao, R.; Gao, L.; Gao, T.; Wang, W.; Bian, J.; Han, S.; Zhu, J.; Xu, Q.; Zhao, Y. A Fiber-Reinforced Solid Polymer Electrolyte by In Situ Polymerization for Stable Lithium Metal Batteries. *Nano Res.* **2023**, *16*, 9259–9266. [[CrossRef](#)]
204. Wang, J.; Tao, C.; Cao, J.; Jiao, X.; Wang, L.; Liu, T. A Quasi-Solid Electrolyte by In Situ Polymerization of Selective Solvent for Lithium-Metal Batteries. *ChemElectroChem* **2022**, *9*, e202200957. [[CrossRef](#)]
205. Ma, J.; Wang, Z.; Wu, J.; Gu, Z.; Xin, X.; Yao, X. In Situ Solidified Gel Polymer Electrolytes for Stable Solid-State Lithium Batteries at High Temperatures. *Batteries* **2022**, *9*, 28. [[CrossRef](#)]
206. Lin, Z.; Guo, X.; Zhang, R.; Tang, M.; Ding, P.; Zhang, Z.; Wu, L.; Wang, Y.; Zhao, S.; Zhang, Q.; et al. Molecular Structure Adjustment Enhanced Anti-Oxidation Ability of Polymer Electrolyte for Solid-State Lithium Metal Battery. *Nano Energy* **2022**, *98*, 107330. [[CrossRef](#)]
207. Zhou, Y.F.; Xie, S.; Chen, C.H. In-Situ Thermal Polymerization of Rechargeable Lithium Batteries with Poly(Methyl Methacrylate) Based Gel-Polymer Electrolyte. *J. Mater. Sci.* **2006**, *41*, 7492–7497. [[CrossRef](#)]
208. Nie, L.; Chen, S.; Zhang, M.; Gao, T.; Zhang, Y.; Wei, R.; Zhang, Y.; Liu, W. An In-Situ Polymerized Interphase Engineering for High-Voltage All-Solid-State Lithium-Metal Batteries. *Nano Res.* **2024**, *17*, 2687–2692. [[CrossRef](#)]
209. Yu, J.; Lin, X.; Liu, J.; Yu, J.T.T.; Robson, M.J.; Zhou, G.; Law, H.M.; Wang, H.; Tang, B.Z.; Ciucci, F. In Situ Fabricated Quasi-Solid Polymer Electrolyte for High-Energy-Density Lithium Metal Battery Capable of Subzero Operation. *Adv. Energy Mater.* **2022**, *12*, 2102932. [[CrossRef](#)]
210. Yang, T.; Zhang, W.; Liu, Y.; Zheng, J.; Xia, Y.; Tao, X.; Wang, Y.; Xia, X.; Huang, H.; Gan, Y.; et al. High-Performance Solid Lithium Metal Batteries Enabled by LiF/LiCl/LiIn Hybrid SEI via InCl₃ -Driven In Situ Polymerization of 1,3-Dioxolane. *Small* **2023**, *19*, 2303210. [[CrossRef](#)]
211. Wu, Y.; Ma, J.; Jiang, H.; Wang, L.; Zhang, F.; Feng, X.; Xiang, H. Confined In-Situ Polymerization of Poly(1,3-Dioxolane) and Poly(Vinylene Carbonate)-Based Quasi-Solid Polymer Electrolyte with Improved Uniformity for Lithium Metal Batteries. *Mater. Today Energy* **2023**, *32*, 101239. [[CrossRef](#)]

212. Xu, R.; Xiao, B.; Xuan, C.; Gao, S.; Chai, J.; Liu, S.; Chen, Y.; Zheng, Y.; Cheng, X.; Guo, Q.; et al. Facile and Powerful In Situ Polymerization Strategy for Sulfur-Based All-Solid Polymer Electrolytes in Lithium Batteries. *ACS Appl. Mater. Interfaces* **2021**, *13*, 34274–34281. [CrossRef] [PubMed]
213. Zhu, M.; Ma, J.; Wang, Z.; He, H.; Yao, X. In-Situ Polymerized Gel Polymer Electrolytes for Stable Solid-State Lithium Batteries with Long-Cycle Life. *J. Power Sources* **2023**, *585*, 233651. [CrossRef]
214. Meisner, Q.J.; Jiang, S.; Cao, P.; Glossmann, T.; Hintennach, A.; Zhang, Z. An *In Situ* Generated Polymer Electrolyte via Anionic Ring-Opening Polymerization for Lithium–Sulfur Batteries. *J. Mater. Chem. A* **2021**, *9*, 25927–25933. [CrossRef]
215. He, Y.; Li, Y.; Tong, Q.; Zhang, J.; Weng, J.; Zhu, M. Highly Conductive and Thermostable Grafted Polyrotaxane/Ceramic Hybrid Polymer Electrolyte for Solid-State Lithium-Metal Batteries. *ACS Appl. Mater. Interfaces* **2021**, *13*, 41593–41599. [CrossRef]
216. Zhao, Z.; Zhang, Y.; Li, S.; Wang, S.; Li, Y.; Mi, H.; Sun, L.; Ren, X.; Zhang, P. A Lithium Carboxylate Grafted Dendrite-Free Polymer Electrolyte for an All-Solid-State Lithium-Ion Battery. *J. Mater. Chem. A* **2019**, *7*, 25818–25823. [CrossRef]
217. Guo, K.; Li, S.; Chen, G.; Wang, J.; Wang, Y.; Xie, X.; Xue, Z. One-Pot Synthesis of Polyester-Based Linear and Graft Copolymers for Solid Polymer Electrolytes. *CCS Chem.* **2022**, *4*, 3134–3149. [CrossRef]
218. Liu, D.; Lu, Z.; Lin, Z.; Zhang, C.; Dai, K.; Wei, W. Organoboron- and Cyano-Grafted Solid Polymer Electrolytes Boost the Cyclability and Safety of High-Voltage Lithium Metal Batteries. *ACS Appl. Mater. Interfaces* **2023**, *15*, 21112–21122. [CrossRef] [PubMed]
219. Colombo, F.; Bonizzoni, S.; Ferrara, C.; Simonutti, R.; Mauri, M.; Falco, M.; Gerbaldi, C.; Mustarelli, P.; Ruffo, R. Polymer-in-Ceramic Nanocomposite Solid Electrolyte for Lithium Metal Batteries Encompassing PEO-Grafted TiO₂ Nanocrystals. *J. Electrochem. Soc.* **2020**, *167*, 070535. [CrossRef]
220. Li, H.; Shen, X.; Hua, H.; Gao, J.; Wen, Z.; Wang, X.; Peng, L.; Wu, D.; Zhang, P.; Zhao, J. A Novel Single-Ion Conductor Gel Polymer Electrolyte Prepared by Co-Irradiation Grafting and Electrospinning Process. *Solid State Ion.* **2020**, *347*, 115246. [CrossRef]
221. Min, H.J.; Park, M.S.; Kang, M.; Kim, J.H. Excellent Film-Forming, Ion-Conductive, Zwitterionic Graft Copolymer Electrolytes for Solid-State Supercapacitors. *Chem. Eng. J.* **2021**, *412*, 127500. [CrossRef]
222. Whba, R.; Su'ait, M.S.; TianKhoon, L.; Ibrahim, S.; Mohamed, N.S.; Ahmad, A. In-Situ UV Cured Acrylonitrile Grafted Epoxidized Natural Rubber (ACN-g-ENR)—LiTFSI Solid Polymer Electrolytes for Lithium-Ion Rechargeable Batteries. *React. Funct. Polym.* **2021**, *164*, 104938. [CrossRef]
223. Huo, H.; Wu, B.; Zhang, T.; Zheng, X.; Ge, L.; Xu, T.; Guo, X.; Sun, X. Anion-Immobilized Polymer Electrolyte Achieved by Cationic Metal-Organic Framework Filler for Dendrite-Free Solid-State Batteries. *Energy Storage Mater.* **2019**, *18*, 59–67. [CrossRef]
224. Zhang, H.; Wang, S.; Wang, A.; Li, Y.; Yu, F.; Chen, Y. Polyethylene Glycol-Grafted Cellulose-Based Gel Polymer Electrolyte for Long-Life Li-Ion Batteries. *Appl. Surf. Sci.* **2022**, *593*, 153411. [CrossRef]
225. Liu, X.; Mao, W.; Gong, J.; Liu, H.; Shao, Y.; Sun, L.; Wang, H.; Wang, C. Enhanced Electrochemical Performance of PEO-Based Composite Polymer Electrolyte with Single-Ion Conducting Polymer Grafted SiO₂ Nanoparticles. *Polymers* **2023**, *15*, 394. [CrossRef] [PubMed]
226. Yuan, B.; Zhao, B.; Cong, Z.; Cheng, Z.; Wang, Q.; Lu, Y.; Han, X. A Flexible, Fireproof, Composite Polymer Electrolyte Reinforced by Electrospun Polyimide for Room-Temperature Solid-State Batteries. *Polymers* **2021**, *13*, 3622. [CrossRef]
227. Hu, T.; Shen, X.; Peng, L.; Liu, Y.; Wang, X.; Ma, H.; Zhang, P.; Zhao, J. Preparation of Single-Ion Conductor Solid Polymer Electrolyte by Multi-Nozzle Electrospinning Process for Lithium-Ion Batteries. *J. Phys. Chem. Solids* **2021**, *158*, 110229. [CrossRef]
228. Gao, L.; Tang, B.; Jiang, H.; Xie, Z.; Wei, J.; Zhou, Z. Fiber-Reinforced Composite Polymer Electrolytes for Solid-State Lithium Batteries. *Adv. Sustain. Syst.* **2022**, *6*, 2100389. [CrossRef]
229. Wang, N.; Wei, Y.; Yu, S.; Zhang, W.; Huang, X.; Fan, B.; Yuan, H.; Tan, Y. A Flexible PEO-Based Polymer Electrolyte with Cross-Linked Network for High-Voltage All Solid-State Lithium-Ion Battery. *J. Mater. Sci. Technol.* **2024**, *183*, 206–214. [CrossRef]
230. Panneerselvam, T.; Rajamani, A.; Janani, N.; Murugan, R.; Sivaprakasam, S. Electrospun Composite Polymer Electrolyte for High-Performance Quasi Solid-State Lithium Metal Batteries. *Ionics* **2023**, *29*, 1395–1406. [CrossRef]
231. Seo, Y.; Jung, Y.-C.; Park, M.-S.; Kim, D.-W. Solid Polymer Electrolyte Supported by Porous Polymer Membrane for All-Solid-State Lithium Batteries. *J. Membr. Sci.* **2020**, *603*, 117995. [CrossRef]
232. Wang, Y.; Liu, T.; Liu, C.; Liu, G.; Yu, J.; Zou, Q. Solid-State Lithium Battery with Garnet Li₇La₃Zr₂O₁₂ Nanofibers Composite Polymer Electrolytes. *Solid. State Ion.* **2022**, *378*, 115897. [CrossRef]
233. Gao, L.; Li, J.; Ju, J.; Cheng, B.; Kang, W.; Deng, N. High-Performance All-Solid-State Polymer Electrolyte with Fast Conductivity Pathway Formed by Hierarchical Structure Polyamide 6 Nanofiber for Lithium Metal Battery. *J. Energy Chem.* **2021**, *54*, 644–654. [CrossRef]
234. Gao, L.; Li, J.; Ju, J.; Cheng, B.; Kang, W.; Deng, N. Polyvinylidene Fluoride Nanofibers with Embedded Li_{6.4}La₃Zr_{1.4}Ta_{0.6}O₁₂ Fillers Modified Polymer Electrolytes for High-Capacity and Long-Life All-Solid-State Lithium Metal Batteries. *Compos. Sci. Technol.* **2020**, *200*, 108408. [CrossRef]
235. Bandyopadhyay, S.; Gupta, A.; Srivastava, R.; Nandan, B. Bio-Inspired Design of Electrospun Poly(Acrylonitrile) and Novel Ionene Based Nanofibrous Mats as Highly Flexible Solid State Polymer Electrolyte for Lithium Batteries. *Chem. Eng. J.* **2022**, *440*, 135926. [CrossRef]
236. Arifeen, W.U.; Abideen, Z.U.; Guru Parakash, N.; Xiaolong, L.; Ko, T.J. Effects of a High-Performance, Solution-Cast Composite Electrolyte on the Host Electrospun Polymer Membrane for Solid-State Lithium Metal Batteries. *Mater. Today Energy* **2023**, *33*, 101270. [CrossRef]

237. Ma, Y.; Wan, J.; Yang, Y.; Ye, Y.; Xiao, X.; Boyle, D.T.; Burke, W.; Huang, Z.; Chen, H.; Cui, Y.; et al. Scalable, Ultrathin, and High-Temperature-Resistant Solid Polymer Electrolytes for Energy-Dense Lithium Metal Batteries. *Adv. Energy Mater.* **2022**, *12*, 2103720. [[CrossRef](#)]
238. Xu, H.; Zhang, X.; Jiang, J.; Li, M.; Shen, Y. Ultrathin $\text{Li}_7\text{La}_3\text{Zr}_2\text{O}_{12}$ @PAN Composite Polymer Electrolyte with High Conductivity for All-Solid-State Lithium-Ion Battery. *Solid State Ion.* **2020**, *347*, 115227. [[CrossRef](#)]
239. Xian, C.; Zhang, S.; Liu, P.; Huang, L.; He, X.; Shen, S.; Cao, F.; Liang, X.; Wang, C.; Wan, W.; et al. An Advanced Gel Polymer Electrolyte for Solid-State Lithium Metal Batteries. *Small* **2024**, *20*, 2306381. [[CrossRef](#)] [[PubMed](#)]
240. Khoon, L.T.; Fui, M.-L.W.; Hassan, N.H.; Su'ait, M.S.; Vedarajan, R.; Matsumi, N.; Bin Kassim, M.; Shyuan, L.K.; Ahmad, A. In Situ Sol-Gel Preparation of ZrO_2 in Nano-Composite Polymer Electrolyte of PVDF-HFP/MG49 for Lithium-Ion Polymer Battery. *J. Sol-Gel Sci. Technol.* **2019**, *90*, 665–675. [[CrossRef](#)]
241. Luu, V.T.; Nguyen, Q.H.; Park, M.G.; Nguyen, H.L.; Seo, M.-H.; Jeong, S.-K.; Cho, N.; Lee, Y.-W.; Cho, Y.; Lim, S.N.; et al. Cubic Garnet Solid Polymer Electrolyte for Room Temperature Operable All-Solid-State-Battery. *J. Mater. Res. Technol.* **2021**, *15*, 5849–5863. [[CrossRef](#)]
242. Azarian, M.H.; Woothikanokkhan, J. In Situ Sol-Gel Synthesis of Tungsten Trioxide Networks in Polymer Electrolyte: Dual-functional Solid State Chromogenic Smart Film. *J. Appl. Polym. Sci.* **2021**, *138*, 49863. [[CrossRef](#)]
243. Liu, Q.; Yu, T.; Yang, H.; Xu, S.; Li, H.; Chen, K.; Xu, R.; Zhou, T.; Sun, Z.; Li, F. Ion Coordination to Improve Ionic Conductivity in Polymer Electrolytes for High Performance Solid-State Batteries. *Nano Energy* **2022**, *103*, 107763. [[CrossRef](#)]
244. Chen, G.; Zhang, K.; Liu, Y.; Ye, L.; Gao, Y.; Lin, W.; Xu, H.; Wang, X.; Bai, Y.; Wu, C. Flame-Retardant Gel Polymer Electrolyte and Interface for Quasi-Solid-State Sodium Ion Batteries. *Chem. Eng. J.* **2020**, *401*, 126065. [[CrossRef](#)]
245. Wang, X.; Liu, Z.; Tang, Y.; Chen, J.; Mao, Z.; Wang, D. PVDF-HFP/PMMA/TPU-Based Gel Polymer Electrolytes Composed of Conductive $\text{Na}_3\text{Zr}_2\text{Si}_2\text{PO}_{12}$ Filler for Application in Sodium Ions Batteries. *Solid State Ion.* **2021**, *359*, 115532. [[CrossRef](#)]
246. Li, L.; Xie, M.; Zhang, Y.; Xu, Y.; Li, J.; Shan, Y.; Zhao, Y.; Zhou, D.; Chen, X.; Cui, W. Thermal Safety and Performances Analysis of Gel Polymer Electrolytes Synthesized by in Situ Polymerization for Li-Ion Battery. *J. Solid State Electrochem.* **2021**, *25*, 2021–2032. [[CrossRef](#)]
247. Wen, P.; Lu, P.; Shi, X.; Yao, Y.; Shi, H.; Liu, H.; Yu, Y.; Wu, Z. Photopolymerized Gel Electrolyte with Unprecedented Room-Temperature Ionic Conductivity for High-Energy-Density Solid-State Sodium Metal Batteries. *Adv. Energy Mater.* **2021**, *11*, 2002930. [[CrossRef](#)]
248. Mohanty, D.; Chen, S.-Y.; Hung, I.-M. Effect of Lithium Salt Concentration on Materials Characteristics and Electrochemical Performance of Hybrid Inorganic/Polymer Solid Electrolyte for Solid-State Lithium-Ion Batteries. *Batteries* **2022**, *8*, 173. [[CrossRef](#)]
249. Lee, T.K.; Andersson, R.; Dzulkurnain, N.A.; Hernández, G.; Mindemark, J.; Brandell, D. Polyester-ZrO₂ Nanocomposite Electrolytes with High Li Transference Numbers for Ambient Temperature All-Solid-State Lithium Batteries. *Batter. Supercaps* **2021**, *4*, 653–662. [[CrossRef](#)]
250. Zhang, P.; Li, R.; Huang, J.; Liu, B.; Zhou, M.; Wen, B.; Xia, Y.; Okada, S. Flexible Poly(Vinylidene Fluoride- Co-Hexafluoropropylene)-Based Gel Polymer Electrolyte for High-Performance Lithium-Ion Batteries. *RSC Adv.* **2021**, *11*, 11943–11951. [[CrossRef](#)]
251. Zhang, Y.; Lu, W.; Cong, L.; Liu, J.; Sun, L.; Mauger, A.; Julien, C.M.; Xie, H.; Liu, J. Cross-Linking Network Based on Poly(Ethylene Oxide): Solid Polymer Electrolyte for Room Temperature Lithium Battery. *J. Power Sources* **2019**, *420*, 63–72. [[CrossRef](#)]
252. Chen, S.; Wang, J.; Wei, Z.; Zhang, Z.; Deng, Y.; Yao, X.; Xu, X. One-Pot Synthesis of Crosslinked Polymer Electrolyte beyond 5V Oxidation Potential for All-Solid-State Lithium Battery. *J. Power Sources* **2019**, *431*, 1–7. [[CrossRef](#)]
253. Wen, S.; Luo, C.; Wang, Q.; Wei, Z.; Zeng, Y.; Jiang, Y.; Zhang, G.; Xu, H.; Wang, J.; Wang, C.; et al. Integrated Design of Ultrathin Crosslinked Network Polymer Electrolytes for Flexible and Stable All-Solid-State Lithium Batteries. *Energy Storage Mater.* **2022**, *47*, 453–461. [[CrossRef](#)]
254. Davino, S.; Callegari, D.; Pasini, D.; Thomas, M.; Nicotera, I.; Bonizzoni, S.; Mustarelli, P.; Quartarone, E. Cross-Linked Gel Electrolytes with Self-Healing Functionalities for Smart Lithium Batteries. *ACS Appl. Mater. Interfaces* **2022**, *14*, 51941–51953. [[CrossRef](#)]
255. Li, X.; Zheng, Y.; Duan, Y.; Shang, M.; Niu, J.; Li, C.Y. Designing Comb-Chain Crosslinker-Based Solid Polymer Electrolytes for Additive-Free All-Solid-State Lithium Metal Batteries. *Nano Lett.* **2020**, *20*, 6914–6921. [[CrossRef](#)] [[PubMed](#)]
256. Zhang, T.; Zhang, J.; Yang, S.; Li, Y.; Dong, R.; Yuan, J.; Liu, Y.; Wu, Z.; Song, Y.; Zhong, Y.; et al. Facile In Situ Chemical Cross-Linking Gel Polymer Electrolyte, Which Confines the Shuttle Effect with High Ionic Conductivity and Li-Ion Transference Number for Quasi-Solid-State Lithium-Sulfur Battery. *ACS Appl. Mater. Interfaces* **2021**, *13*, 44497–44508. [[CrossRef](#)] [[PubMed](#)]
257. Zhou, B.; Jiang, J.; Zhang, F.; Zhang, H. Crosslinked Poly(Ethylene Oxide)-Based Membrane Electrolyte Consisting of Polyhedral Oligomeric Silsesquioxane Nanocages for All-Solid-State Lithium Ion Batteries. *J. Power Sources* **2020**, *449*, 227541. [[CrossRef](#)]
258. Olmedo-Martínez, J.L.; Meabe, L.; Riva, R.; Guzmán-González, G.; Porcarelli, L.; Forsyth, M.; Mugica, A.; Calafel, I.; Müller, A.J.; Lecomte, P.; et al. Flame Retardant Polyphosphoester Copolymers as Solid Polymer Electrolyte for Lithium Batteries. *Polym. Chem.* **2021**, *12*, 3441–3450. [[CrossRef](#)]
259. Tang, L.; Chen, B.; Zhang, Z.; Ma, C.; Chen, J.; Huang, Y.; Zhang, F.; Dong, Q.; Xue, G.; Chen, D.; et al. Polyfluorinated Crosslinker-Based Solid Polymer Electrolytes for Long-Cycling 4.5 V Lithium Metal Batteries. *Nat. Commun.* **2023**, *14*, 2301. [[CrossRef](#)] [[PubMed](#)]

260. Kuai, Y.; Wang, F.; Yang, J.; Lu, H.; Xu, Z.; Xu, X.; NuLi, Y.; Wang, J. Silica-Nanoresin Crosslinked Composite Polymer Electrolyte for Ambient-Temperature All-Solid-State Lithium Batteries. *Mater. Chem. Front.* **2021**, *5*, 6502–6511. [[CrossRef](#)]
261. Cai, X.; Cai, Z.; Yuan, H.; Zhang, W.; Wang, S.; Wang, H.; Lan, J.; Yu, Y.; Yang, X. An Initiator-Free and Solvent-Free in-Situ Self-Catalyzed Crosslinked Polymer Electrolyte for All-Solid-State Lithium-Metal Batteries. *J. Colloid Interface Sci.* **2023**, *648*, 972–982. [[CrossRef](#)]
262. Xu, R.; Xu, S.; Wang, F.; Xiao, R.; Tang, P.; Zhang, X.; Bai, S.; Sun, Z.; Li, F. Double Crosslinked Polymer Electrolyte by C–S–C Group and Metal–Organic Framework for Solid-State Lithium Batteries. *Small Struct.* **2023**, *4*, 2200206. [[CrossRef](#)]
263. Ji, X.; Li, S.; Cao, M.; Liang, R.; Xiao, L.; Yue, K.; Liu, S.; Zhou, X.; Guo, Z. Crosslinked Polymer-Brush Electrolytes: An Approach to Safe All-Solid-State Lithium Metal Batteries at Room Temperature. *Batter. Supercaps* **2022**, *5*, e202100319. [[CrossRef](#)]
264. Maddu, A.; Sulaeman, A.S.; Tri Wahyudi, S.; Rifai, A. Enhancing Ionic Conductivity of Carboxymethyl Cellulose-Lithium Perchlorate with Crosslinked Citric Acid as Solid Polymer Electrolytes for Lithium Polymer Batteries. *Int. J. Renew. Energy Dev.* **2022**, *11*, 1002–1011. [[CrossRef](#)]
265. Wang, X.; Sun, J.; Feng, C.; Wang, X.; Xu, M.; Sun, J.; Zhang, N.; Ma, J.; Wang, Q.; Zong, C.; et al. Lithium Bis(Oxalate)Borate Crosslinked Polymer Electrolytes for High-Performance Lithium Batteries. *J. Energy Chem.* **2021**, *55*, 228–235. [[CrossRef](#)]
266. Ma, F.; Zhang, Z.; Yan, W.; Ma, X.; Sun, D.; Jin, Y.; Chen, X.; He, K. Solid Polymer Electrolyte Based on Polymerized Ionic Liquid for High Performance All-Solid-State Lithium-Ion Batteries. *ACS Sustain. Chem. Eng.* **2019**, *7*, 4675–4683. [[CrossRef](#)]
267. Mendes, T.C.; Goujon, N.; Malic, N.; Postma, A.; Chieffari, J.; Zhu, H.; Howlett, P.C.; Forsyth, M. Polymerized Ionic Liquid Block Copolymer Electrolytes for All-Solid-State Lithium-Metal Batteries. *J. Electrochem. Soc.* **2020**, *167*, 070525. [[CrossRef](#)]
268. Sun, Y.; Zhang, X.; Ma, C.; Guo, N.; Liu, Y.; Liu, J.; Xie, H. Fluorine-Containing Triblock Copolymers as Solid-State Polymer Electrolytes for Lithium Metal Batteries. *J. Power Sources* **2021**, *516*, 230686. [[CrossRef](#)]
269. Zhang, B.; Liu, Y.; Pan, X.; Liu, J.; Doyle-Davis, K.; Sun, L.; Liu, J.; Jiao, X.; Jie, J.; Xie, H.; et al. Dendrite-Free Lithium Metal Solid Battery with a Novel Polyester Based Triblock Copolymer Solid-State Electrolyte. *Nano Energy* **2020**, *72*, 104690. [[CrossRef](#)]
270. Yang, L.; Nie, Y.; Liu, Y.; Zheng, Y.; Luo, D.; Yang, N.; Ma, Q.; Xu, M.; Ma, X.; Yu, A.; et al. The Plasticizer-Free Composite Block Copolymer Electrolytes for Ultralong Lifespan All-Solid-State Lithium-Metal Batteries. *Nano Energy* **2022**, *100*, 107499. [[CrossRef](#)]
271. Khudyshkina, A.D.; Butzelaar, A.J.; Guo, Y.; Hoffmann, M.; Bergfeldt, T.; Schaller, M.; Indris, S.; Wilhelm, M.; Théato, P.; Jeschull, F. From Lithium to Potassium: Comparison of Cations in Poly(Ethylene Oxide)-Based Block Copolymer Electrolytes for Solid-State Alkali Metal Batteries. *Electrochim. Acta* **2023**, *454*, 142421. [[CrossRef](#)]
272. Guan, M.; Liu, S.; Jiao, K.; Huang, Y.; Zhao, J.; Yan, J. Designing Thermomechanical Stable Gel-Polymer Electrolytes Mediated by Block-Copolymer Nanofibers for Quasi-Solid-State Lithium Batteries. *Adv. Energy Sustain. Res.* **2022**, *3*, 2200022. [[CrossRef](#)]
273. He, Y.; Liu, N.; Kohl, P.A. Difunctional Block Copolymer with Ion Solvating and Crosslinking Sites as Solid Polymer Electrolyte for Lithium Batteries. *J. Power Sources* **2021**, *481*, 228832. [[CrossRef](#)]
274. Gregory, G.L.; Gao, H.; Liu, B.; Gao, X.; Rees, G.J.; Pasta, M.; Bruce, P.G.; Williams, C.K. Buffering Volume Change in Solid-State Battery Composite Cathodes with CO₂-Derived Block Polycarbonate Ethers. *J. Am. Chem. Soc.* **2022**, *144*, 17477–17486. [[CrossRef](#)]
275. Butzelaar, A.J.; Röring, P.; Mach, T.P.; Hoffmann, M.; Jeschull, F.; Wilhelm, M.; Winter, M.; Brunklaus, G.; Théato, P. Styrene-Based Poly(Ethylene Oxide) Side-Chain Block Copolymers as Solid Polymer Electrolytes for High-Voltage Lithium-Metal Batteries. *ACS Appl. Mater. Interfaces* **2021**, *13*, 39257–39270. [[CrossRef](#)] [[PubMed](#)]
276. Butzelaar, A.J.; Röring, P.; Hoffmann, M.; Atik, J.; Paillard, E.; Wilhelm, M.; Brunklaus, G.; Theato, P. Advanced Block Copolymer Design for Polymer Electrolytes: Prospects of Microphase Separation. *Macromolecules* **2021**, *54*, 11101–11112. [[CrossRef](#)]
277. Sun, Y.; Zhang, X.; Xu, P.; Liu, Y.; Dong, F.; Ma, C.; Liu, J.; Xie, H. Perfluoropolyether-Based Block Copolymer Electrolytes Enabling High-Temperature-Resistant Solid-State Lithium Metal Batteries. *J. Power Sources* **2023**, *561*, 232751. [[CrossRef](#)]
278. Zhu, X.; Fang, Z.; Deng, Q.; Zhou, Y.; Fu, X.; Wu, L.; Yan, W.; Yang, Y. Poly(Ionic Liquid)@PEGMA Block Polymer Initiated Microphase Separation Architecture in Poly(Ethylene Oxide)-Based Solid-State Polymer Electrolyte for Flexible and Self-Healing Lithium Batteries. *ACS Sustain. Chem. Eng.* **2022**, *10*, 4173–4185. [[CrossRef](#)]
279. Zhou, X.; Ye, Q.; Pang, B.; Wu, Z.; Yang, T.; Zhang, W.; Xia, Y.; Huang, H.; Xia, X.; He, X.; et al. Styrene–Butadiene–Styrene Block Copolymer-Li_{5.5}PS_{4.5}Cl_{1.5} Composite Solid-State Electrolyte Enabling a High-Performance All-Solid-State Lithium Battery. *ACS Appl. Energy Mater.* **2023**, *6*, 12120–12127. [[CrossRef](#)]
280. Meng, N.; Lian, F.; Cui, G. Macromolecular Design of Lithium Conductive Polymer as Electrolyte for Solid-State Lithium Batteries. *Small* **2021**, *17*, 2005762. [[CrossRef](#)] [[PubMed](#)]
281. Mohamed Ali, T.; Padmanathan, N.; Selladurai, S. Effect of Nanofiller CeO₂ on Structural, Conductivity, and Dielectric Behaviors of Plasticized Blend Nanocomposite Polymer Electrolyte. *Ionics* **2015**, *21*, 829–840. [[CrossRef](#)]
282. Lin, C.W.; Hung, C.L.; Venkateswarlu, M.; Hwang, B.J. Influence of TiO₂ Nano-Particles on the Transport Properties of Composite Polymer Electrolyte for Lithium-Ion Batteries. *J. Power Sources* **2005**, *146*, 397–401. [[CrossRef](#)]
283. Ni'mah, Y.L.; Saputra, M.A.E.; Suprapto, S.; Fansuri, H.; Suwarta, P.; Subhan, A.; Pradanawati, S.A. The Fabrication of Solid Polymer Electrolyte from CS/PEO/NaClO₄/Fly Ash Composite. *Polymers* **2022**, *14*, 4792. [[CrossRef](#)] [[PubMed](#)]
284. Yang, Z.; Sun, Z.; Liu, C.; Li, Y.; Zhou, G.; Zuo, S.; Wang, J.; Wu, W. Lithiated Nanosheets Hybridized Solid Polymer Electrolyte to Construct Li⁺ Conduction Highways for Advanced All-Solid-State Lithium Battery. *J. Power Sources* **2021**, *484*, 229287. [[CrossRef](#)]
285. Shenbagavalli, S.; Muthuvinayagam, M.; Revathy, M.S. Preparation and Characterization of Proton (H⁺) Conducting Solid Blend Polymer Electrolytes Based on PEO/P(VdF-HFP) Incorporated with NH₄SCN. *J. Non-Cryst. Solids* **2022**, *579*, 121368. [[CrossRef](#)]

286. Laxmiprasanna, N.; Reddy, P.S.; Kumar, G.S.; Reddy, M.B.; Ganta, K.K.; Jeedi, V.R.; Praveen, B.V.S. A Review on Nano Composite Polymer Electrolytes for High-Performance Batteries. *Mater. Today Proc.* **2023**, *72*, 286–292. [[CrossRef](#)]
287. Deka, M.; Kumar, A. Electrical and Electrochemical Studies of Poly(Vinylidene Fluoride)-Clay Nanocomposite Gel Polymer Electrolytes for Li-Ion Batteries. *J. Power Sources* **2011**, *196*, 1358–1364. [[CrossRef](#)]
288. Karan, S.; Sahu, T.B.; Sahu, M.; Mahipal, Y.K.; Agrawal, R.C. Characterization of Ion Transport Property in Hot-Press Cast Solid Polymer Electrolyte (SPE) Films: [PEO: Zn(CF₃SO₃)₂]. *Ionics* **2017**, *23*, 2721–2726. [[CrossRef](#)]
289. Ashrafi, R.; Sahu, D.K.; Kesharwani, P.; Ganjir, M.; Agrawal, R.C. Ag⁺-Ion Conducting Nano-Composite Polymer Electrolytes (NCPEs): Synthesis, Characterization and All-Solid-Battery Studies. *J. Non-Cryst. Solids* **2014**, *391*, 91–95. [[CrossRef](#)]
290. Klongkan, S.; Pumchusak, J. Effects of Nano Alumina and Plasticizers on Morphology, Ionic Conductivity, Thermal and Mechanical Properties of PEO-LiCF₃SO₃ Solid Polymer Electrolyte. *Electrochim. Acta* **2015**, *161*, 171–176. [[CrossRef](#)]
291. Borah, S.; Deka, M. Study of Electrical and Electrochemical Properties of P(VdF-HFP)-MMT Based Nanocomposite Gel Polymer Electrolytes for Application in Energy Storage Devices. *Mater. Sci. Eng. B* **2021**, *263*, 114822. [[CrossRef](#)]
292. Wu, Z.; Xie, Z.; Yoshida, A.; Wang, J.; Yu, T.; Wang, Z.; Hao, X.; Abudula, A.; Guan, G. Nickel Phosphate Nanorod-Enhanced Polyethylene Oxide-Based Composite Polymer Electrolytes for Solid-State Lithium Batteries. *J. Colloid Interface Sci.* **2020**, *565*, 110–118. [[CrossRef](#)]
293. Liew, J.W.Y.; Loh, K.S.; Ahmad, A.; Lim, K.L.; Wan Daud, W.R. Effect of Modified Natural Filler O-Methylene Phosphonic κ -Carrageenan on Chitosan-Based Polymer Electrolytes. *Energies* **2018**, *11*, 1910. [[CrossRef](#)]
294. Dhatarwal, P.; Choudhary, S.; Sengwa, R.J. Electrochemical Performance of Li⁺-Ion Conducting Solid Polymer Electrolytes Based on PEO-PMMA Blend Matrix Incorporated with Various Inorganic Nanoparticles for the Lithium Ion Batteries. *Compos. Commun.* **2018**, *10*, 11–17. [[CrossRef](#)]
295. Arya, A.; Sharma, A.L. Tailoring of the Structural, Morphological, Electrochemical, and Dielectric Properties of Solid Polymer Electrolyte. *Ionics* **2019**, *25*, 1617–1632. [[CrossRef](#)]
296. Deshmukh, K.; Ahamed, M.B.; Polu, A.R.; Sadashivuni, K.K.; Pasha, S.K.K.; Ponnamma, D.; AlMaadeed, M.A.-A.; Deshmukh, R.R.; Chidambaram, K. Impedance Spectroscopy, Ionic Conductivity and Dielectric Studies of New Li⁺ Ion Conducting Polymer Blend Electrolytes Based on Biodegradable Polymers for Solid State Battery Applications. *J. Mater. Sci: Mater. Electron.* **2016**, *27*, 11410–11424. [[CrossRef](#)]
297. Nofal, M.M.; Aziz, S.B.; Ghareeb, H.O.; Hadi, J.M.; Dannoun, E.M.A.; Al-Saeedi, S.I. Impedance and Dielectric Properties of PVC:NH4I Solid Polymer Electrolytes (SPEs): Steps toward the Fabrication of SPEs with High Resistivity. *Materials* **2022**, *15*, 2143. [[CrossRef](#)] [[PubMed](#)]
298. Rauf, H.G.; Hadi, J.M.; Aziz, S.B.; Abdulwahid, R.T.; Mustafa, M.S. A Novel Approach to Design High Resistive Polymer Electrolytes Based on PVC: Electrochemical Impedance and Dielectric Properties. *Int. J. Electrochem. Sci.* **2022**, *17*, 22051. [[CrossRef](#)]
299. Ramesh, S.; Yin, T.S.; Liew, C.-W. Effect of Dibutyl Phthalate as Plasticizer on High-Molecular Weight Poly(Vinyl Chloride)-Lithium Tetraborate-Based Solid Polymer Electrolytes. *Ionics* **2011**, *17*, 705–713. [[CrossRef](#)]
300. Ganta, K.K.; Jeedi, V.R.; Katrapally, V.K.; Yalla, M.; Emmadi, L.N. Effect of TiO₂ Nano-Filler on Electrical Properties of Na⁺ Ion Conducting PEO/PVDF Based Blended Polymer Electrolyte. *J. Inorg. Organomet. Polym.* **2021**, *31*, 3430–3440. [[CrossRef](#)]
301. Kulshrestha, N.; Chatterjee, B.; Gupta, P.N. Structural, Thermal, Electrical, and Dielectric Properties of Synthesized Nanocomposite Solid Polymer Electrolytes. *High. Perform. Polym.* **2014**, *26*, 677–688. [[CrossRef](#)]
302. Zamri, S.F.M.; Latif, F.A.; Ali, A.M.M.; Ibrahim, R.; Kamaluddin, N.; Hadip, F. Ionic Conductivity and Dielectric Properties of LiBF₄ Doped PMMA/ENR 50 Filled Acid Modified SiO₂ Electrolytes. *Procedia Technol.* **2014**, *15*, 849–855. [[CrossRef](#)]
303. Quartarone, E. PEO-Based Composite Polymer Electrolytes. *Solid State Ion.* **1998**, *110*, 1–14. [[CrossRef](#)]
304. *Solid State Electrochemistry*; Bruce, P.G., Ed.; Chemistry of solid state materials; Cambridge University Press: Cambridge, UK; New York, NY, USA, 1995; ISBN 978-0-521-40007-7.
305. Lu, Q.; He, Y.; Yu, Q.; Li, B.; Kaneti, Y.V.; Yao, Y.; Kang, F.; Yang, Q. Dendrite-Free, High-Rate, Long-Life Lithium Metal Batteries with a 3D Cross-Linked Network Polymer Electrolyte. *Adv. Mater.* **2017**, *29*, 1604460. [[CrossRef](#)] [[PubMed](#)]
306. Lin, Y.-C.; Ito, K.; Yokoyama, H. Solid Polymer Electrolyte Based on Crosslinked Polyrotaxane. *Polymer* **2018**, *136*, 121–127. [[CrossRef](#)]
307. Li, Z.; Guo, D.; Li, F.; Hou, G.; Liu, X.; Li, C.; Cao, L.; Wei, R.; Zhou, Z.; Lai, Z. Nerve Network-Inspired Solid Polymer Electrolytes (NN-SPE) for Fast and Single-Ion Lithium Conduction. *Energy Storage Mater.* **2022**, *49*, 575–582. [[CrossRef](#)]
308. Lee, J.-Y.; Yu, T.-Y.; Chung, P.-H.; Lee, W.-Y.; Yeh, S.-C.; Wu, N.-L.; Jeng, R.-J. Semi-Interpenetrating Polymer Network Electrolytes Based on a Spiro-Twisted Benzoxazine for All-Solid-State Lithium-Ion Batteries. *ACS Appl. Energy Mater.* **2021**, *4*, 2663–2671. [[CrossRef](#)]
309. Kim, G.-T.; Appeteccchi, G.B.; Alessandrini, F.; Passerini, S. Solvent-Free, PYR1ATFSI Ionic Liquid-Based Ternary Polymer Electrolyte Systems. *J. Power Sources* **2007**, *171*, 861–869. [[CrossRef](#)]
310. Cha, E.H.; Macfarlane, D.R.; Forsyth, M.; Lee, C.W. Ionic Conductivity Studies of Polymeric Electrolytes Containing Lithium Salt with Plasticizer. *Electrochim. Acta* **2004**, *50*, 335–338. [[CrossRef](#)]
311. Young, W.-S.; Epps, T.H. Ionic Conductivities of Block Copolymer Electrolytes with Various Conducting Pathways: Sample Preparation and Processing Considerations. *Macromolecules* **2012**, *45*, 4689–4697. [[CrossRef](#)]
312. Aldalur, I.; Martínez-Ibañez, M.; Piszcza, M.; Rodriguez-Martinez, L.M.; Zhang, H.; Armand, M. Lowering the Operational Temperature of All-Solid-State Lithium Polymer Cell with Highly Conductive and Interfacially Robust Solid Polymer Electrolytes. *J. Power Sources* **2018**, *383*, 144–149. [[CrossRef](#)]

313. Forsyth, M.; MacFarlane, D.R.; Hill, A.J. Glass Transition and Free Volume Behaviour of Poly(Acrylonitrile)/LiCF₃SO₃ Polymer-in-Salt Electrolytes Compared to Poly(Ether Urethane)/LiClO₄ Solid Polymer Electrolytes. *Electrochim. Acta* **2000**, *45*, 1243–1247. [CrossRef]
314. Sandner, B.; Steurich, T.; Wiesner, K.; Bischoff, H. Solid Polymer Electrolytes Based on Oligo(Ethylene Glycol)Methacrylates: 1. Conductivity of Plasticized Networks Containing a Polar Comonomer. *Polym. Bull.* **1992**, *28*, 355–360. [CrossRef]
315. Dannoun, E.M.A.; Aziz, S.B.; Abdullah, S.N.; Nofal, M.M.; Mahmoud, K.H.; Murad, A.R.; Abdullah, R.M.; Kadir, M.F.Z. Characteristics of Plasticized Lithium Ion Conducting Green Polymer Blend Electrolytes Based on CS: Dextrans with High Energy Density and Specific Capacitance. *Polymers* **2021**, *13*, 3613. [CrossRef] [PubMed]
316. Mauger, A.; Julien, C.M. V₂O₅ Thin Films for Energy Storage and Conversion. *AIMS Mater. Sci.* **2018**, *5*, 349–401. [CrossRef]
317. Tasheva, T.; Dimitrov, V. Correlation between Structure and Optical Basicity of Glasses in the TeO₂-V₂O₅-MoO₃ System. *J. Non-Cryst. Solids* **2021**, *570*, 120981. [CrossRef]
318. Logan, E.R.; Hall, D.S.; Cormier, M.M.E.; Taskovic, T.; Bauer, M.; Hamam, I.; Hebecker, H.; Molino, L.; Dahn, J.R. Ester-Based Electrolytes for Fast Charging of Energy Dense Lithium-Ion Batteries. *J. Phys. Chem. C* **2020**, *124*, 12269–12280. [CrossRef]
319. Xu, K.; Von Cresce, A.; Lee, U. Differentiating Contributions to “Ion Transfer” Barrier from Interphasial Resistance and Li⁺ Desolvation at Electrolyte/Graphite Interface. *Langmuir* **2010**, *26*, 11538–11543. [CrossRef]
320. Xu, K.; Von Wald Cresce, A. Li⁺-Solvation/Desolvation Dictates Interphasial Processes on Graphitic Anode in Li Ion Cells. *J. Mater. Res.* **2012**, *27*, 2327–2341. [CrossRef]
321. Cho, Y.-G.; Kim, Y.-S.; Sung, D.-G.; Seo, M.-S.; Song, H.-K. Nitrile-Assistant Eutectic Electrolytes for Cryogenic Operation of Lithium Ion Batteries at Fast Charges and Discharges. *Energy Environ. Sci.* **2014**, *7*, 1737–1743. [CrossRef]
322. Yao, Y.-X.; Chen, X.; Yan, C.; Zhang, X.-Q.; Cai, W.-L.; Huang, J.-Q.; Zhang, Q. Regulating Interfacial Chemistry in Lithium-Ion Batteries by a Weakly-Solvating Electrolyte. *Angew. Chem. Int. Ed.* **2020**, *60*, 4090–4097. [CrossRef]
323. Chen, X.; Yao, N.; Zeng, B.-S.; Zhang, Q. Ion-Solvent Chemistry in Lithium Battery Electrolytes: From Mono-Solvent to Multi-Solvent Complexes. *Fundam. Res.* **2021**, *1*, 393–398. [CrossRef]
324. Lei, S.; Zeng, Z.; Liu, M.; Zhang, H.; Cheng, S.; Xie, J. Balanced Solvation/de-Solvation of Electrolyte Facilitates Li-Ion Intercalation for Fast Charging and Low-Temperature Li-Ion Batteries. *Nano Energy* **2022**, *98*, 107265. [CrossRef]
325. Ong, M.T.; Verners, O.; Draeger, E.W.; Van Duin, A.C.T.; Lordi, V.; Pask, J.E. Lithium Ion Solvation and Diffusion in Bulk Organic Electrolytes from First-Principles and Classical Reactive Molecular Dynamics. *J. Phys. Chem. B* **2015**, *119*, 1535–1545. [CrossRef]
326. Jiang, H.; Han, X.; Du, X.; Chen, Z.; Lu, C.; Li, X.; Zhang, H.; Zhao, J.; Han, P.; Cui, G. A PF₆⁻-Permselective Polymer Electrolyte with Anion Solvation Regulation Enabling Long-Cycle Dual-Ion Battery. *Adv. Mater.* **2022**, *34*, 2108665. [CrossRef] [PubMed]
327. Chernyak, A.V.; Slesarenko, N.A.; Slesarenko, A.A.; Baymuratova, G.R.; Tulibaeva, G.Z.; Yudina, A.V.; Volkov, V.I.; Shestakov, A.F.; Yarmolenko, O.V. Effect of the Solvate Environment of Lithium Cations on the Resistance of the Polymer Electrolyte/Electrode Interface in a Solid-State Lithium Battery. *Membranes* **2022**, *12*, 1111. [CrossRef]
328. Wen, P.; Liu, Y.; Mao, J.; Liu, X.; Li, W.; Ren, Y.; Zhou, Y.; Shao, F.; Chen, M.; Lin, J.; et al. Tuning Desolvation Kinetics of In-Situ Weakly Solvating Polyacetal Electrolytes for Dendrite-Free Lithium Metal Batteries. *J. Energy Chem.* **2023**, *79*, 340–347. [CrossRef]
329. Wang, T.; Zhang, Y.; Huang, X.; Su, P.; Xiao, M.; Wang, S.; Huang, S.; Han, D.; Meng, Y. Designing Weakly and Strongly Solvating Polymer Electrolytes: Systematically Boosting High-voltage Lithium Metal Batteries. *SusMat* **2024**, *4*, e219. [CrossRef]
330. Kido, R.; Ueno, K.; Iwata, K.; Kitazawa, Y.; Imaizumi, S.; Mandai, T.; Dokko, K.; Watanabe, M. Li⁺ Ion Transport in Polymer Electrolytes Based on a Glyme-Li Salt Solvate Ionic Liquid. *Electrochim. Acta* **2015**, *175*, 5–12. [CrossRef]
331. Lin, Z.; Wang, Y.; Li, Y.; Liu, Y.; Zhong, S.; Xie, M.; Yan, F.; Zhang, Z.; Peng, J.; Li, J.; et al. Regulating Solvation Structure in Gel Polymer Electrolytes with Covalent Organic Frameworks for Lithium Metal Batteries. *Energy Storage Mater.* **2022**, *53*, 917–926. [CrossRef]
332. Liu, X.; Wang, D.; Zhang, Z.; Li, G.; Wang, J.; Yang, G.; Lin, H.; Lin, J.; Ou, X.; Zheng, W. Gel Polymer Electrolyte Enables Low-Temperature and High-Rate Lithium-Ion Batteries via Bionic Interface Design. *Small* **2024**, *20*, 2404879. [CrossRef]
333. Yu, Y.; Lu, F.; Sun, N.; Wu, A.; Pan, W.; Zheng, L. Single Lithium-Ion Polymer Electrolytes Based on Poly(Ionic Liquid)s for Lithium-Ion Batteries. *Soft Matter* **2018**, *14*, 6313–6319. [CrossRef]
334. Kitazawa, Y.; Iwata, K.; Kido, R.; Imaizumi, S.; Tsuzuki, S.; Shinoda, W.; Ueno, K.; Mandai, T.; Kokubo, H.; Dokko, K.; et al. Polymer Electrolytes Containing Solvate Ionic Liquids: A New Approach To Achieve High Ionic Conductivity, Thermal Stability, and a Wide Potential Window. *Chem. Mater.* **2018**, *30*, 252–261. [CrossRef]
335. Lee, K.-H.; Lim, H.S.; Wang, J.H. Effect of Unreacted Monomer on Performance of Lithium-Ion Polymer Batteries Based on Polymer Electrolytes Prepared by Free Radical Polymerization. *J. Power Sources* **2005**, *139*, 284–288. [CrossRef]
336. Swiderska-Mocek, A.; Kubis, A. Preparation and Electrochemical Properties of Polymer Electrolyte Containing Lithium Difluoro(Oxalato)Borate or Lithium Bis(Oxalate)Borate for Li-Ion Polymer Batteries. *Solid State Ion.* **2021**, *364*, 115628. [CrossRef]
337. Wang, S.; Li, J.; Li, T.; Huang, W.; Wang, L.; Tao, S. Li⁺ Affinity Ultra-Thin Solid Polymer Electrolyte for Advanced All-Solid-State Lithium-Ion Battery. *Chem. Eng. J.* **2023**, *461*, 141995. [CrossRef]
338. Zhu, Y.; Liu, C.; Yang, Y.; Li, Y.; Wu, Q.-H. A Novel Design of Inorganic-Polymer Gel Electrolyte/Anode Interphase in Quasi-Solid-State Lithium-Ion Batteries. *Electrochim. Acta* **2023**, *446*, 142097. [CrossRef]
339. Li, H.; Kuai, Y.; Yang, J.; Hirano, S.; Nuli, Y.; Wang, J. A New Flame-Retardant Polymer Electrolyte with Enhanced Li-Ion Conductivity for Safe Lithium-Sulfur Batteries. *J. Energy Chem.* **2022**, *65*, 616–622. [CrossRef]

340. Chen, J.; Lu, H.; Zhang, X.; Zhang, Y.; Yang, J.; Nuli, Y.; Huang, Y.; Wang, J. Electrochemical Polymerization of Nonflammable Electrolyte Enabling Fast-Charging Lithium-Sulfur Battery. *Energy Storage Mater.* **2022**, *50*, 387–394. [[CrossRef](#)]
341. Guo, Y.; Lu, J.; Jin, Z.; Chen, H.; Wang, W.; Huang, Y.; Wang, A. InPc-Modified Gel Electrolyte Based on in Situ Polymerization in Practical High-Loading Lithium-Sulfur Batteries. *Chem. Eng. J.* **2023**, *469*, 143714. [[CrossRef](#)]
342. Ling, W.; Fu, N.; Yue, J.; Zeng, X.; Ma, Q.; Deng, Q.; Xiao, Y.; Wan, L.; Guo, Y.; Wu, X. A Flexible Solid Electrolyte with Multilayer Structure for Sodium Metal Batteries. *Adv. Energy Mater.* **2020**, *10*, 1903966. [[CrossRef](#)]
343. Liu, X.; Li, X.; Yang, X.; Lu, J.; Zhang, X.; Yuan, D.; Zhang, Y. Influence of Water on Gel Electrolytes for Zinc-Ion Batteries. *Chem. Asian J.* **2023**, *18*, e202201280. [[CrossRef](#)]
344. Yu, Z.; Jiao, S.; Li, S.; Chen, X.; Song, W.; Teng, T.; Tu, J.; Chen, H.; Zhang, G.; Fang, D. Flexible Stable Solid-State Al-Ion Batteries. *Adv. Funct. Mater.* **2019**, *29*, 1806799. [[CrossRef](#)]
345. Xie, Y.; Feng, L.; Li, D.; Tang, Y.; Zhu, C.; Wang, M.; Xu, J. A Novel Flame-Retardant Nitrile-Based Gel Polymer Electrolyte for Quasi-Solid-State Lithium Metal Batteries. *Colloids Surf. A Physicochem. Eng. Asp.* **2023**, *670*, 131487. [[CrossRef](#)]
346. Callegari, D.; Colombi, S.; Nitti, A.; Simari, C.; Nicotera, I.; Ferrara, C.; Mustarelli, P.; Pasini, D.; Quartarone, E. Autonomous Self-Healing Strategy for Stable Sodium-Ion Battery: A Case Study of Black Phosphorus Anodes. *ACS Appl. Mater. Interfaces* **2021**, *13*, 13170–13182. [[CrossRef](#)]
347. West, K.; Zachau-Christiansen, B.; Jacobsen, T.; Hiort-Lorenzen, E.; Skaarup, S. Poly(Ethylene Oxide)-sodium Perchlorate Electrolytes in Solid-state Sodium Cells. *Br. Polym. J.* **1988**, *20*, 243–246. [[CrossRef](#)]
348. Ma, Y.; Doyle, M.; Fuller, T.F.; Doeff, M.M.; De Jonghe, L.C.; Newman, J. The Measurement of a Complete Set of Transport Properties for a Concentrated Solid Polymer Electrolyte Solution. *J. Electrochem. Soc.* **1995**, *142*, 1859–1868. [[CrossRef](#)]
349. Song, S.; Kotobuki, M.; Zheng, F.; Xu, C.; Savilov, S.V.; Hu, N.; Lu, L.; Wang, Y.; Li, W.D.Z. A Hybrid Polymer/Oxide/Ionic-Liquid Solid Electrolyte for Na-Metal Batteries. *J. Mater. Chem. A* **2017**, *5*, 6424–6431. [[CrossRef](#)]
350. Zheng, Y.; Pan, Q.; Clites, M.; Byles, B.W.; Pomerantseva, E.; Li, C.Y. High-Capacity All-Solid-State Sodium Metal Battery with Hybrid Polymer Electrolytes. *Adv. Energy Mater.* **2018**, *8*, 1801885. [[CrossRef](#)]
351. Zhou, D.; Liu, R.; Zhang, J.; Qi, X.; He, Y.-B.; Li, B.; Yang, Q.-H.; Hu, Y.-S.; Kang, F. In Situ Synthesis of Hierarchical Poly(Ionic Liquid)-Based Solid Electrolytes for High-Safety Lithium-Ion and Sodium-Ion Batteries. *Nano Energy* **2017**, *33*, 45–54. [[CrossRef](#)]
352. Zhang, Z.; Xu, K.; Rong, X.; Hu, Y.-S.; Li, H.; Huang, X.; Chen, L. $\text{Na}_{3.4}\text{Zr}_{1.8}\text{Mg}_{0.2}\text{Si}_2\text{PO}_{12}$ Filled Poly(Ethylene Oxide)/ $\text{Na}(\text{CF}_3\text{SO}_2)_2\text{N}$ as Flexible Composite Polymer Electrolyte for Solid-State Sodium Batteries. *J. Power Sources* **2017**, *372*, 270–275. [[CrossRef](#)]
353. Reddeppa, N.; Sharma, A.K.; Narasimha Rao, V.V.R.; Chen, W. Preparation and Characterization of Pure and KBr Doped Polymer Blend (PVC/PEO) Electrolyte Thin Films. *Microelectron. Eng.* **2013**, *112*, 57–62. [[CrossRef](#)]
354. Gao, H.; Xue, L.; Xin, S.; Goodenough, J.B. A High-Energy-Density Potassium Battery with a Polymer-Gel Electrolyte and a Polyaniline Cathode. *Angew. Chem. Int. Ed.* **2018**, *57*, 5449–5453. [[CrossRef](#)]
355. Singh, R.; Baghel, J.; Shukla, S.; Bhattacharya, B.; Rhee, H.-W.; Singh, P.K. Detailed Electrical Measurements on Sago Starch Biopolymer Solid Electrolyte. *Phase Transit.* **2014**, *87*, 1237–1245. [[CrossRef](#)]
356. Lee, K.J.; Park, J.T.; Koh, J.H.; Min, B.R.; Kim, J.H. Graft Polymerization of Poly(Epichlorohydrin-g-Poly((Oxyethylene) Methacrylate)) Using ATRP and Its Polymer Electrolyte with KI. *Ionics* **2009**, *15*, 163–167. [[CrossRef](#)]
357. Yang, J.; Zhang, H.; Zhou, Q.; Qu, H.; Dong, T.; Zhang, M.; Tang, B.; Zhang, J.; Cui, G. Safety-Enhanced Polymer Electrolytes for Sodium Batteries: Recent Progress and Perspectives. *ACS Appl. Mater. Interfaces* **2019**, *11*, 17109–17127. [[CrossRef](#)]
358. Kesharwani, P.; Sahu, D.K.; Sahu, M.; Sahu, T.B.; Agrawal, R.C. Study of Ion Transport and Materials Properties of K+-Ion Conducting Solid Polymer Electrolyte (SPE):[(1-x)PEO:xCH₃COOK]. *Ionics* **2017**, *23*, 2823–2827. [[CrossRef](#)]
359. Zhao, T.; Zhang, G.; Zhou, F.; Zhang, S.; Deng, C. Toward Tailorable Zn-Ion Textile Batteries with High Energy Density and Ultrafast Capability: Building High-Performance Textile Electrode in 3D Hierarchical Branched Design. *Small* **2018**, *14*, 1802320. [[CrossRef](#)] [[PubMed](#)]
360. Liu, J.; Guan, C.; Zhou, C.; Fan, Z.; Ke, Q.; Zhang, G.; Liu, C.; Wang, J. A Flexible Quasi-Solid-State Nickel-Zinc Battery with High Energy and Power Densities Based on 3D Electrode Design. *Adv. Mater.* **2016**, *28*, 8732–8739. [[CrossRef](#)] [[PubMed](#)]
361. Li, H.; Han, C.; Huang, Y.; Huang, Y.; Zhu, M.; Pei, Z.; Xue, Q.; Wang, Z.; Liu, Z.; Tang, Z.; et al. An Extremely Safe and Wearable Solid-State Zinc Ion Battery Based on a Hierarchical Structured Polymer Electrolyte. *Energy Environ. Sci.* **2018**, *11*, 941–951. [[CrossRef](#)]
362. Ye, H.; Xu, J.J. Zinc Ion Conducting Polymer Electrolytes Based on Oligomeric Polyether/PVDF-HFP Blends. *J. Power Sources* **2007**, *165*, 500–508. [[CrossRef](#)]
363. Liu, B.; Huang, Y.; Wang, J.; Li, Z.; Yang, G.; Jin, S.; Iranmanesh, E.; Hiralal, P.; Zhou, H. Highly Conductive Locust Bean Gum Bio-Electrolyte for Superior Long-Life Quasi-Solid-State Zinc-Ion Batteries. *RSC Adv.* **2021**, *11*, 24862–24871. [[CrossRef](#)] [[PubMed](#)]
364. Chen, Z.; Wang, P.; Ji, Z.; Wang, H.; Liu, J.; Wang, J.; Hu, M.; Huang, Y. High-Voltage Flexible Aqueous Zn-Ion Battery with Extremely Low Dropout Voltage and Super-Flat Platform. *Nano-Micro Lett.* **2020**, *12*, 75. [[CrossRef](#)]
365. Huang, S.; Wan, F.; Bi, S.; Zhu, J.; Niu, Z.; Chen, J. A Self-Healing Integrated All-in-One Zinc-Ion Battery. *Angew. Chem. Int. Ed.* **2019**, *58*, 4313–4317. [[CrossRef](#)]
366. Li, X.; Wang, D.; Ran, F. Key Approaches and Challenges in Fabricating Advanced Flexible Zinc-Ion Batteries with Functional Hydrogel Electrolytes. *Energy Storage Mater.* **2023**, *56*, 351–393. [[CrossRef](#)]
367. Wu, F.; Zhu, N.; Bai, Y.; Gao, Y.; Wu, C. An Interface-Reconstruction Effect for Rechargeable Aluminum Battery in Ionic Liquid Electrolyte to Enhance Cycling Performances. *Green. Energy Environ.* **2018**, *3*, 71–77. [[CrossRef](#)]

368. Gu, S.; Wang, H.; Wu, C.; Bai, Y.; Li, H.; Wu, F. Confirming Reversible Al_{3+} Storage Mechanism through Intercalation of Al_{3+} into V₂O₅ Nanowires in a Rechargeable Aluminum Battery. *Energy Storage Mater.* **2017**, *6*, 9–17. [CrossRef]
369. Wu, F.; Yang, H.; Bai, Y.; Wu, C. Paving the Path toward Reliable Cathode Materials for Aluminum-Ion Batteries. *Adv. Mater.* **2019**, *31*, 1806510. [CrossRef]
370. Wang, H.; Gu, S.; Bai, Y.; Chen, S.; Wu, F.; Wu, C. High-Voltage and Noncorrosive Ionic Liquid Electrolyte Used in Rechargeable Aluminum Battery. *ACS Appl. Mater. Interfaces* **2016**, *8*, 27444–27448. [CrossRef]
371. Elia, G.A.; Marquardt, K.; Hoeppner, K.; Fantini, S.; Lin, R.; Knipping, E.; Peters, W.; Drillet, J.; Passerini, S.; Hahn, R. An Overview and Future Perspectives of Aluminum Batteries. *Adv. Mater.* **2016**, *28*, 7564–7579. [CrossRef]
372. Yao, T.; Genier, F.S.; Biria, S.; Hosein, I.D. A Solid Polymer Electrolyte for Aluminum Ion Conduction. *Results Phys.* **2018**, *10*, 529–531. [CrossRef]
373. Song, S.; Kotobuki, M.; Zheng, F.; Li, Q.; Xu, C.; Wang, Y.; Li, W.D.Z.; Hu, N.; Lu, L. Al Conductive Hybrid Solid Polymer Electrolyte. *Solid State Ion.* **2017**, *300*, 165–168. [CrossRef]

Disclaimer/Publisher’s Note: The statements, opinions and data contained in all publications are solely those of the individual author(s) and contributor(s) and not of MDPI and/or the editor(s). MDPI and/or the editor(s) disclaim responsibility for any injury to people or property resulting from any ideas, methods, instructions or products referred to in the content.